

IDENTIFICATION OF IMMUNOLOGICAL GENES IMPORTANT FOR  
CYTOTOXICITY

by

SİNEM USLUER

Submitted to the Institute of Engineering and Natural Sciences  
in partial fulfillment of  
the requirements for the degree of  
Master of Science

Sabanci University

Jan 2019


# IDENTIFICATION OF IMMUNOLOGICAL GENES FOR CYTOTOXICITY

APPROVED BY:

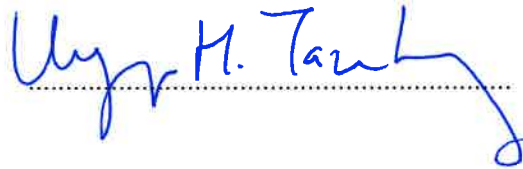
Prof. Dr. Batu Erman  
(Thesis Supervisor)

  
.....

Asst. Prof. Tolga Sütli

  
.....

Prof. Dr. Uygur Halis Tazebay

  
.....

DATE OF APPROVAL: 07/01/2019

© Sinem Usluer 2019

All Rights Reserved

## ABSTRACT

### IDENTIFICATION OF IMMUNOLOGICAL GENES FOR CYTOTOXICITY

SİNEM USLUER

Molecular Biology, Genetics and Bioengineering, MSc Thesis, Jan 2019

Thesis Supervisor: Prof. Batu Erman

Keywords: NK-92 cells, single cell clone, HSV-TK, CRISPR/Cas9, cytotoxicity

Natural Killer (NK) cells and Cytotoxic T lymphocytes (CTLs) are essential to defend the body against foreign or transformed cells. An understanding of the mechanism of their cytotoxicity can result in the generation of genetically modified cells with higher cytotoxicity and to identify drug-targets that increase cytotoxicity. In this thesis, genes which have a role in the cytotoxicity of CTLs were targeted by the CRISPR/Cas9 system to check whether they also play a role in the cytotoxicity of Natural Killer cells (NK-92 cell line). These cells are difficult to transfect with plasmid DNA and to generate single cell clones. In this thesis we attempted to optimize the Neon Electroporation method for the NK-92 cell line. Unfortunately, we could not obtain high transfection efficiency and high cell viability. We thus performed gene transfer into these cells by lentiviral infection. In order to obtain single cell cloned NK-92 cells, we generated a feeder cell line by transduction with lentivirus encoding the HSV-TK gene into the NK-92 cell line. Cell containing the TK gene can be negatively selected by ganciclovir treatment. We performed coculture experiments with this feeder line mixed with ganciclovir resistant, unmodified NK cells at different ratios under different doses of ganciclovir selection. We were able to initiate a healthy culture starting with only 17 NK-92 cells, using a 1:10000 ratio of ganciclovir sensitive feeder cells selected under increasing doses of ganciclovir from 0.01  $\mu\text{g/ml}$  to 1  $\mu\text{g/ml}$ . To mutate selected cytotoxicity genes, we expressed CRISPR/Cas9 by third generation lentivirus. Presence of a mutation and a decrease in mRNA expression level of the target genes was confirmed by the T7 assay and QRT-PCR. The cytotoxicity of mutated pools were assessed by a degranulation assay and by xCELLigence real time cell analysis. We identified several genes that are important for the cytotoxic response towards the MCF-7 cell line.

## ÖZET

### SİTOTOKSİSİTE İÇİN İMMÜNÖLOJİK GENLERİN TANIMI

SİNEM USLUER

Moleküler Biyoloji, Genetik and Biyomühendislik, Yüksek Lisans Tezi, Ocak 2019

Tez Danışmanı: Prof. Batu Erman

Anahtar Kelimeler: NK-92 Hücreleri, Tek Hücreli Klon, HSV-TK, CRISPR/Cas9,  
Sitotoksosite

Doğal Öldürücü (NK) hücreleri ve sitotoksik T-lenfositleri (CTL) vücudu yabancı hücelere karşı korumak için önemlidir. Sitotoksosite mekanizmalarının ayrıntılı olarak anlaşılması daha yüksek sitotoksositeye sahip genetiği değiştirilmiş hücreler üretme ve sitotoksitelerini arttırmak için ilaçla hedeflenebilir bölgeler bulma şansı verir. Bu tezde, CTL'nin sitotoksitesinde rol oynayan genlerin, NK-92 hücrelerinin sitotoksitesinde de önemli olup olmadıklarını kontrol etmek için CRISPR/Cas9 sistemini kullandık. NK-92 hücrelerine plazmit transfeksiyonu ve tek hücreli klon yapmak zordur. Bu adımlar, CRISPR / Cas9 sistemi kullanarak mutasyona uğramış bir hücre popülasyonu oluşturmak için gereklidir. Neon Elektroporasyon transfeksiyon yöntemi ile NK-92 hücre hattına gen aktarımını optimize etmeye çalıştık, ancak CRISPR/Cas9 vektörünü yüksek transfeksiyon verimliliği ve yüksek hücre canlılığı ile hücreye gönderimini sağlayamadık. Besleyici hücre hattı, HSV-TK genli virüsün NK-92 hücre hattına transfer edilmesi ile üretildi. Tek NK-92 hücrelerini büyütme için en iyi koşulu bulmak amacıyla farklı oranlarda ve farklı konsantrasyonlarda gansiklovir kullanılarak birlikte kültür deneyleri yaptık. Yaklaşık 17 NK-92 hücresinin 1:10000 oranı ve 0.01 µg/ml ile 1 µg/ml gansiklovir muamelesi sonucunda saf bir popülasyon oluşturduğunu belirledik. Seçilen genleri mutasyona uğratmak için, CRISPR/Cas9 plazmitleri, üçüncü nesil lentivirüs metotları ile iletildi. Mutasyonun varlığı ve hedef genin mRNA ifade seviyesindeki azalma, T7 tahlili ve QRT-PCR ile doğrulandı. Mutasyona uğramış popülasyonların sitotoksitesisi ve degranülasyonu xCELLigence deneyi ile kontrol edildi. Bu tez çalışmasında bazı genlerdeki mutasyonların NK-92 hücrelerinin MCF-7 hücrelerine karşı sitotoksosite yanıtlarının azalttığını belirledik.

*To my beloved family...*

*Canım Aileme...*

*#UMUT*

## ACKNOWLEDGEMENTS

I would like to express my appreciation to my thesis advisor Prof. Batu Erman for his endless support and continuous encouragement throughout my MSc study. Being a member of his research laboratory improved me a lot in critical thinking and broaden my scientific perspective thanks to his huge knowledge. Prof. Batu Erman is a great group leader and great teacher. I am grateful for this opportunity to become a member of his research lab and professional support that I always received and hope to continue in the future. I am thankful to my thesis jury members Prof. Uygur Tazebay and Dr. Tolga Sütü for their supports and feedbacks about my thesis project. I am very appreciative to Dr. Tolga Sütü for his all support and his valuable scientific comments.

I would like to thank all the past and present members of our lab: Dr. Bahar Shamloo, Nazife Tolay, Hakan Taşkıran, Liyne Noğay, Melike Gezen, Sanem Sarıyar, Sofia Piepoli, Sarah Mohammed Barakat, Ronay Çetin. I am appreciative to Bahar for her help and unique friendship. I am thankful to Sofia and Ronay for their help and scientific comments. I am appreciative to Liyne, Sanem and Melike for their friendship. I would like to express my great appreciation to Nazife for her pure friendship, her endless help and strong comments about the experiment and in my life. I am very grateful to Hakan for his support, guidance and deep friendship. I am also thankful to my undergrad student Anna for her friendship.

I would like to thank all members of Sütü lab: Ayhan Parlar, Cevriye Pamukçu, Mertkaya Aras, Didem Özkazanç, Alp Ertunga Eyüpoğlu, Elif Çelik, Pegah Zahedimaram, Lolai Ikromzoda, Dr. Başak Özata for their help and friendship.

I am very grateful to all my friends for their love and friendship, especially to Sevde Nur Karataş, Nazlı Kocatuğ, Cansu Karahan and Buket Sakinci. They always support me for my studies and for my life.

I am very grateful to my family for their endless support and faith in me. Their love and support always with me during my journey. I could not have fulfilled my studies without having their supports and love.

## TABLE OF CONTENT

<b>ABSTRACT</b> .....	<b>iv</b>
<b>ÖZET</b> .....	<b>v</b>
<b>ACKNOWLEDGEMENTS</b> .....	<b>vii</b>
<b>TABLE OF CONTENT</b> .....	<b>viii</b>
<b>LIST OF FIGURES</b> .....	<b>xii</b>
<b>LIST OF TABLES</b> .....	<b>xiv</b>
<b>LIST OF ABBREVIATIONS</b> .....	<b>xv</b>
<b>1. INTRODUCTION</b> .....	<b>1</b>
<b>1.1. The Immune System</b> .....	<b>1</b>
1.1.1. Innate Immune System .....	1
1.1.2. Adaptive Immune System.....	2
<b>1.2. Activation of Cytotoxic Lymphocytes of Immune Cells</b> .....	<b>3</b>
1.2.1. Activation of T cells .....	3
1.2.2. Activation of NK cells.....	6
1.2.3. NK-92 cell lines.....	8
<b>1.3 Function and Cytotoxicity of Lymphocytes</b> .....	<b>10</b>
1.3.1. T cells.....	10
1.3.1.1. Function of Helper T cells .....	10
1.3.1.2. Function of Cytotoxic T cells .....	10
1.3.2. NK cell.....	11
1.3.2.1. Activating the NK Cell Immunological Synapse .....	12
1.3.2.2. Inhibitory NK Cell Immunological Synapse(iNKIS) .....	13
1.3.3. Comparison of T and NK cell cytotoxicity.....	13
<b>1.4. Genetic Modification of the NK-92 Cell Line by Clustered Regularly Interspaced Short Palindromic Repeats (CRISPR)</b> .....	<b>14</b>
<b>1.5. Function of Target Proteins</b> .....	<b>16</b>
1.5.1. Actin Related Protein 2/3 Complex Subunit 1B (Apc1b) .....	16
1.5.2. Chromosome 12 Open Reading Frame 4 (C12orf4).....	17
1.5.3. Coiled-coil domain containing 124 (Ccdc124).....	17
1.5.4. CTR9 Homolog, Paf1/RNA Polymerase II Complex Component (Ctr9) .....	18
1.5.5. DNA Fragmentation Factor Subunit Beta (Dffb) .....	18
1.5.6. Ubiquitin-specific-processing protease 30 (Usp30) .....	18



1.5.7. Tumor susceptibility gene 101 (Tsg101)	19
<b>2. AIM OF THE STUDY</b>	<b>20</b>
<b>3. MATERIALS AND METHODS</b>	<b>22</b>
<b>3.1. Materials</b>	<b>22</b>
3.1.1. Chemicals	22
3.1.2. Equipment	22
3.1.3. Buffer and Solutions	22
3.1.4. Growth Medium	22
3.1.5. Commercial kits used in this study	23
3.1.6. Enzymes	23
3.1.7. Antibodies	24
3.1.8. Bacterial Strains	24
3.1.9. Mammalian cell lines	24
3.1.10. Plasmids and Oligonucleotides	24
3.1.11. DNA Ladder	28
3.1.12. DNA sequencing	28
3.1.13. Software, Computer-based Programs, and Websites	28
<b>3.2. Methods</b>	<b>29</b>
3.2.1. Bacterial Cell Culture	29
3.2.1.1. Growth of bacterial culture	29
3.2.1.2. Preparation of competent bacteria	30
3.2.1.3. Transformation of Competent Bacteria	30
3.2.1.4. Plasmid DNA Isolation	31
3.2.2. Mammalian Cell Culture	31
3.2.2.1. Maintenance of Cell Lines	31
3.2.2.2. Cryopreservation of the cells	31
3.2.2.3. Thawing frozen mammalian cells	32
3.2.2.4. Transient Transfection of mammalian cells by Electroporation	32
3.2.2.5. Transfection of HEK293FT cells to produce virus with target vector	32
3.2.2.6. Determination of the amount of virus	33
3.2.2.7. Lentiviral Transduction	34
3.2.2.8. Flow Cytometer	34
3.2.2.9. Degranulation Assay for NK cells	34

3.2.2.10. Cytotoxicity of NK cells by xCELLigence RTCA .....	35
3.2.2.11. Genomic DNA Isolation .....	35
3.2.2.12. RNA Isolation and qRT-PCR .....	35
3.2.2.13. Optimization for Concentration of Ganciclovir Drug and Feeder Cells Ratio.....	36
3.2.3. Vector Constructions .....	36
3.2.3.1. General Vector Constructions Protocol.....	36
3.2.3.2. Donor DNA construction.....	37
3.2.4. CRISPR/Cas9 Genome Editing by using pLentiCRISPRv2 .....	40
3.2.4.1. sgRNA Design and off-target analysis .....	40
3.2.4.2. Phosphorylation and annealing of top and bottom oligonucleotide pairs.....	40
3.2.4.4. LentiCRISPRv2 plasmid digestion and dephosphorylation .....	41
3.2.4.5. Transformation of Cas9 plasmids .....	42
3.2.5. CRISPR/Cas9 Genome Editing by using pSpCas9(BB)-2A-GFP .....	42
3.2.5.1. pSpCas9(BB)-2A-GFP plasmid digestion and ligation .....	42
3.2.5.2. Transformation of Cas9 plasmids .....	43
3.2.6. Determination Genome Targeting Efficiency by T7 endonuclease I assay .....	43
<b>4. RESULTS .....</b>	<b>46</b>
<b>4.1. Optimization Trials of Electroporation for NK-92 cells by Neon Transfection     System .....</b>	<b>46</b>
4.1.1. Neon Optimization Using Different Electroporation Conditions.....	46
4.1.2. Neon Optimization Using Conditioned Medium .....	47
4.1.3. Neon Optimization with Increasing Doses of Plasmid DNA.....	48
4.1.4. Neon Optimization using Alternative Electroporation Pipet Tips .....	49
4.1.5. Neon Optimization by Changing Plasmid and Target Cell Identity.....	50
<b>4.2. Generation of Feeder Cell Line and Single Cell Cloning Trials .....</b>	<b>51</b>
4.2.1. Cloning of the TK gene into the LegoiG2puro vector .....	51
4.2.2. Production and Transduction of Virus into NK-92 cell line .....	52
4.2.3. Ganciclovir Titration .....	53
4.2.4. Making a Single Cell Cloning From NK-92 Cells .....	55
4.2.5. Single Cell Cloning by Using Feeder Cell Lines .....	57
4.2.6. Coculturing feeder and target cells by using different ratios and different ganciclovir concentrations.....	62

4.2.6.1. Coculture Experiment 1 .....	62
4.2.6.2. Coculture Experiment 2 .....	64
4.2.6.3. Coculture Experiment 3 .....	65
4.2.6.4. Coculture Experiment 4 .....	67
<b>4.3. Production of Mutated Pools by CRISPR/Cas9 Genome Editing Method.....</b>	<b>69</b>
4.3.1. Cloning of gRNA into pLentiCRISPR_v2 plasmid .....	70
4.3.2. Production and Transduction of Lentivirus into the NK-92 cell line .....	72
4.3.3. Analysis of Mutations by the T7 Assay and QRT-PCR.....	74
<b>4.4. Cytotoxic Tests for Mutated Pools.....</b>	<b>76</b>
4.4.1. Degranulation Assay .....	76
4.4.2. xCELLigence Real Time Cell Analysis Assay .....	77
<b>5. DISCUSSION.....</b>	<b>80</b>
<b>6. REFERENCES.....</b>	<b>84</b>
<b>7. APPENDICES.....</b>	<b>93</b>
7.1. APPENDIX A- Chemicals .....	93
7.2 APPENDIX B – Equipment .....	95
7.3. APPENDIX C- Molecular Biology Kits .....	97
7.4. APPENDIX D- Antibodies .....	97
7.5. APPENDIX E – DNA Molecular Weight Marker .....	98
7.6. APPENDIX F- Plasmid Maps .....	99

## LIST OF FIGURES

<b>Figure 1. 1. Activation of Cytotoxic T and NK Cells</b> .....	2
<b>Figure 1. 2. Activation and Immunological Synapse Formation of Cytotoxic T cells</b> ....	5
<b>Figure 1. 3. Receptors of NK Cells.</b> .....	6
<b>Figure 1. 4. Activation of NK Cells.</b> .....	8
<b>Figure 1. 5. CRISPR/Cas9 System and Double Strand Break Repair</b> .....	16
<b>Figure 4. 1. Cloning of the TK gene into the pLego-iG2Puro plasmid</b> .....	51
<b>Figure 4. 2. Experimental design of the production of the virus with TK gene and transduction into NK-92 cells.</b> .....	52
<b>Figure 4. 3. FACS Analysis of Virus Transduction Efficiency.</b> .....	53
<b>Figure 4. 4. Cell concentration under different selection conditions with increasing concentrations of ganciclovir.</b> .....	54
<b>Figure 4. 5. Percentage of GFP positive cells in the cell culture under ganciclovir treatment.</b> .....	54
<b>Figure 4. 6. Cell concentration under the different selection conditions with increasing concentrations of ganciclovir and 1µg/ml puromycin.</b> .....	55
<b>Figure 4. 7. Percentage of GFP positive cells in the cell culture under ganciclovir treatment and 0.01 µg/ml puromycin treatment.</b> .....	55
<b>Figure 4. 8. Different dilutions of NK-92 cells</b> .....	56
<b>Figure 4. 9. Schematic showing ganciclovir treatment of mixtures of the TK-GFP feeder cells and iT2 cells.</b> .....	57
<b>Figure 4. 10. Experimental setups for single cell clone by co-incubation with feeder cells.</b> .....	58
<b>Figure 4. 11. Fluorescent Imaging of a mixed origin colony.</b> .....	59
<b>Figure 4. 12. Experimental Design for D4 and F8 mixed colonies undergoing ganciclovir treatment.</b> .....	59
<b>Figure 4. 13. Confocal Z-stack Image of the F1 population</b> .....	60
<b>Figure 4. 14. Experimental Design for F1 colony ganciclovir treatment</b> .....	61
<b>Figure 4. 16. The percentage of GFP and tdTomato positive cells in Coculture Experiment 1</b> .....	64
<b>Figure 4. 17. The percentage of GFP and tdTomato positive cells in Coculture Experiment 2</b> .....	65
<b>Figure 4. 18. The percentage of GFP and tdTomato positive cells in Coculture Experiment 3</b> .....	67
<b>Figure 4. 19. The percentage of GFP and tdTomato positive cells in Coculture Experiment 4</b> .....	69
<b>Figure 4. 20. Expression pattern of candidate genes in NK-92 cells.</b> .....	70

<b>Figure 4. 21. Guide RNA design for targeting candidate genes</b> .....	71
<b>Figure 4. 22. Map of the pLentiCRISPRv2 plasmid and a representative annealed oligonucleotide inserted into the BsmBI site.</b> .....	72
<b>Figure 4. 23. Vectors for third generation virus production.</b> .....	72
<b>Figure 4. 24. Experimental design of the production of lentivirus with expressing CRISPR/Cas9 targeting different genes in NK-92 cells.</b> .....	73
<b>Figure 4. 25. T7 Assay Results.</b> .....	74
<b>Figure 4. 26. RNA Isolation Results.</b> .....	75
<b>Figure 4. 27. QRT-PCR quantification of gene expression in targeted NK-92 cells.</b> .....	75
<b>Figure 4. 28. Expression of CD107<math>\alpha</math> in the Degranulation Assay.</b> .....	77
<b>Figure 4. 29. Proliferation of MCF-7 cells in the xCELLigence RTCA machine.</b> .....	78
<b>Figure 4. 30. xCELLigence RTCA results for NK-92 WT and Mutant &amp; MCF-7 target cells</b> .....	79
<b>Figure 7. 1. Thermo Scientific GeneRuler DNA Ladders</b> .....	98
<b>Figure 7. 2. The plasmid map of pMDLg_pRRE</b> .....	99
<b>Figure 7. 3. The plasmid map of pRSV-Rev</b> .....	99
<b>Figure 7. 4. The plasmid map of pCMV-VSV-G</b> .....	100
<b>Figure 7. 5. The plasmid map of LegoiG2puro</b> .....	100
<b>Figure 7. 6. The plasmid map of LegoiT2puro.</b> .....	101
<b>Figure 7. 7. The plasmid map of pLentiCRISPRv2</b> .....	101
<b>Figure 7. 8. The plasmid map of pSpCas9(BB)-2A-GFP</b> .....	102
<b>Figure 7. 9. The plasmid map of PL253</b> .....	102
<b>Figure 7. 10. The plasmid map of LegoiG2puro_TK</b> .....	103

## LIST OF TABLES

<b>Table 3. 1. List of plasmids used in this study.</b> .....	26
<b>Table 3. 2. List of oligonucleotides used in this study.</b> .....	28
<b>Table 3. 3. List of computer-based programs, software and websites used in this study</b> .....	29
<b>Table 3. 4. Determination of the optimal LeGO-iG2-puro virus concentration</b> .....	33
<b>Table 3. 5. Determination of the optimal LeGO-iG2-puro-TK virus concentration</b> ....	33
<b>Table 4. 1. Programs for Neon Transfection</b> .....	46
<b>Table 4. 2. Programs for Neon Transfection Optimization</b> .....	46
<b>Table 4. 3. Cell Viability and Transfection Efficiency of Neon Electroporation Using Different Electroporation Conditions</b> .....	47
<b>Table 4. 4. Cell Viability and Transfection Efficiency of Neon Electroporation Using Conditioned Medium</b> .....	48
<b>Table 4. 5. Cell Viability and Transfection Efficiency of Neon Electroporation with Increasing Doses of Plasmid DNA</b> .....	49
<b>Table 4. 6. Cell Viability and Transfection Efficiency of Neon Electroporation using Alternative Electroporation Pipet Tips</b> .....	49
<b>Table 4. 7. Cell Viability and Transfection Efficiency of Neon Electroporation by Changing Plasmid and Target Cell Identity</b> .....	50
<b>Table 4. 8. GFP and tdTomato Expressing Cell Ratio</b> .....	58
<b>Table 4. 9. The percentage of GFP and tdTomato positive cells after ganciclovir treatment.</b> .....	61
<b>Table 4. 10. Experimental Design for Coculture Experiments</b> .....	62
<b>Table 4. 11. Cell Numbers and Ratios for NK92 iT2 and TK/GFP populations in Coculture Experiment 1</b> .....	63
<b>Table 4. 12. Cell Numbers and Ratios for NK92 iT2 and TK/GFP populations in Coculture Experiment 2</b> .....	64
<b>Table 4. 13. Cell Numbers and Ratios for NK92 iT2 and TK/GFP populations in Coculture Experiment 3</b> .....	66
<b>Table 4. 14. Cell Numbers and Ratios for NK92 iT2 and TK/GFP populations in Coculture Experiment 4.</b> .....	68
<b>Table 4. 15. Length of DNA fragment with targeted part.</b> .....	74

## LIST OF ABBREVIATIONS

$\alpha$	Alpha
$\beta$	Beta
$\varepsilon$	Epsilon
$\gamma$	Gamma
$\kappa$	Kappa
$\delta$	Sigma
$\zeta$	Zeta
$\mu$	Micro
ADCC	Antibody Dependent Cell-Mediated Cytotoxicity
Amp	Ampicillin
AP-1	Activator Protein-1
APCs	Antigen presenting cells
Arp2/3	Actin-Related Protein 2/3 Complex
Arpc1b	Actin Related Protein 2/3 Complex Subunit 1B
ATP	Adenosine triphosphate
Bach2	BTB Domain and CNC Homolog 2
bp	Basepair
BSA	Bovine Serum Albumin
C12orf4	Chromosome 12 Open Reading Frame 4
Cas9	CRISPR associated protein 9
Ccdc124	Coiled-Coil Domain Containing 124
CD	Cluster of Differentiation
CIAP	Calf intestinal alkaline phosphatase
CLP	common lymphoid progenitor
CMV	Cytomegalovirus
cPPT	Central Polypurine Tract
CRISPR	Clustered Regularly Interspaced Short Palindromic Repeats
crRNA	CRISPR RNA
cSMAC	Central Supramolecular Activation Complex
CTL	Cytotoxic T Lymphocyte
Ctr9	CTR9 Homolog, Paf1/RNA Polymerase II Complex Component
DAG	Diacylglycerol
DAMPs	Damage-Associated Molecular Pattern Molecules
DAP	DNAX-activating Protein
DCs	Dendritic cells
Dffb	DNA Fragmentation Factor Subunit Beta
DMEM	Dulbecco's Modified Eagle Medium
DMSO	Dimethyl sulfoxide
DNA	Deoxyribonucleic acid
dNTPs	Deoxynucleotide triphosphates
DSB	Double Strand Break
dsDNA	Double Strand DNA

dSMAC	Distal Supramolecular Activation Complex
DTT	Dithiothreitol
EAT-2	Ewing's sarcoma-associated transcript 2
E.coli	Escherichia coli
EDTA	Ethylenediaminetetraacetic acid
ER	Endoplasmid Reticulum
ERK	Extracellular Receptor-Stimulated Kinase
ERM	Ezrin-Radixin-Moesin
ERT	EAT-2-related transducer
ESCRT-I	Endosomal Sorting Complex Required for Transport I
FACS	Fluorescence Activated Cell Sorting
FasL	Fas ligand
FBS	Fetal Bovine Serum
Fc	Fragment Crystallizable
GAC	GTPase activation center
Gag	Group-specific antigen
GFP	Green Fluorescent Protein
gRNA	Guide RNA
GTPase	GTP hydrolase
HBS	HEPES-buffered Saline
HDR	Homology-Directed Repair
HEPES	4-(2-hydroxyethyl)-1-piperazineethanesulfonic acid
HLA	Human leukocyte antigen
HSV-TK	Herpes Simplex Virus Thymidine kinase
ICAM-1	Intercellular Adhesion Molecule-1
ICAM-5	Intercellular Adhesion Molecule-5
IFN- $\gamma$	Interferon- $\gamma$
Ig	Immunoglobulin
IKK	Inhibitor of $\kappa$ B Kinase
IL	Interleukin
ILT2	Immunoglobulin-Like Transcript 2
iNKIS	Inhibitory NK Cell Immunological Synapse
Iono	Ionmycin
IP <sub>3</sub>	Inositol Trisphosphate
IRES	Internal Ribosomal Entry Site
IS	Immunological Synapse
ITAM	Immunoreceptor Tyrosine-Based Activation Motifs
ITIMs	Immunoreceptor Tyrosine-Based Inhibitory Motifs
JAK	Janus kinase
JEV	Japanese Encephalitis Virus
JNK	c-JUN terminal kinase
kb	Kilobase
KIR	Killer immunoglobulin like receptor
KK3	Kaposi's Sarcoma-Associated Herpes Virus Gene Product K3
LAT	Linker for Activation of T Cells
LB	Luria Broth
LeGO	Lentiviral Gene Ontology vectors



LFA-1	Lymphocyte function-associated antigen 1
LGLs	Large Granular Lymphocytes
(li)	Invariant Chain
Lso2	Late-Annotated Short Open Reading Frame 2
LTR	Long Terminal Repeat
Lys	Lysine
Mac-1	Macrophage-1 antigen
MAP	Mitogen-Activated Protein
MBV	Multivesicular Body
MCs	Microclusters
MDM2	Murine double minute 2
MHCI	Major Histocompatibility Complex class 1
MHCII	Major Histocompatibility Complex class 2
MIP	Macrophage Inflammatory Protein
MOI	Multiplicity of Infection
mRNA	Messenger ribonucleic acid
MTOC	Microtubule Organizing Center
Munc13-4	Unc-13 homolog D
Munc18	mammalian uncoordinated 18
NEAA	Non-essential Amino Acid
NFκB	Nuclear Factor kappa B
NFAT	Nuclear factor of activated T cells
NHEJ	Nonhomologous End Joining
NK	Natural Killer
NKP	NK cell precursors
NPFs	Nucleation-Promoting Factors
NS3	Non-Structural Protein 3
Oaf	Out At First Homolog
PAM	Protospacer Adjacent Motif
PAMPs	Pathogen Associated Molecular Patterns
PBS	Phosphate-buffered saline
PCR	Polymerase Chain Reaction
PI	Propidium Iodide
PI3K	Phosphoinositide 3-kinase
PIPES	Piperazine-N,N'-bis (2-ethanesulfonic acid)
PKC	Protein Kinase C
PLC-γ	Phospholipase C-γ
PMA	Phorbol 12-myristate 13-acetate
pMHC	Peptide-Major Histocompatibility Complex
Pol	Polymerase
PRRs	Pattern recognition receptors
pSMAC	Peripheral Supramolecular Activation Complex
PTK	Protein Tyrosine Kinase
Puro	Puromycin
qRT-PCR	quantitative Reverse-Transcription PCR
Rab-27A	Ras-Related Protein Rab-27A
RANTES	Regulated on Activation Normal T cell Expressed and Secreted

RasGRP	Ras guanyl nucleotide-releasing protein
Rev	Regulator of virion gene expression
RNA	Ribonucleic acid
Rpm	Revolution per minute
RPMI	Roswell Park Memorial Institute
RRE	Rev Response Element
RT	Reverse-Transcriptase
RT	Room Temperature
RTCA	Real time cell analysis
SAP	SLAM associated protein
SDS	Sodium Dodecyl Sulfate
Ser	Serine
SFFV	Spleen Focus Forming Virus
SHP1 or 2	Src Homology 2 Domain Containing Phosphatases-1 or -2
SIN	Self-inactivating
siRNA	small interfering RNA
SLAM	The signaling lymphocytic activation molecule
SLP	Src homology 2 domain-containing leukocyte phosphoprotein.
SNARE	N-ethylmaleimide- Sensitive Protein Attachment Protein Receptor
ssODNs	single-stranded DNA Oligonucleotides
STAT	Signal Transducer and Activator of Transcription
T7E1	T7 endonuclease I
TAP	Transporter Associated with Antigen Presentation
TBE	Tris-Borate-EDTA
TBK1	TANK Binding Kinase-1
TCR	T cell receptor
tdTomato	Tandem dimer Tomato
TERRA	Telomere Repeat Containing RNA
Th	T helper
TNF- $\alpha$	Tumor Necrosis Factor
TOM20	Translocase of Outer Membrane of Mitochondria
tracrRNA	Trans-Activating crRNA
TRAIL	TNF-Related Apoptosis-Inducing Ligand
Tsg101	Tumor Susceptibility Gene 101
Ub	Ubiquitin
Usp30	Ubiquitin-specific-processing protease 30
VAMP7	Vesicle-Associated Membrane Protein 7
WASp	Wiskott-Aldrich Syndrome Protein
WAVE2	WASp Family Verprolin-homologous Protein-2
wPRE	Woodchuck hepatitis virus post-transcriptional regulatory element
WT	Wild Type
ZAP70	Zeta-chain-associated protein kinase 70

# 1. INTRODUCTION

## 1.1.The Immune System

There are many pathogenic organisms which threaten the health of the body and cause diseases. The mammalian immune system recognizes intrinsic and extrinsic threats and protects the body against diseases. The initial immune response results in the recognition of the presence of an infection. Then, specialized immune cells use their effector functions to eliminate foreign organisms which cause this infection. The immune system is divided into two main arms which are the innate and adaptive immune system.

### 1.1.1. Innate Immune System

The innate immune system provides physical and chemical barriers against viruses, bacteria, parasites and other foreign substances. Macrophages, mast cells, granulocytes, natural killer (NK) cells and dendritic cells (DCs) are the fundamental members of the innate immune system. Pattern recognition receptors (PRRs), which are inherited through the germline, are expressed on the surface of these innate immune cells. PRRs are responsible for the recognition of a broad range of pathogens (non-self) and damaged self-tissues. After this recognition, a rapid immune response is generated against the pathogens to protect host cells and organs [1]. The pathogen derived molecules which are recognized by PRRs are named Pathogen Associated Molecular Patterns (PAMPs) and Damage-Associated Molecular Pattern Molecules (DAMPs). The PAMPs are composed of exogenous molecules such as viral nucleic acids, cell wall components of bacteria and fungi [2]. On the other hand, DAMPs originated from endogenous molecules such as cytosolic and nuclear 'altered self' proteins [3]. Recognition of PAMPs and DAMPs by PRRs results in inflammatory responses. The first inflammatory response is the synthesis of cytokines and chemokines at the site of infection. Phagocytic cells of the innate immune system reach the site of infection by following the concentration gradient of these cytokines and chemokines. Apart from these, the adaptive immune system is also activated when PRRs expressed on the antigen presenting cells (APCs) detect the pathogens [4].

The innate immune system has no antigen specificity. The receptors involved in this response are encoded in the germline in a non-clonally fashion by many cell types. Therefore, the

innate immune system has limited diversity. Yet this primary rapid response is crucial to initiate and develop the adaptive immune response [5].

### 1.1.2. Adaptive Immune System

The adaptive immune system protects host cells from pathogens. T cells and B cells are the members of the adaptive immune system. Receptors of T and B cells are produced by gene rearrangements, so they are very specific to antigens and their response are slower than the innate immune system. B cells are produced in the bone marrow and they migrate through the lymphatic system into secondary lymphoid organs such as spleen and lymph nodes where they encounter antigen and differentiate into plasma cells. This provides them to give a quicker and more effective response against exposure of the same antigens. T cells precursors are also produced in the bone marrow. However, they move to the thymus where their final development takes place. Their receptors undergo gene rearrangement, get expressed on the thymocyte cell surface and gets selected by positive or negative selection to become mature T lymphocytes. Thus, in the thymus, thymocytes differentiate into either  $CD4^+$  T helper or  $CD8^+$  T cytotoxic lymphocytes. The recognition of antigens by T cell receptors is Major Histocompatibility Complex (MHC) restricted. Antigens are presented on MHC class I molecules to  $CD8^+$  T cells and on MHC class II to  $CD4^+$  T cells [6].

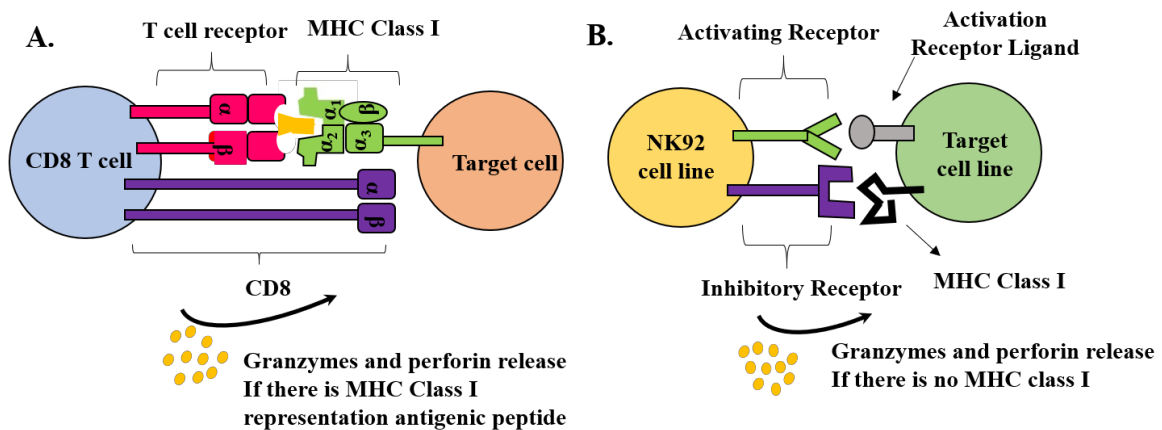


Figure 1. 1. Activation of Cytotoxic T and NK Cells

## 1.2. Activation of Cytotoxic Lymphocytes of Immune Cells

### 1.2.1. Activation of T cells

T cells are divided into two groups according to coreceptors which they express: CD4<sup>+</sup> helper T cells and CD8<sup>+</sup> cytotoxic T cells. Both CD4<sup>+</sup> and CD8<sup>+</sup> T cells have T cell receptor (TCR) on their surface. As mentioned before, CD4<sup>+</sup> T cells recognize antigens which are presented by MHC class II whereas CD8<sup>+</sup> T cells recognize antigens which are presented by MHC class I. All nucleated cells express MHC class I molecules on their surface which present peptides from intracellular sources. The presentation of peptides on MHC class I molecules follows specific steps (REF). Self-origin or viral proteins expressed by self cells are degraded by nuclear or cytosolic proteasomes. These cytosolic peptides are transported by TAP (transporter associated with antigen presentation) into the Endoplasmic Reticulum (ER) where they bind to the peptide binding groove of MHC class I. Chaperone proteins stabilize MHC-I in the ER in the absence of peptide, and binding of peptide leads to the release of chaperone proteins and the formation of a stable MHC-I:peptide complex which can move to the surface of the cell [7]. On the other hand, the presentation of peptides on the MHC class II molecule follows the following steps. Professional APCs such as DCs, B cells and macrophages express MHC class II molecules on their surface. Extracellular peptides, which are degraded in the endocytic pathway, are bound to MHC class II in a specialized endocytic multi-vesicular body called the MIIC. The MIIC compartment receives both extracellular derived peptides and the MHC II molecules with an invariant peptide called the CLIP peptide. The CLIP peptide is derived from an invariant chain (Ii) protein that associates with the MHC II in the ER. Ii bound MHC class II molecules are stable, and can be transported through the Golgi complex, into the MIIC compartment where Ii is digested by proteases because of low pH. Interaction of the Ii bound MHC II with another invariant protein called the HLA-DM results in the exchange of CLIP peptide with antigenic peptides, after which the MHC class II:peptide complex goes to cell surface [8].

TCRs have a heterodimer structure which consists of two subunits; TCR  $\alpha$  and TCR  $\beta$ . The cytoplasmic tail of TCR  $\alpha\beta$  is not long and not sufficient for signaling. Its variable transmembrane part recognizes antigens presented by MHC class I or II by the help of CD4 and CD8 coreceptors [9].  $\alpha\beta$  TCR associates with CD3 molecules CD3 $\gamma$ ,  $\epsilon$ ,  $\zeta$  and  $\delta$ . Immunoreceptor tyrosine-based activation motifs (ITAMs), which provide a specific

sequence for tyrosine phosphorylation, are on the cytoplasmic tail of CD3 molecules. CD3 molecules mediate all proximal signaling events [10]. Antigen binding to  $\alpha\beta$  TCR causes a conformational change on the cytoplasmic tail of the CD3 complex. Thus, ITAMs on the cytoplasmic tails of CD3 molecules can be phosphorylated by the protein tyrosine kinase (PTK) (Lck), which associates with CD4 and CD8 co-receptors [11]. Phosphorylated ITAMs provide a docking stage for signaling proteins with tandem SH2 domains. ZAP70, which is also a PTK, is recruited to phosphorylated ITAMs and is phosphorylated by Lck. Intracellular signaling molecules like LAT and SLP-76 are phosphorylated by activated ZAP70. The Gads:SLP-76:LAT complex is formed by Gads, and Phospholipase C- $\gamma$  (PLC- $\gamma$ ) [12,13]. Activated PLC- $\gamma$  cleaves phosphatidylinositol bisphosphate (PIP<sub>2</sub>) into diacylglycerol (DAG) and inositol trisphosphate (IP<sub>3</sub>) that are two important signaling molecules. IP<sub>3</sub> diffuses into the cytosol and binds to calcium channels on the ER membrane. Ca<sup>2+</sup> is released from the ER into the cytosol where it binds to Calmodulin [14,15]. Calcineurin is activated by the Ca<sup>2+</sup>: calmodulin complex, and activated calcineurin dephosphorylates the NFAT transcription factor. Thus, NFAT can enter nucleus and activate the transcription of genes that have a role in cell proliferation and differentiation. DAG stays in the membrane and recruits protein kinase C  $\theta$  (PKC  $\theta$ ) and RasGRP. Recruitment of PKC  $\theta$  leads to the activation of CARMA, which activates the NF $\kappa$ B transcription factor. AP-1 transcription factor is also activated through activation of MAP kinase cascade which is activated by Ras [15](Figure 1. 2). As a result of the activation of the NFAT, NF $\kappa$ B and AP1 transcription factor pathways, the metabolism, proliferation and microtubule networks of CTLs are activated. These changes results in the programming of the CD8<sup>+</sup> T lymphocyte for directed cytotoxicity.

CTLs have two main mechanisms to kill target cells. First, MHC class I presents intracellular ligands to the TCR receptor, and by the help of CD8 receptor, T cells are activated. TCR signaling and further signaling cascades are activated by phosphorylation of tyrosine residues on ITAM. Then, immunological synapse (IS) is formed (Figure 1. 2), and cytoplasmic granules fuse to the plasma membrane of the CTL near the IS, releasing their cytotoxic contents toward the target cells [16]. These cytotoxic molecules activate the intrinsic apoptotic pathways in the target cells. The second mechanism depends on the expression of FasL (Fas ligand) on the CTLs after recognition of MHC class I. FasL binds to Fas death

receptors on the target cells and activates the extrinsic apoptotic pathways in the target cells [17].

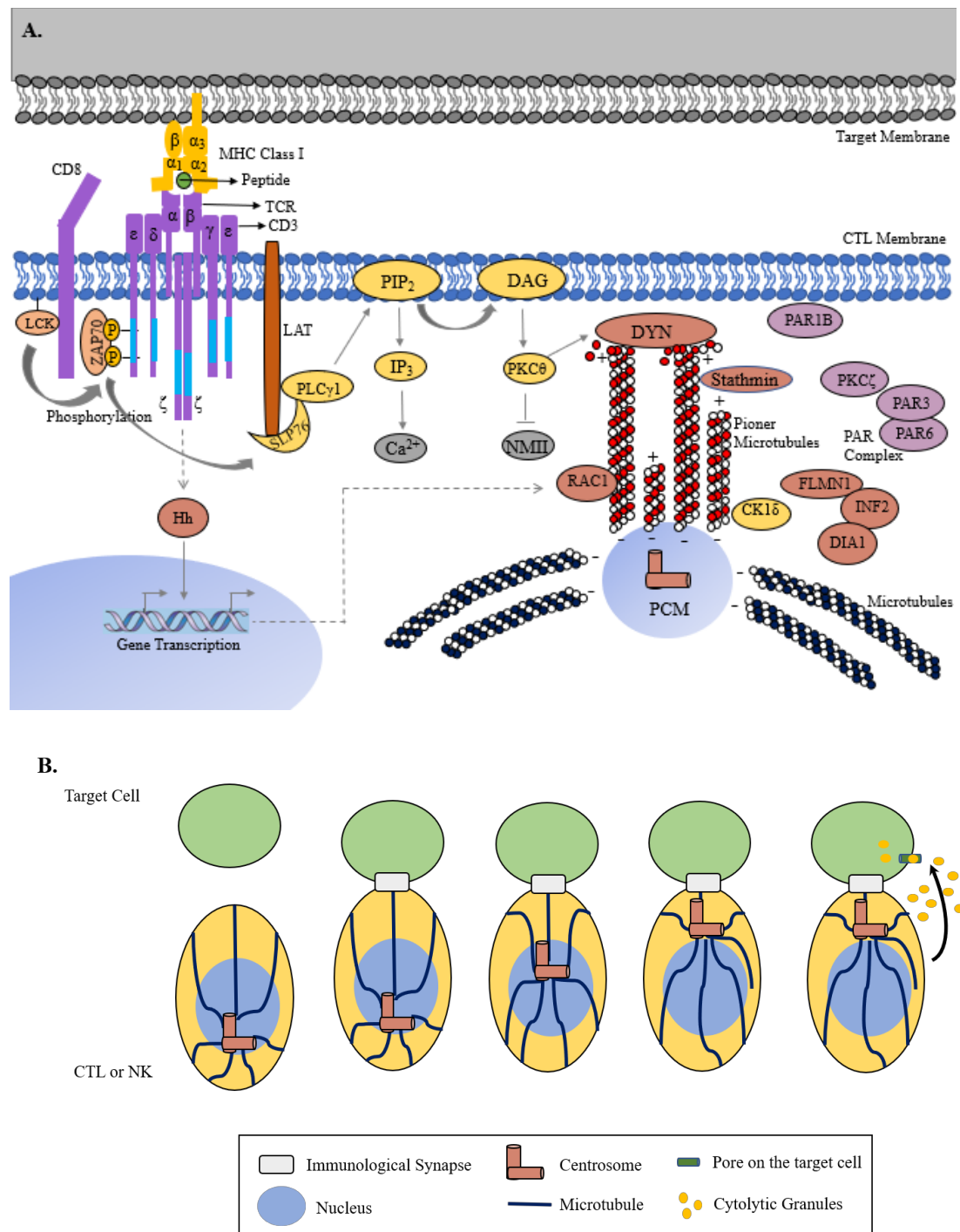


**Figure 1. 2. Activation and Immunological Synapse Formation of Cytotoxic T cells. A.** Activation of CTLs and further signaling cascades are shown. **B.** Centrosome moves toward the IS by help of microtubules. The activated lymphocyte or NK cell centrosome generates

a microtubule organizing center (MTOC) that orchestrates the orientation of cytoplasmic microtubules on which cytotoxic organelles travel and are directed towards the target cell.

### 1.2.2. Activation of NK cells

NK cells are members of the innate immune system and they are the first line of protection of the body against intracellular pathogens. 5–10% of peripheral blood lymphocytes are NK cells. This proportion can change with age [18]. NK cells are originated from the common lymphoid progenitor (CLP). Transcription factors such as Eomes and Tbx21 convert them into NK cell precursors (NKP) which do not have surface markers. Then, they become mature NK cells which express NKp46<sup>+</sup>, NK 1.1<sup>+</sup>, CD56<sup>+</sup>, NKp30<sup>+</sup> [19,20]. NK cell receptors, which are expressed by germline encoded genes which do not undergo recombination like the genes encoding T cell receptors, are divided into two main categories. These are the activating and inhibitory NK receptors. NK cells are educated to prevent killing of self-cells during their development and this is called priming [21]. Inhibitory receptors recognize MHC class I on self-cells and cytotoxicity of these targets is prevented [22].

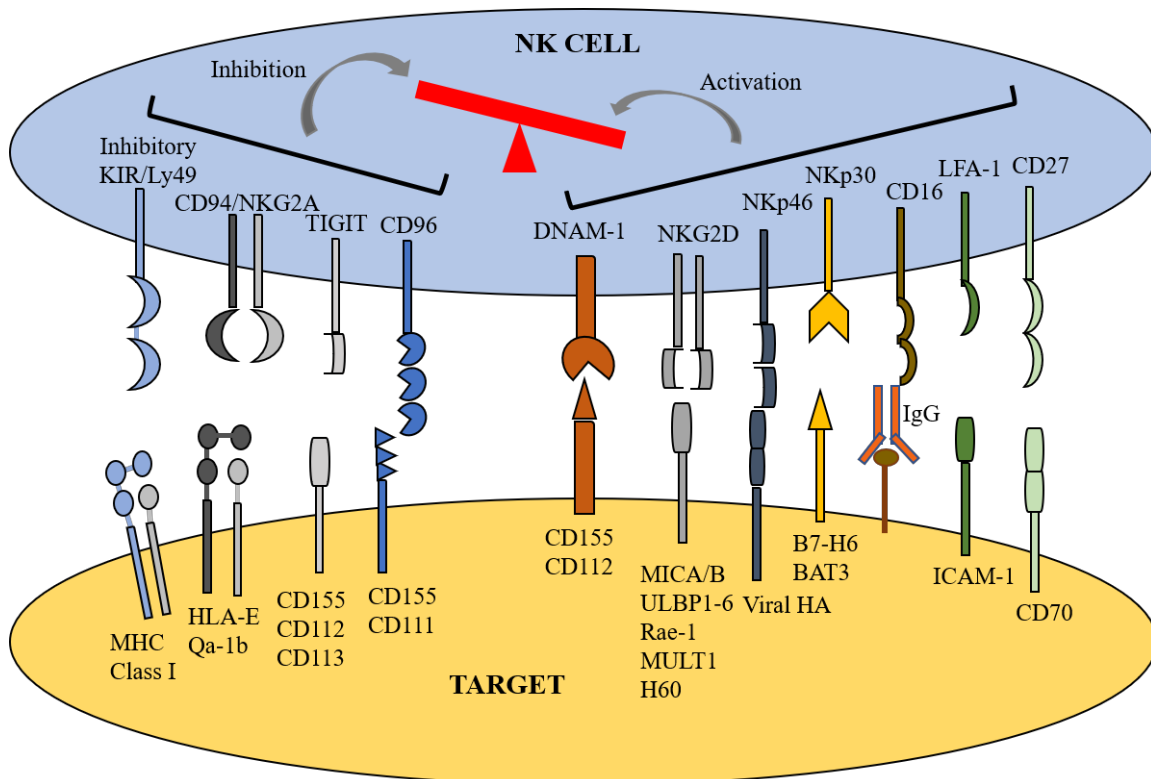


**Figure 1. 3. Receptors of NK Cells.** Activating and inhibitory receptors, and their ligands on target cells are shown. Activation of NK cells is not controlled by the triggering of a single



receptor like in the case of the TCR. Rather, NK cells can be activated by the balance between the signals received by the ITAM containing activating receptors and the ITIM containing inhibitory receptors. Thus, the balance between the expression of activating and inhibitory ligands on the target cells is what determines the triggering of cytotoxicity.

NK cells use three different mechanisms for immune defense. First one is the perforin-independent and NK cells are activated by cytokine secretion like interferon (IFN)- $\gamma$  and tumor necrosis factor (TNF)- $\alpha$  [23]. The second one is also perforin-independent, and it depends on FasL and TNF-related apoptosis-inducing ligand (TRAIL) expression [24]. The third one is related to balance between activating and inhibitory receptors. Activation of NK cells leads to movement towards target cells and to the exocytosis of cytolytic granules which contain perforin and granzyme B. NK cells can also be regulated by DCs and macrophages [23,25].

Perforin-dependent NK cell cytotoxicity is regulated by balance between activating and inhibitory receptors (Figure 1. 3). Cytoplasmic tails of inhibitory receptors have immunoreceptor tyrosine-based inhibitory motifs (ITIMs) whose tyrosine residue is phosphorylated, and Src homology 2 domain containing phosphatases (SHP1 or 2) are recruited. This leads to dephosphorylation and phosphorylation of intracellular components [26]. ITAMs are found in the adaptor molecules and cytoplasmic tail of activating receptor. Those are also phosphorylated and lead to the recruitment of Src homology 2 domain containing kinases (Syk or ZAP70) and further signal cascades. Finally, cytokines and chemokines are secreted by NK cells, and cytolytic granules are released to target cells [27]. Activating receptor NKG2D uses different signaling mechanism by DAP10 and DAP12. NKG2D is homodimer and recruits DAP10 and DAP12. NKG2D activation via DAP10 (Figure 1. 4) leads to cytotoxicity and via DAP12 causes cytokine secretion and cytotoxicity [28]. CD244 (2B4) receptor has both activating and inhibitory function. There is an immunoreceptor tyrosine-based switch motif in the cytoplasmic tail of 2B4 receptor. Adaptor proteins SAP and ERT with Src homolog 2 domain can be recruited onto immunoreceptor tyrosine-based switch motif. SAP recruitment results in activation and ERT recruitment results in inhibition of NK cell function [29]. Furthermore, there is a different category for activating receptors of NK cells which are signaled by integrins. For example, LFA-1

provides natural cytotoxicity by binding to intercellular adhesion molecule-1 (ICAM-1) through ICAM-5 [30].

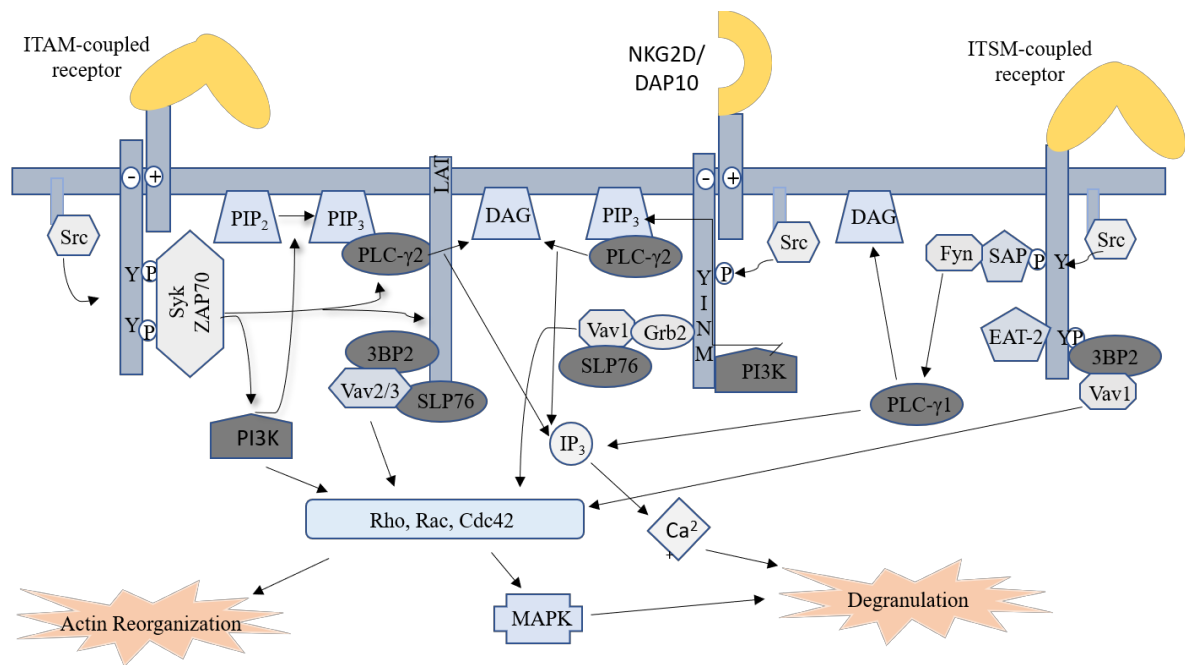


**Figure 1. 4. Activation of NK Cells.** Activation of NK cells and further signaling cascades are shown.

### 1.2.3. NK-92 cell lines

NK-92 is an interleukin-2 (IL-2) dependent and high cytotoxic NK cell line. It was established from the peripheral blood of a 50-year-old male who was diagnosed with non-Hodgkin's lymphoma. Being large granular lymphocytes (LGLs) is one of the morphological features of the NK-92 cell line. They show anti-tumor activity against a wide range of malignancies such as malignant melanoma, leukemia, viral infected cells, lymphoma, prostate cancer, breast cancer and squamous cell carcinoma [31,32]. NK-92 cell lines are stimulated by IL-2 for cytotoxicity and proliferation. Besides IL-2 stimulation, IL-7 stimulation is an alternative way for short term proliferation of the NK-92 cell line [33]. In addition to these, IL-18 and IL-12 stimulation leads to an increase in cytotoxicity and widens the range of target cells [34].

Phenotype of NK-92 cell line is different from NK cells. They express high levels of CD56 and CD7. CD2 and CD122 are expressed at an intermediate level, and CD25 is expressed at

a low level. NK-92 cells do not express surface CD3, CD4, CD8 and CD16 [35,36]. Because they are CD16 negative, NK-92 cell lines are crucial for the study of direct cell-mediated cytotoxicity and therapeutic approaches without antibody-dependent cell-mediated cytotoxicity (ADCC). This is an advantage because primary NK cells can kill their target by ADCC using the CD16 receptor which recognizes antigen bound antibodies by the Fc region of IgG [37]. In the absence of this form of triggering, NK-92 cells can be triggered by target cell-mediated means.

Receptor expression of the NK-92 cell line is different from NK cells. They express a few inhibitory receptors, which are NKGA/B, and low levels of KIR2DL4 and ILT- 2. The p58 complex of KIR receptors are absent in NK-92 cell lines so their cytotoxicity against tumor cells are very high. Exogenous expression of the p58 complex in NK-92 cells prevents their cytotoxicity toward targets [38]. In contrast to inhibitory receptors, NK-92 cells express a large number of activating receptors such as NKG2D-E, NKp30, NKp46, 2B4, CD28 activating receptors, but not NKG2C, NKp44 [33,35]. NK-92 cell lines use alternative mechanisms to kill their targets. They can release cytolytic granules containing perforin and granzyme, and cytotoxic effector molecules such as tumor necrosis factor (TNF)-super family members FasL, TRAIL, TWEAK, TNF- $\alpha$  [35]. Moreover, NK-92 cell lines express regulators of immune effector cells such as CD80, CD86, CD40L and TRANCE. Expression of CD40L is induced by IL-2 stimulation [39] and it is not expressed in NK cells [40].

Higher cytotoxicity of NK-92 according to other NK cell lines makes them crucial for treatment approaches. Genetic modifications on the cytotoxic genes can be performed to make them more cytotoxic or more specific to their target. Therefore, plasmid delivery into NK-92 cell lines and obtaining single cell cloned NK-92 cell should be improved. To prevent immunological response of NK-92 cells to vector delivery, BX795, which is an inhibitor of the TBK1/IKK $\epsilon$ , kinases was used in this study for transducing these cells with third generation lentivirus [41]. Moreover, the Herpes Simplex Virus Thymidine kinase (HSV-TK) suicide gene [42] was used to create a feeder cell line and to obtain single cell cloned NK-92 in this thesis.

## 1.3 Function and Cytotoxicity of Lymphocytes

### 1.3.1. T cells

#### 1.3.1.1. Function of Helper T cells

Interaction between MHC class II and CD4 TCR causes the movement of microtubule organizing center (MTOC) and polarization towards APC. The microtubules which are originated from MTOC grow toward to IS (Figure 1. 2). Many cytoskeletal proteins have certain roles in this organization [43].

When CD4<sup>+</sup> T cells interact with APCs, receptors and adaptor proteins are recruited to the contact site which is specifically called the immunological synapse which has 3 regions. The central supramolecular activation complex (cSMAC), which is located in the center, consists of TCRs and recruited proteins [44]. The peripheral supramolecular activation complex (pSMAC), which is in the middle, contains adhesion proteins like LFA-1 and associated talin. The distal supramolecular activation complex (dSMAC), which is the third layer, is composed of actin and actin-interacting protein, phosphatases like CD45. The IS between CD4<sup>+</sup> T cells and APC are stable and intact for longer time to allow a proper cytokine secretion [45]. Actin flow and microtubule movement driven by dynein motors have a function in the formation of cSMAC. Actin filament formation is controlled by nucleation-promoting factors (NPFs) such as Wiskott-Aldrich syndrome protein (WASp) and WAVE2 which work with Arp2/3 Complex. In addition, cofilin promotes depolymerization and generates fresh barbed ends by dividing actin filaments [46]. T cell integrins, particularly LFA-1, undergo a conformational change after TCR activation, and can bind tightly to the ICAM-1 on the APC [47]. This process is regulated by the interaction between actin-binding proteins and integrin [48]. This interaction between T cell and APC helps to recruitment and activation of actin polymerizing proteins. Eventually, activated T cells secrete cytokines and chemokines [49].

#### 1.3.1.2. Function of Cytotoxic T cells

Interaction between MHC class I and CD8 plus TCR results in the movement of the MTOC and secretory organelles towards the target cells in the cytoplasm of the lymphocytes. Then, the immunological synapse is formed (Figure 1. 2). Actin rearrangement, formation of the

cSMAC, MTOC reorientation, polarization of centrosome mechanisms are similar to CD4<sup>+</sup> T cells [50]. However, there are separate secretory domains in the central area of the CTL synapse instead of the secretory cleft in CD4<sup>+</sup> T cells. The IS of CD8<sup>+</sup> T cells are dynamic and transient. Activation of CD8<sup>+</sup> T cells results in the production of lytic granules which consist of perforin and granzyme. Perforin has a calcium-dependent C2 domain that is a lipid-recognition motif. This domain helps perforin to insert itself into target membrane and then perforin is able to form a pore on the surface of target membrane. Perforin is produced in an inactive form to prevent damage to the CTL. Granzyme is also produced in an inactive form. It enters target cell through the pores created by perforin and cleaves and activates initiator caspases. These cytotoxic effectors result in the cell to undergo apoptosis [51]. Thanks to the MTOC, the cytotoxic cell is polarized and lytic granules can reach IS [52]. Here, they are secreted towards the target cells in the form of small packets. This provides a small area which is quite crucial to ensure that the concentration of lytic granules is high and to prevent leakage into the CTL. Lytic granules are not permeable to the granule membrane. This is a critical point to protect the CTL from the harmful effect of lytic granules [15,53].

Before the target cell dies, centrosomes separated from plasma membrane. This separation is controlled by the rearrangement of the microtubule network. Granules that do not contact with the plasma membrane, MTOC and membrane receptors are recycled back into the CTL. This recycling is performed by minus-end-directed transport and MTOC localization [54].

### **1.3.2. NK cell**

Upon the interact between NK cells and their target, two different immunological synapses can be formed. The balance between inhibitory and activating receptors controls activation of NK cells. Individual engagement of activating receptors is not sufficient for activation of NK cells. Also, there should be a correct combination between activating receptors. However, engagement of specific activating receptor which is Fc receptor CD16 is enough for activation of NK cells [55].

Mature NK cells can be categorized into two subtypes which are CD56<sup>bright</sup> and CD56<sup>dim</sup>. Their functions are different from each other. CD56<sup>bright</sup> NK cells highly express NKG2a/CD94 inhibitory receptor complex and produce the highest amount of cytokines. In

contrast, CD56<sup>dim</sup> NK cells express killer cell Ig-like receptors (KIRs) and are more positive for CD16. Also, their function is generally related to cytotoxicity [56].

#### **1.3.2.1. Activating the NK Cell Immunological Synapse**

LFA-1 and Mac-1 which are adhesion molecules move to the peripheral supramolecular activation cluster (pSMAC) and provide tight conjugation between the NK and target cell [57]. Divalent cations are necessary for the function of LFA-1. Binding of Mg<sup>2+</sup> or Mn<sup>2+</sup> makes the affinity of LFA-1 higher whereas binding of Ca<sup>2+</sup> makes it lower [58]. Receptor re-localization in the membrane is regulated by the conformational change of LFA-1. Accumulation of receptors helps LFA-1 bind to ICAM. This binding mediates signaling which is important for both tight adhesion to target cells and lytic granules polarization to the target cells [55]. In addition to LFA-1, actin nucleators Arp2/3 and hDia1 control cell adhesion and actin assembly at the immunological synapse [59]. Accumulation of filamentous (F)-actin at the pSMAC contributes to formation of tight junction and it is controlled by LFA-1, talin, ezrin-radixin-moesin (ERM) proteins and WASp [60,61]. Without actin polymerization and accumulation in the pSMAC, actin cytoskeleton is disrupted, and activity and cytotoxicity of NK cells are impaired. In the meantime, activating receptors accumulate in the cSMAC. Activation of PI3K–ERK2 and PLC $\gamma$ –JNK pathways polarize the MTOC into the IS. Microtubules which are released from the MTOC [62] and dynein as a minus-ended microtubule motor take a role in the accumulation of lytic granules into the cSMAC of the IS. For the secretion of granules, firstly vesicles tether to membrane by small GTPase rab27a and Munc13-4. The tethering step helps vesicles come closer to the membrane. Then, N-ethylmaleimide-sensitive protein attachment protein receptor (SNARE) proteins such as vesicle-associated membrane protein 7 (VAMP7), syntaxin-11 and Munc18-2 help fusion of lytic granules to the membrane [63]. Perforin opens a pore on the plasma membrane of the target cell and granzyme B enters through that pore. Granzyme B cleaves caspases and cell undergoes apoptosis. At the same time, chemokines (MIP-1 $\alpha$ , MIP-1 $\beta$  and RANTES), and cytokines (TNF- $\alpha$  and IFN- $\gamma$ ) are secreted by the effector cell [64]. TNF- $\alpha$  initiates proinflammatory cytokine cascade, and IFN- $\gamma$  promotes differentiation of T-helper 1 cell and enhances the expression of MHC class I [65].

### **1.3.2.2. Inhibitory NK Cell Immunological Synapse(iNKIS)**

NK cells recognize MHC class I on the healthy cells by inhibitory receptors (KIR and NKG2A). Dimerization and multimerization of KIR receptors depend on divalent cations such as  $Zn^{2+}$  and  $Co^{2+}$  [66]. Inhibitory receptors accumulate in the center of the iNKIS while LFA-1 moves away from these NK cell receptors to the periphery of the synapse. The dynamic structure of the IS depends on the expression of inhibitory receptors on the NK cell and MHC class I on the target cell. KIR or NKG2A binding to MHC class I leads to the phosphorylation and recruitment of SHP-1 and SHP-2. These protein tyrosine phosphatases prevent the phosphorylation of activating receptors, cytoskeletal rearrangement, and integrin mediated adhesion which are important in the formation of the activating immunological synapse [67,68].

### **1.3.3. Comparison of T and NK cell cytotoxicity**

NK cells and T cells kill their target by releasing of lysosomal vesicles. Although their mechanisms are similar at some points, they are quite different from each other. Interaction of NK cells with their targets are dynamic, indefinite and temporary because NK cells have active LFA-1. However, CTLs rapidly set up cytoskeletal polarity so CTLs interactions with their target are more stable [59,69]. Rab27a, MuNC13-4 and Syntaxin 11 play a role in the exocytosis of granules in both NK and CTL cells. Deficiency or knockout of these proteins result in the impaired exocytosis of cytotoxic granules even though granule polarization proceeds as normal [70]. Integrin is vital for granule polarization in NK cells whereas it might not be crucial for T cell granule polarization. In T cells, the strength of signal is important. Strong signals provide movement of lytic granules to the IS. In contrast, in NK cells, mechanism of lytic granule delivery to pSMAC is not very clear. Clearance of F-actin from IS of both NK and T cells allows granules to pass through the membrane [71]. WASp and its homolog WAVE2, which are expressed by both NK and T cells, regulate F-actin polymerization. However, only WAVE2 might be important in the CTL and only WASp might be dominant in NK cells. Furthermore, the MTOC docks in the plasma membrane at IS of T cells, however, it is not observed at IS of NK cells [72].

Examples for similarities and differences for mechanisms of NK and T cells cytotoxicity can be expanded. There are many mysteries which must be solved. The Infection and Immunity Immunophenotyping (3i) project (<http://www.immunophenotype.org>) conducts research on

the function of immunological genes. This project randomly knocked out murine genes important for CTL mediated cytotoxicity. This study identified Arpc1b (Actin Related Protein 2/3 Complex Subunit 1B), C12orf4 (Chromosome 12 Open Reading Frame 4), Ctr9 (CTR9 Homolog, Paf1/RNA Polymerase II Complex Component), Dffb (DNA Fragmentation Factor Subunit Beta), Usp30 (Ubiquitin-specific-processing protease 30), Oaf (Out At First Homolog), Bach2 (BTB Domain And CNC Homolog 2). We checked the expression of these genes in the NK-92 cell line from our RNA-seq results. We found that Arpc1b, C12orf4, Ctr9, Dffb, Usp30 are expressed by NK-92 cell line. We aimed to identify the role of these genes in the cytotoxicity of NK-92 cells. In addition to these genes, two other genes were also targeted: Ccdc124 (Coiled-Coil Domain Containing 124) and Tsg101 (Tumor susceptibility gene 101). Ccdc124 is found in the centrosome which forms the MTOC [73]. Tsg101 is a member of the endosomal sorting complex required for transport (ESCRT)-I. Mutation of Tsg101 in T cells disrupt the translocation of the TCR to the plasma membrane and causes a reduction in microvesicle production [74].

#### **1.4. Genetic Modification of the NK-92 Cell Line by Clustered Regularly Interspaced Short Palindromic Repeats (CRISPR)**

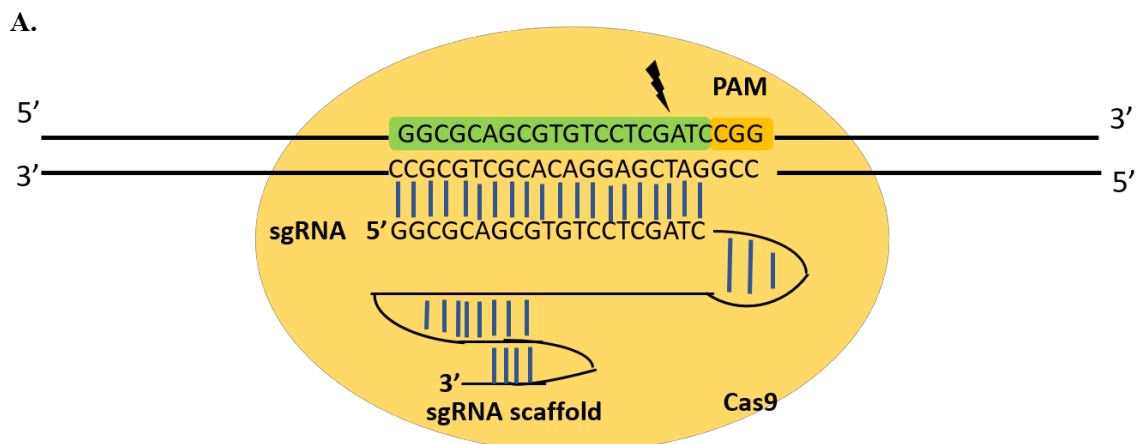
Clustered Regularly Interspaced Short Palindromic Repeats/Cas9 is a method for manipulation of genes. CRISPR/Cas9 system is a part of microbial adaptive immune systems. This enzyme RNA-guided nuclease cleaves foreign genetic elements. There are three types of CRISPR systems, and simplest one is the Type II CRISPR system. Type II CRISPR/Cas9 originated from *Streptococcus pyogenes*. It comprises of a CRISPR RNA (crRNA) array which encodes guide RNAs, Cas9 nuclease and auxiliary trans-activating crRNA (tracrRNA) which promotes processing of crRNA array into different units. For this nuclease to function an NGG protospacer adjacent motif (PAM) has to come downstream of the target DNA sequence. The crRNA consists of 20 nucleotides and must be complementary to the target DNA [75,76].

The Cas9 enzyme recognizes the PAM sequence and cuts the target DNA 3 bp upstream of the PAM sequence. Cas9 enzyme makes a double-stranded break which can be repaired by two different DNA repair mechanisms ( Figure 1. 5). The more common form of repair is



nonhomologous end joining (NHEJ) which is an error-prone mechanism. Cells use NHEJ in the absence of donor DNA. It re-ligates DSBs by random insertion/deletion (INDEL) mutations which can result in premature stop codon formation due to the frameshift mutations. The second method is homology-directed repair (HDR) where homologous donor DNA in the form of long dsDNA or shorter single-stranded DNA oligonucleotides (ssODNs) are used to repair the double stranded break. Donor DNAs must have homology arms which must be identical to the break spanning regions on the target [75,77].

There are some limitations for the CRISPR/Cas9 genome engineering method. The most important limitation is the off-target mutagenesis activity. The 20 nucleotide long gRNA is not exactly specific for only one target sequence in the genome. gRNAs can bind to partially mismatched DNA sequences and guide the Cas9 enzyme to create double strand breaks in these off-target sequences. To prevent this, there are bioinformatic tools that can be used for identification of best gRNAs with minimal off target specificity [78]. The second limitation is the dependence on the PAM sequence. For efficient cleavage there has to be a PAM sequence downstream of the target sequence. This decreases the frequency of targetable sites on the genome. The third limitation is dependent on the gRNA sequence which affects the CRISPR/Cas9 genome editing efficiency. Experiments have shown that different gRNAs targeting sequences in close proximity results in very different efficiencies. Because there is no bioinformatic tool that can measure these variables, optimization of gRNAs can only be determined by experiments [79]. With these limitations, CRISPR/Cas9 genome editing has become the most popular tool for creating knock-out and, knock-in cell lines. It can also be used for transcription regulation, gene therapy and genome-wide screens.



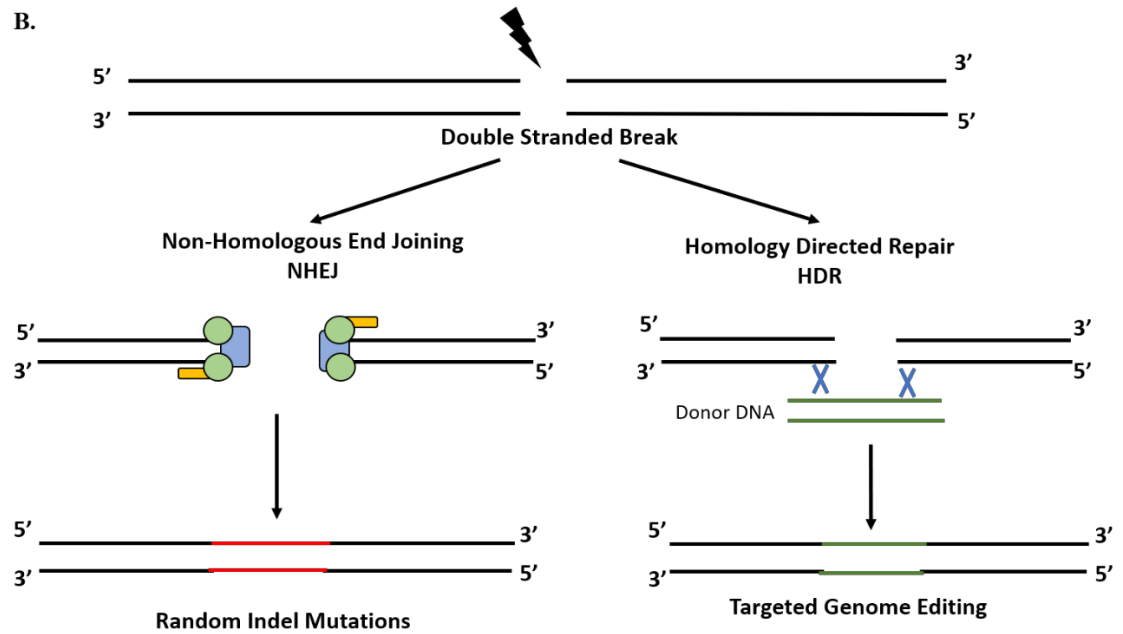


**Figure 1. 5. CRISPR/Cas9 System and Double Strand Break Repair**

## 1.5.Function of Target Proteins

### 1.5.1. Actin Related Protein 2/3 Complex Subunit 1B (Arpc1b)

Human actin-related protein 2/3 complex (Arp2/3) consists of seven components and one of them is Arpc1b. Arp2/3 complex has a role in actin filament branching [80]. ARPC1 component has two isoforms which are Arpc1b and Arpc1a. Arpc1b deficiency leads to impairment of Arp2/3 actin filament branching (cell secretion, lamellipodia-mediated cell migration, phagocytosis, autophagy, migration, vesicle trafficking and transcytosis in the small intestine), and abnormalities in platelets and their distributions (microthrombocytes, leukocytoclastic vasculitis, eosinophilia and elevated IgA and IgE.). Besides these, most crucially in our case, loss of Arpc1b function impairs Arp2/3 actin filament branching which is important for T cell development and formation of the IS [81,82]. T cells cocultured with their target P815 cells showed that Arpc1b can be colocalized with F-actin in the IS. In contrast, Arpc1b deficient T cells had decreased amounts of F-actin in the IS [83]. Somech et al. worked with two genetically related patients who have a homozygous 2 bp deletion in Arpc1b and this results in a premature stop codon formation [84]. These patients show

symptoms like microthrombocytopenia, eosinophilia, and inflammatory bowel disease. They used zebrafish and mice as model organisms and showed that there was a disruption of the IS of T cells in zebrafish models. However, they did not see any impairments in mice models like Brigida et al [83]. They explained that mice did not become totally knock-out and loss of function mutation might not give same results. Also, they added that Arpc1b might have a different function in mice [84]. In light of these findings, we want to study the function of Arpc1b in the formation of the IS and the cytotoxicity of the NK-92 cell line.

### **1.5.2. Chromosome 12 Open Reading Frame 4 (C12orf4)**

C12orf4 is a highly conserved gene which is conserved from nematodes to humans. It is a cytoplasmic protein that has a role in the degranulation of mast cells. Antigen-IgE recognition by FcεRI results in the degranulation of cytoplasmic granules, synthesis of proinflammatory lipid mediators, and synthesis and secretion of growth factors, cytokines, and chemokines. The function of C12orf4 in FcεRI-mediated mast cell responses was controlled by using shRNA targeting C12orf4. Analysis of these experiments have shown that deficiency of C12orf4 results in impairment of activation of mast cells [85]. Some aspects of the degranulation mechanism may be shared between mast cells and NK cells. As such targeting this gene in NK cells may also affect their degranulation.

### **1.5.3. Coiled-coil domain containing 124 (Ccdc124)**

Ccdc124 is a centrosomal and midbody protein and it is conserved from fungi to humans. The midbody is important for completion of cell division (cytokinesis). Ccdc124 deficiency in human HeLa cells results in the accumulation of multinucleated and enlarged cells [41]. The MTOC is formed by centrosomes and it is important for the polarity of immune cells during the formation of an IS. Ccdc124, which is the ortholog of late-annotated short open reading frame 2 (Lso2) in yeast, interacts with near A site of the 25S ribosomal RNA, where it overlaps with GTPase activation center (GAC) of the ribosomal large subunit. Ccdc124 may also have a conserved function in translation [86]. The function and regulation of this protein is not extensively studied. However there is a documented interaction between Ccdc124 and protein kinase R during HEK293 cells innate immune stimulation [87].

#### **1.5.4. CTR9 Homolog, Paf1/RNA Polymerase II Complex Component (Ctr9)**

Ctr9 is the component of PAF complex which is evolutionary conserved and interacts with RNA polymerase II [88]. It has a role in cell cycle progression [88], transcription [89], histone modifications [89,90,91], post transcriptional RNA processing [91], poly(A) site utilization [91], and cancer [90,91]. Ctr9 repression increases in differentiation of naive T cells into Th17 cells [88]. Activation of immune cells against foreign cells results in production and release of cytokines such as interleukin (IL)-1 $\beta$ , tumor necrosis factor (TNF)- $\alpha$ , and IL-6 which cause inflammatory response [89]. Ctr9 repression abolishes IL-6 responsive gene expression [88,89]. Mechanism of this abolishment is histone methylation modification and interacting with JAK/STAT3 pathway [89]. IL-6 stimulation leads to the activation of STAT3 that binds to promoter of target genes and associates with CTR9-containing complex. This complex induces target gene expression by recruitment of histone methyltransferase complex [89]. Moreover, three of the 35 Wilms tumor family members showed inactivating Ctr9 mutations. According to an experiment's results, Ctr9 was called as a cancer predisposition gene [90]. PAF complex has a role in telomere function in yeast. Low level of TERRA (telomere repeat containing RNA) is maintained by Paf1 and Ctr9 component of PAF complex [91].

#### **1.5.5. DNA Fragmentation Factor Subunit Beta (Dffb)**

Dffb encodes a protein which is a nuclease DNA fragmentation factor. It has a role in degradation of naked DNA, chromatin condensation DNA fragmentation during apoptosis [92]. Expression of Dffb is changed by inhibition of 26S proteasome [93]. Ovarian cancer cells were disrupted by exogenous targeted recombinant expression of Dffb in vitro assays without affecting healthy cells [94]. There is no clear information about functions of Dffb in immunological systems.

#### **1.5.6. Ubiquitin-specific-processing protease 30 (Usp30)**

Usp30 is a negative regulator of mitophagy [95,96]. It deubiquitylates Parkin-mediated ubiquitination of TOM20 (translocase of outer membrane of mitochondria)[97,98]. Generally, polyubiquitin at the Lys-6 and Lys-11 are cleaved by Usp30. However, it cannot cleave polyubiquitin at the Ser-65 [98,99]. There is no information about its function in the immunological systems.

### **1.5.7. Tumor susceptibility gene 101 (Tsg101)**

Tsg101 has a role in cell cycle control [100], transcriptional regulation [100], turnover of endocytosed proteins [100], regulation of multivesicular body (MBV) formation [101], regulation of MDM2/p53 circuitry [102,103], development and progression of several human cancer [104]. MHC class I molecules are released from Endoplasmic Reticulum and are sent to plasma membrane to present their ligands. After releasing from ER, MHC class I is ubiquitylated by Kaposi's sarcoma-associated herpes virus gene product K3 (KK3) and is internalized into plasma membrane. Ubiquitylated MHC class I goes to late endocytic pathway and it is degraded. Tsg101, which is a ubiquitin enzyme 2 variant protein, has a role in late endosomal sorting. Degradation of MHC class I in the KK3-expressing cells is prevented by depletion of Tsg101 [105]. Like ubiquitylated MHC class I, ubiquitylated proteins are also associated with Tsg101 which is the part of endosomal sorting complex required for transport (ESCRT- I). ESCRT-0, -I, -II, -III have a role in the biogenesis of MBV and degradation of ubiquitylated proteins [105,106,107]. During the cell division process, Tsg101 is localized into Golgi apparatus in interphase and is connected to spindle fibres in mitosis. In a research, it was reported that Tsg101 and non-structural protein 3 (NS3) of Japanese encephalitis virus (JEV) is associated with microtubules during JEV replication [106].

Tsg101 controls vesicle budding and fission. Depletion of Tsg101 by small interfering RNA (siRNA) prevents translocation of TCR into IS and incorporation of TCR into microvesicles [74]. Moreover, Tsg101 and ubiquitin (Ub) have a crucial role in signaling events at cSMAC. Formation of cSMAC is maintained by microclusters (MCs), and recognition of Ub by ESCRT-I component TSG101 is necessary for cSMAC formation. TCR and pMHC are recruited into cSMAC, and cytolytic vesicles are secreted towards target cells. Then, TCRs are downregulated and degraded by internalization into lysosomes [108].

## 2. AIM OF THE STUDY

NK cells and Cytotoxic T lymphocytes are very crucial for the immune system. NK cells are members of the innate immune system and they give a fast response against foreign or altered self cells. CTLs belong to the adaptive immune system and their response to foreign or infected cells is more specific but much slower. Activation of NK cells depends on the balance between activating and inhibitory receptors, and cytotoxic T cells activation depends on the recognition of peptide ligands on MHC class I by the TCR. Activation of NK cells and CTLs causes further signaling by phosphorylation and the recruitment of adaptor proteins to the cytoplasmic tails of the signaling receptors. Finally, they produce and release cytolytic granules towards the target cells. There is not so much information about these mechanisms. Details of mechanisms give us opportunity about new targetable sites for immunotherapy which is the most effective way to protect healthy cells from cancer and foreign cells. The Infection and Immunity Immunophenotyping (3i) project searches for important genes for immunological pathways. This project assessed the CTLs responses of random mutagenized mice. They have shown that mice that carry mutations in 7 genes have significantly different CTL responses compared to WT. We aimed to find out if these genes are also important for the cytotoxicity of the NK-92 cell line.

First, we tried to optimize the Neon Electroporation transfection method for the NK-92 cell line. NK-92 cells are notoriously difficult to transfect. Transduction of this cell line with lentiviral vectors is also inefficient but with high virus titers it is possible. Our ultimate goal was to induce gene mutations in this cell line using CRISPR/Cas9 genome editing. While it is possible to transduce cells with lentiviral constructs expressing CRISPR/Cas9, this leads to the insertion and continuous expression of the genes of interest into genome of the NK-92 cells and increases the risk of off-target effects. For this purpose, we tried to optimize the delivery of plasmids transiently expressing CRISPR/Cas9. We aimed to find the best condition to get high number of live cells with high transfection efficiency. To assess transient transfection efficiency and cell viability, we used a GFP expressing plasmid and analyzed the cells by flow cytometry.

The second part of this thesis focusses on the generation of single cell clone from NK-92 cells using a feeder cell system. Single cell cloning is an essential part of CRISPR/Cas9 genome editing, yet the NK-92 cell line is notoriously difficult to grow starting from a single cell. First, we conducted two trials were to make a single cell clones from NK-92 but were not successful. To generate a feeder cell line system, we transduced NK-92 cells by lentivirus encoding the HSV-TK gene. The Thymidine Kinase gene is a suicide gene and it is toxic in the presence of Ganciclovir. NK-92 cells which were transduced with lentivirus expressing tdTomato-puro were mixed with HSV-TK transduced NK-92 cells in different ratios. We titrated Ganciclovir treatment with various concentrations and tried to optimize the ratio of target to feeder cells, concentration of ganciclovir and the length of culturing to growth a healthy culture starting with a single NK-92 iT2 cell.

Finally, we confirmed the expression of selected cytotoxicity related genes from the 3i project in NK-92 cells using RNA-seq analysis conducted with this cell line. Five of these candidate genes were expressed by NK-92 cells. In addition to these, Ccdc124 and Tsg101 genes were also targeted. Ccdc124 gene is found in the centrosome which forms the MTOC. MTOC is known to reorient the cytotoxic cell towards the target cell. The Tsg101 gene is a part of ESCRT-1 which is an endosomal sorting complex and is required for transport. In total seven genes were mutated by the CRISPR/Cas9 genome editing method and unique CRISPR/Cas9 vectors were delivered using third generation lentivirus. To assess successful genome editing and a decrease in mRNA expression of the targeted genes, we performed T7 assays and QRT-PCR, respectively. We also performed Degranulation assays and xCELLigence RTCA experiments to assess deficiencies of cytotoxicity of the mutated NK-92 cells.

### 3. MATERIALS AND METHODS

#### 3.1. Materials

##### 3.1.1. Chemicals

Chemicals which were used in this thesis are listed in Appendix A.

##### 3.1.2. Equipment

Equipment which were used in this thesis is listed in Appendix B.

##### 3.1.3. Buffer and Solutions

Agarose Gel: For 100 ml 1% w/v gel, 1 g of agarose powder was dissolved in 100 ml 0.5X TBE buffer by heating. 0.002% (v/v) ethidium bromide was added to the solution.

Calcium Chloride (CaCl<sub>2</sub>) Solution: 60 mM CaCl<sub>2</sub>, 15% Glycerol, and 10 mM PIPES (pH 7.0) were mixed with ddH<sub>2</sub>O until a total volume of 500 ml. The solution was filter-sterilized and stored at 4°C.

Tris-Borate-EDTA (TBE) Buffer: For 1 L 5X stock solution, 54 g Tris-base, 27.5 g boric acid, and 20 ml 0.5M EDTA (pH 8.0) were dissolved in 1 L ddH<sub>2</sub>O. The solution was stored at room temperature (RT) and diluted 1 to 10 with ddH<sub>2</sub>O for working solution of 0.5X TBE.

Phosphate-buffered saline (PBS): For 1 L 1X solution, 100 ml 10X DPBS was added to 900 ml ddH<sub>2</sub>O and the solution was filter-sterilized.

FACS Buffer: For 500 ml 1X solution, 0.5 g bovine serum albumin (BSA) and 0.5 g sodium azide were mixed in 500 ml 1X PBS and the solution was kept at +4°C.

HEPES-buffered Saline (HBS): Solution of 21 mM HEPES (pH 7.05), 137 mM NaCl, 5 mM KCl, 0.7 mM Na<sub>2</sub>HPO<sub>4</sub>, and 6 mM Glucose was prepared. Solution was filter-sterilized and stored at -20°C

##### 3.1.4. Growth Medium

Luria Broth (LB): For 1 L 1X LB media, 20 g LB powder was dissolved in 1 L ddH<sub>2</sub>O and then autoclaved at 121°C for 15 minutes. For selection, kanamycin at a final concentration



of 50 µg/ml or ampicillin at a final concentration of 100 µg/ml was added to liquid medium just before use.

LB-Agar: For 1 L 1X agar medium, 35 g LB-Agar powder were dissolved in 1 L ddH<sub>2</sub>O and then autoclaved at 121°C for 15 minutes. For selection, kanamycin at a final concentration of 50 µg/ml or ampicillin at a final concentration of 100 µg/ml was added to the medium after autoclaved medium was cooled down to 50°C. LB-Agar medium was poured into sterile petri dishes under the hood. Lids of petri dishes were closed after 15-20 min. Sterile agar plates were kept at 4°C.

DMEM: 293FT cells were maintained in culture in DMEM supplemented with 10% heat inactivated fetal bovine serum, 2mM L-Glutamine, 1mM Sodium Pyruvate, 1% PenStrep (100 U/mL Penicilium and 100 µg/mL Streptomycin), and 25mM HEPES solution. MCF-7 cells were maintained in culture in DMEM supplemented with 10% heat inactivated fetal bovine serum, 2mM L-Glutamine, 1% PenStrep (100 U/mL Penicilium and 100 µg/mL Streptomycin).

RPMI: NK92 cell line was maintained in culture in RPMI1640 supplemented with 20% heat-inactivated fetal bovine serum, 25mM HEPES, 2mM L-Glutamine, 1mM Sodium Pyruvate and 1% PenStrep (100 U/mL Penicilium and 100 µg/mL Streptomycin). 1000 U/ml Interleukin-2 is added to culture every 48 hours. K562 cell line was maintained in culture in RPMI1640 supplemented with 10% heat-inactivated fetal bovine serum, 2mM L-Glutamine, 1% PenStrep (100 U/mL Penicilium and 100 µg/mL Streptomycin).

Freezing medium: All the cell lines were frozen in heat-inactivated fetal bovine serum containing 6% DMSO (v/v).

### **3.1.5. Commercial kits used in this study**

Commercial kits which were used in this thesis is listed in Appendix C.

### **3.1.6. Enzymes**

All of the restriction enzymes, DNA modifying enzymes, polymerases and their corresponding buffers used in this study were from either Fermentas or New England Biolabs.

### 3.1.7. Antibodies

Antibodies which were used in this thesis is listed in Appendix D.

### 3.1.8. Bacterial Strains

*Escherichia coli* (*E.coli*) DH-5 $\alpha$  strain is used for general plasmid amplifications and Top10 strain is used for lentiviral construct amplifications.

### 3.1.9. Mammalian cell lines

HEK293FT: Human embryonic kidney 293 (HEK293) cell line derivative that stably expresses the large T antigen of SV40 virus and has fast-growing specificity (Invitrogen R70007).

NK-92: Human natural killer cell line isolated in the year 1992 from a non-Hodgkin's lymphoma patient (ATCC® CRL 2407™).

K562: K562 is the first established human immortalized myelogenous leukemia line which is derived from a 53-year-old female chronic myelogenous leukemia patient in blast crisis (ATCC® CCL-243™).

MCF-7: Human breast cancer cell line which is derived from 69-year-old female adenocarcinoma patient (ATCC® HTB-22™)

### 3.1.10. Plasmids and Oligonucleotides

The plasmids and the primers used in this thesis are listed in Table 3. 1 and Table 3. 2, respectively.

PLASMID NAME	PURPOSE OF USE	SOURCE
pMDLg/pRRE	Virus production/packaging plasmid (Gag/Pol)	Addgene (#12251)
pRSV-REV	Virus production/packaging plasmid (Rev)	Addgene (#12253)
pCMV-VSV-g	Virus production/packaging plasmid (Env)	Addgene (#8454)
LeGO-iG2-Puro	Lentiviral construct for GFP expression with Puromycin resistance gene	Kind gift from Prof. Boris Fehse of University Medical

		Center Hamburg-Eppendorf, Hamburg, Germany
lentiCRISPRv2	Lentiviral construct for CRISPR/Cas9 expression with Puromycin resistance gene	Addgene (#52961)
pSpCas9(BB)-2A-GFP	Mammalian expression plasmid for the CRISPR/Cas9 system with GFP expression gene	Addgene (#48138)
PL253	Getting Thymidine Kinase Gene	Addgene
LeGO-iG2-Puro_TK	Expression of TK	Lab construct
Ccdc124_lentiCRISPRv2	Lentiviral construct for Ccdc124-targeting CRISPR/Cas9 expression with Puromycin resistance	Lab construct
C12orf4_lentiCRISPRv2	Lentiviral construct for C12orf4-targeting CRISPR/Cas9 expression with Puromycin resistance	Lab construct
Ctr9_lentiCRISPRv2	Lentiviral construct for Ctr9-targeting CRISPR/Cas9 expression with Puromycin resistance	Lab construct
Dffb_lentiCRISPRv2	Lentiviral construct for Dffb-targeting CRISPR/Cas9 expression with Puromycin resistance	Lab construct
Usp30_lentiCRISPRv2	Lentiviral construct for Usp30-targeting CRISPR/Cas9 expression with Puromycin resistance	Lab construct
Arpc1b_lentiCRISPRv2	Lentiviral construct for Arpc1b-targeting CRISPR/Cas9 expression with Puromycin resistance	Lab construct
Tsg101_lentiCRISPRv2	Lentiviral construct for Tsg101-targeting CRISPR/Cas9 expression with Puromycin resistance	Lab construct

**Table 3. 1. List of plasmids used in this study.**

<b>PRIMER NAME</b>	<b>SEQUENCE (5' to 3')</b>	<b>PURPOSE OF USE</b>
Ccdc124_Top	CACCGGCGCAGCGTGTCTCG ATC	LentiCRISPRv2 cloning
Ccdc124_Bottom	AAACGATCGAGGACACGCTGC GCC	LentiCRISPRv2 cloning
Ccdc124_CRISPR_fwd	GTTCTGGTATGTCCCCTGC	T7 endonuclease I assay for Ccdc124 binding site
Ccdc124_CRISPR_rev	CTCAAGGTCCACTGCCTCTG	T7 endonuclease I assay for Ccdc124 binding site
C12orf4_Top	CACCGAGATCAAGATGTAAAT TCAC	LentiCRISPRv2 cloning
C12orf4_Bottom	AAACGTGAATTTACATCTTGAT CTC	LentiCRISPRv2 cloning
C12orf4_CRISPR_fwd	TAAGGGAGCTGTTGTTGGGG	T7 endonuclease I assay for C12orf4 binding site
C12orf4_CRISPR_rev	AGTCATGCAGGAATTGGGAA	T7 endonuclease I assay for C12orf4 binding site
Ctr9_Top	CACCGACTTCGATCAGTTACC GGA	LentiCRISPRv2 cloning
Ctr9_Bottom	AAACTCCGGTAACTGATCGAA GTC	LentiCRISPRv2 cloning
Ctr9_CRISPR_fwd	GGGGACAAGTAGCAGGGTTT	T7 endonuclease I assay for Ctr9 binding site
Ctr9_CRISPR_rev	TGACCGCCAAAGCAATCCAT	T7 endonuclease I assay for Ctr9 binding site
Dffb_Top	CACCGTGTTCCTCGACAACGCC GAGC	LentiCRISPRv2 cloning
Dffb_Bottom	AAACGCTCGGCGTTGTCGGGA ACAC	LentiCRISPRv2 cloning

Dffb_CRISPR_fwd	AGCTCATTCCGGTCGTTTGT	T7 endonuclease I assay for Dffb binding site
Dffb_CRISPR_rev	TCCTCCTTGAGACCCGAGAG	T7 endonuclease I assay for Dffb binding site
Usp30_Top	CACCGAAGAAGTGGGGAGTTA TAGG	LentiCRISPRv2 cloning
Usp30_Bottom	AAACCCTATAACTCCCCAGTTC TTC	LentiCRISPRv2 cloning
Usp30_CRISPR_fwd	TGTGTTTGTGTGAGGGAAGAC A	T7 endonuclease I assay for Usp30 binding site
Usp30_CRISPR_rev	AAAGCATGCCTCCA ACTCCA	T7 endonuclease I assay for Usp30 binding site
Arpc1b_Top	CACCGTGCGGTCCTTGTTCAG GCG	LentiCRISPRv2 cloning
Arpc1b_Bottom	AAACCGCCTGGAACAAGGACC GCAC	LentiCRISPRv2 cloning
Arpc1b_CRISPR_fwd	GTGTGAGGCCTGTGAGGATC	T7 endonuclease I assay for Arpc1b binding site
Arpc1b_CRISPR_rev	CTCCAGAGTCCCCATGTGTG	T7 endonuclease I assay for Arpc1b binding site
Tsg101_Top	CACCGTCCAGTAGCCATAGGC ATAT	LentiCRISPRv2 cloning
Tsg101_Bottom	AAACATATGCCTATGGCTACT GGAC	LentiCRISPRv2 cloning
Tsg101_CRISPR_fwd	TCTTCCCATTTCATCAACATG	T7 endonuclease I assay for Tsg101 binding site
Tsg101_CRISPR_rev	ACTTTGCTATTGCCCTCAGGA	T7 endonuclease I assay for Tsg101 binding site
Ccdc124_QRTPCR_fwd	GAGGACTCCAAGCTCAAGGG	QRTPCR
Ccdc124_QRTPCR_rev	TTGGCTTTCTCGGCTGTGTC	QRTPCR
C12orf4_QRTPCR_fwd	AGGAAATGACTATACCCTGGT GC	QRTPCR

C12orf4_QRTPCR_rev	CCTCCATCCCATGAAGCCATTT C	QRTPCR
Ctr9_QRTPCR_fwd	TCCAGCCCTTCTTGGTAAAGC	QRTPCR
Ctr9_QRTPCR_rev	CGCTGGACATCCTGGGTTAG	QRTPCR
Dffb_QRTPCR_fwd	ACCTGGAACCTGGATCACATA A	QRTPCR
Dffb_QRTPCR_rev	CTTGGGTCACAGTTGAGCTT	QRTPCR
Usp30_QRTPCR_fwd	TGAAGAACAGGATGCTCACGA A	QRTPCR
Usp30_QRTPCR_rev	TATTTCTGACTGCTGCTCCAGG	QRTPCR
Arpc1b_QRTPCR_fwd	CTATGAAAAGAGCGGTGCCAA	QRTPCR
Arpc1b_QRTPCR_rev	CCAGTCGATGCCTGTCACCT	QRTPCR
Tsg101_QRTPCR_fwd	ACGGGGCCACCAAATACTTC	QRTPCR
Tsg101_QRTPCR_rev	GGAGGCTGAGAAGGGTACTG	QRTPCR
GAPDH_QRTPCR_fwd	TCCTGCACCACCAACTG	QRTPCR
GAPDH_QRTPCR_rev	TCTGGGTGGCAGTGATG	QRTPCR
hU6_forward	GAGGGCCTATTTCCCATGATTC C	lentiCRISPRv2 sequencing primer
TK_fwd_BamHI	GGGGGATCCACCATGGCTTCG TACCCCGGCCA	LeGO-iG2-puro cloning
TK_rev_EcoRI	GGGGGAATTCTCAGTTAGCCT CCCCATCTCC	LeGO-iG2-puro cloning

**Table 3. 2. List of oligonucleotides used in this study.**

### 3.1.11. DNA Ladder

DNA Ladders which were used in this thesis are listed in Appendix E.

### 3.1.12. DNA sequencing

DNA sequencing service was commercially provided by MCLAB, CA, USA. (<https://www.mclab.com/home.php>)

### 3.1.13. Software, Computer-based Programs, and Websites

The software and computer-based programs used in this project are listed in Table 3. 3

<b>SOFTWARE, PROGRAM, WEBSITE NAME</b>	<b>COMPANY/WEBSITE</b>	<b>PURPOSE OF USE</b>
CLC Main Workbench v7.9.4	QIAGEN Bioinformatics	DNA Sequencing Analysis, Molecular Cloning, DNA Alignment, Primer Design,
FlowJo v10	FlowJo, LLC	Analysis of Flow cytometry data
LightCycler 480 SW 1.5	ROCHE	Analyzing qPCR results
BD FACSDiva	BD Biosciences	Collecting flow cytometry data
Ensembl Genome Browser	<a href="http://www.ensembl.org/index.html">http://www.ensembl.org/index.html</a>	Human genome sequence information
NCBI BLAST	<a href="http://blast.ncbi.nlm.nih.gov/Blast.cgi">http://blast.ncbi.nlm.nih.gov/Blast.cgi</a>	Basic local alignment search tool
Addgene	<a href="https://www.addgene.org">https://www.addgene.org</a>	Plasmid sequence and map information
CRISPR design tool (MIT, Zhang Lab)	<a href="http://crispr.mit.edu/">http://crispr.mit.edu/</a>	Website for designing of sgRNA and analysis of off-target
CRISPOR	<a href="http://crispor.tefor.net">http://crispor.tefor.net</a>	Website for designing of sgRNA and analysis of off-target
RTCA Software 2.0	ACEA Biosciences	Real-time cell growth analysis

**Table 3. 3. List of computer-based programs, software and websites used in this study**

## **3.2. Methods**

### **3.2.1. Bacterial Cell Culture**

#### **3.2.1.1. Growth of bacterial culture**

*E.coli* DH5 $\alpha$  or Top10 strains were cultured in LB medium with required antibodies at 37°C with shaking 220 rpm for overnight. To select a single colony, overnight culture was spread

on a petri dish with a required antibiotic by using glass beads and it was incubated overnight at 37°C without shaking. Overnight bacterial culture was stored with glycerol at final concentration 10%(v/v) in 1 ml in a cryo-vial for long term storage. Cryo-vial was stored at -80°C.

### **3.2.1.2. Preparation of competent bacteria**

Competent cell with high efficiency was put into 40 ml LB without any antibiotic. Culture was incubated for overnight at 37°C with shaking 220 rpm. 4 ml of overnight culture was transferred into 400 ml LB without antibiotic and it was inoculated at 37°C with shaking 220 rpm. Every 30 minutes, OD<sub>590</sub> was measured and incubation continued until OD reached 0.375. Culture was aliquoted into eight pre-chilled 50 ml falcons. They were stored on ice for 5-10 minutes. They were centrifuged at 1600 g at 4°C for 10 minutes. Supernatant was discarded, and each pellet was resuspended in 10 mL ice-cold CaCl<sub>2</sub> buffer. They were centrifuged at 1100 g at 4°C for 5 minutes. Supernatant was discarded, and each pellet was resuspended in 10 mL ice-cold CaCl<sub>2</sub> buffer. They were kept on ice for 30 minutes. Then, they were centrifuged at 1100 g at 4°C for 5 minutes. Supernatant was removed, and bacterial pellet was resuspended in 2 mL ice-cold CaCl<sub>2</sub> buffer. Bacterial suspensions were combined into single 50 ml falcon divided into 200 µl aliquots into pre-cooled microcentrifuge tubes. Bacterial cells were immediately frozen into liquid nitrogen and stored in -80°C. Efficiency of competent cells was decided by transforming of PUC19 plasmid by using different concentrations that were 10 pg/µl, 100 pg/µl, 1000 pg/µl.

### **3.2.1.3. Transformation of Competent Bacteria**

Competent cell was taken from -80°C and was thawed on ice. Desired amount of plasmid was added into cells and they were kept on ice for 30 min. They were heat-shocked at 42°C for 90 seconds and they were put into ice again for 1min. 800 µl LB was added onto competent cells and they were incubated at 37°C for 45 minutes. Then, they were centrifuged at 13000 rpm for 30 sec and 900 µl of supernatant was discarded. Bacteria cells were resuspended into 100 µl supernatant and they were spread onto LB-Agar plate with a proper antibiotic by using glass beads. Plates were incubated at 37°C for overnight.



#### **3.2.1.4. Plasmid DNA Isolation**

Plasmid DNA was isolated from bacteria by using alkaline lysis protocol which is described in Molecular Cloning: A Laboratory Manual [110]. Besides the alkaline lysis protocol, PureLink HiPure Plasmid Midiprep or Macherey-Nagel Midiprep Kits were performed according to manufacturer's protocols. Purity and concentration of plasmid were checked by NanoDrop spectrophotometer.

#### **3.2.2. Mammalian Cell Culture**

##### **3.2.2.1. Maintenance of Cell Lines**

HEK293FT cells and MCF-7 were maintained in complete DMEM (10% FBS) in a sterile flask with filtered cap at an incubator set to 37°C and 5% CO<sub>2</sub>. They were split before their confluency reached 90-95%. Medium was removed, and cells were washed with sterile 1X PBS. 1ml of trypsin was added and cells were incubated at incubator for 4-5 minutes. Fresh complete DMEM was added and cells were resuspended into medium. HEK293FT cells were split at from 1:4 to 1:8 ratio into a new sterile flask with filtered cap every 2 days and MCF-7 cells were split at from 1:3 to 1:4 ratio into new sterile flask with a filtered cap every 3 days. K562 cells were maintained in complete RPMI (10% FBS) in a sterile flask with filtered cap at an incubator set to 37°C and 5% CO<sub>2</sub>. Their densities were set between 180000 cells/ml and 300000 cells/ml every 3 or 2 days respectively. NK-92 cells were maintained in complete RPMI with 20% FBS and 1000 U/ml human Interleukin-2 (IL-2) in a sterile flask with a filtered cap at an incubator set to 37°C and 5% CO<sub>2</sub>. Their densities were set between 300000 cells/ml and 400000 cells/ml every 3 or 2 days respectively.

##### **3.2.2.2. Cryopreservation of the cells**

Suspension cells were set to 500000 cells/ml and adherent cells were seed 30-40% one day before. Next day, cells were counted and centrifuged at 300 g for 5 min. 3-5x10<sup>6</sup> cells were resuspended into 0.5 ml FBS and they were kept onto ice for 20 minutes. 0.5 ml FBS with 12% DMSO was prepared freshly and stored on the ice. After 20 min, 0.5 ml FBS with 12% DMSO was added onto 0.5 ml FBS with cells and final concentration of DMSO was 6% in 1 ml. Cells were transferred into cryovials and transferred into Mr. Frosty freezing containers. The Freezing container was placed in -80°C for one day and for long storage cryovials were transferred into liquid nitrogen storage tanks.

### **3.2.2.3. Thawing frozen mammalian cells**

Cryovial was removed from a nitrogen tank and it was stored on ice. 9 ml fresh complete medium was put into 15 ml falcon. Frozen cells were thawed by using fresh medium immediately and they were centrifuged at 300 g for 5 minutes to get rid of DMSO. Supernatant was removed, and pellet was resuspended with fresh 7-8 ml complete medium. Cells were transferred into T25 sterile flask with filter cap. Next day, cells were checked and if they looked healthy, medium was changed to remove dead cells.

### **3.2.2.4. Transient Transfection of mammalian cells by Electroporation**

Transient transfection by Electroporation was tried to optimize for NK-92 cell line. Neon transfection kit from Invitrogen was used. Transfection programs indicated in the results section were used using 10 µl or 100 µl tips and with cells solubilized in either R buffer or HBS buffer. Different number of cells and different concentration of DNAs were used to identify optimal transfection conditions.

### **3.2.2.5. Transfection of HEK293FT cells to produce virus with target vector**

100 mm dishes were covered by 2 ml filtered Poly-l-lysine and were incubated for 5 minutes. Poly-l-lysine was discarded, and dishes were washed with 5 ml ddH<sub>2</sub>O two times. Lids of dishes were left open for 1 hour to dry them. 5x10<sup>6</sup> HEK293FT cells were seeded onto each 100 mm dishes. Cells were incubated at an incubator set to 37°C and 5% CO<sub>2</sub> for 12-16 hours. 3.5 µg pMDLg/pRRE(Gag/Pol), 2.25 µg pRSV-Rev (Rev), 1.50 µg pCMV-VSV-G (Env) plasmids and 7.5 µg gene of interest plasmids(ccdc124\_pLentiCRISPRv2, c12orf4\_pLentiCRISPRv2,ctr9\_pLentiCRISPRv2,ddfb\_pLentiCRISPRv2,usp30\_pLentiCRISPRv2, arpc1b\_pLentiCRISPRv2, tsg101\_pLentiCRISPRv2, LeGO-iG2-Puro\_TK and LeGO-iG2-Puro) were used for transfection of cells. Necessary volume of plasmid was put into a microcentrifuge tube and ddH<sub>2</sub>O was added up to 450 µl. Lastly, 50 µl CaCl<sub>2</sub> from 2.5 M stock solution was taken and added into plasmid+ddH<sub>2</sub>O mix. 500 µl 2xHBS (pH=7.04) was put into 50 ml falcon. Then, bubbling was made by using pipettor with 2 ml stereological pipet. 500 µl mix (plasmid+ ddH<sub>2</sub>O+ CaCl<sub>2</sub>) was added onto 2xHBS by drop by drop using bubbling technique. Then they were incubated for 15-20 minutes under the hood. Medium of cells was changed by 11 ml DMEM+GlutaMAX for each dish with 25 µM final concentration chloroquine. After 15-20 minutes, 1 ml mix was added onto cell by drop by drop and at that

time dish was swirled. After 8-10 hours, medium of cells was changed by fresh 11 ml DMEM+GlutaMAX for each dish. Media with virus was collected at 24h and 36h, was filtered by 0.45  $\mu$ m filters, was aliquoted and was stored at -80°C.

### 3.2.2.6. Determination of the amount of virus

Virus Titration: 50000 HEK293FT cells were seeded into 24 well plate and serial dilution of viral supernatant (LeGO-iG2-puro and LeGO-iG2-puro-TK) were transduced after 4-5 hours in the presence of 8  $\mu$ g/ml proteamine sulfate. FACS analysis was done after 48 hours of transduction. Transduced GFP+ cells were analyzed by FACS. Calculation for the number of infectious particles in 1 ml is shown in the Table 3. 4 and Table 3. 5.

Virus amount ( $\mu$ l)	GFP <sup>+</sup> cell number	Infectious particles in 1ml
0.5 $\mu$ l	$50000 \times 0.05 / 100 = 25$	$25 \times 2000 = 50000$
1 $\mu$ l	$50000 \times 1.29 / 100 = 645$	$645 \times 1000 = 645000$
5 $\mu$ l	$50000 \times 5.38 / 100 = 2690$	$2690 \times 200 = 538000$
10 $\mu$ l	$50000 \times 10.4 / 100 = 5200$	$5200 \times 100 = 520000$

**Table 3. 4. Determination of the optimal LeGO-iG2-puro virus concentration**

Virus amount ( $\mu$ l)	GFP <sup>+</sup> cell number	Infectious particles in 1ml
0.5 $\mu$ l	$50000 \times 0.94 / 100 = 470$	$470 \times 2000 = 940000$
1 $\mu$ l	$50000 \times 2.39 / 100 = 1195$	$1195 \times 1000 = 1195000$
2 $\mu$ l	$50000 \times 3.9 / 100 = 1950$	$1950 \times 500 = 975000$
5 $\mu$ l	$50000 \times 9.4 / 100 = 4700$	$4700 \times 200 = 940000$

**Table 3. 5. Determination of the optimal LeGO-iG2-puro-TK virus concentration**

Volume titration of Virus: pLentiCRISPRv2 vector does not express any fluorescent protein so general virus titration protocol is not proper for it.  $2.5 \times 10^5$  NK-92 cells were resuspended with serial dilution of viral supernatant (625  $\mu$ l, 1.25 ml, 2.5 ml) in the presence of 8  $\mu$ g/ml proteamine sulfate, 3  $\mu$ M inhibitor BX795 and 1000 U/ml IL-2, and medium was changed after 6 hours of transduction. On day 3 post-transduction, 1  $\mu$ g/ml puromycin selection was done for untransduced and transduced cells for 6-8 days. Cells were counted every two days and transduction efficiency was calculated by dividing number of transduced cells to number of untransduced cells.

### **3.2.2.7. Lentiviral Transduction**

Lentiviral transduction (LeGO-iG2-puro) of K562 cells were done by placing  $4 \times 10^6$  cells into the T25 flask at a multiplicity of infection (MOI) 2.5 in the presence 8  $\mu\text{g/ml}$  Proteamine Sulfate for 6 hours. Cells were centrifuged at 300 g for 5 min to remove medium with virus and were cultured 12 ml fresh complete RPMI for 48 hours. Then, GFP expression was analyzed by FACS. 1.5  $\mu\text{g/ml}$  puromycin was given to select transduced cells for 4 days and FACS was repeated to see GFP expression.

Lentiviral transduction (LeGO-iG2-puro-TK) of NK-92 cells was performed  $2 \times 10^6$  cells into T25 flask at multiplicity of infection (MOI) 5 in the presence 8  $\mu\text{g/ml}$  Proteamine Sulfate, 3  $\mu\text{M}$  inhibitor BX795, and 1000 U/ml IL-2 for 6 hours. After that time, cells were centrifuged to remove medium with virus at 300 g for 5 min and cells were cultured 4 ml fresh complete RPMI with 1000 U/ml IL-2 for 72 hours. FACS was performed to analyze GFP expression and 1  $\mu\text{g/ml}$  puromycin selection was done for 10 days to select cells with TK gene.

Lentiviral transduction (pLentiCRISPRv2) of NK-92 cells was done by using  $1 \times 10^6$  or  $2 \times 10^6$  cells that were resuspended into 5- or 10-ml virus suspension respectively in the presence 8  $\mu\text{g/ml}$  Proteamine Sulfate, 3  $\mu\text{M}$  inhibitor BX795, and 1000 U/ml IL-2 for 6 hours. Medium with virus were discarded and cells were resuspended into 2 or 4 ml fresh complete RPMI with 1000 U/ml IL-2 for 72 hours. 1  $\mu\text{g/ml}$  puromycin selection was done for transduced cells for 6-8 days.

### **3.2.2.8. Flow Cytometer**

Cells were washed with 1X PBS. 7AAD antibody staining was performed to select live cells. An antibody was added to cells and they were incubated at RT for 15 min. BD LSR Fortessa was used to acquire cells. Voltages and gates were arranged according to WT cells. Firstly, a gate was put for single cells and then 7AAD negative gate was put for all samples. According to the experiment, proper channels were opened, and expression of proteins were recorded. They were analyzed by using FlowJo v10 software.

### **3.2.2.9. Degranulation Assay for NK cells**

1:1 Effector: Target ratio was used for that assay.  $2 \times 10^5$  cells were used for each effector and target cells in 100  $\mu\text{l}$  in V-bottom 96-well plate. 1.25  $\mu\text{g}$  PMA and 0.25  $\mu\text{g}$  ionomycin was used as a positive control. Chemicals and  $2 \times 10^5$  of target cells (K562 and MCF-7) were

resuspended into 100  $\mu$ l complete RPMI with 20%FBS and were put into V bottom 96-well plate.  $2 \times 10^5$  effector cells (WT and Mutated NK-92 cell lines) were resuspended into 100  $\mu$ l complete RPMI with 20%FBS. Fluorochrome-conjugated anti-CD107 $\alpha$  mAb (1:1000) was added medium of target cells and target cells were given onto effector cells. Cells were mixed by using multichannel pipet. Plate was centrifuged at 50 g for 2 min and was incubated at an incubator set to 37°C and 5% CO<sub>2</sub> for 1 hour. 2 $\mu$ M Monensin was given to each cell and incubation was continued 4 more hours. Then, cells were washed and resuspended into 400  $\mu$ l of 1X PBS and cells were acquired by BD FACS Fortessa machine.

#### **3.2.2.10. Cytotoxicity of NK cells by xCELLigence RTCA**

xCELLigence RTCA DP device was placed into an incubator set to 37°C and 5% CO<sub>2</sub>. 100  $\mu$ l of complete DMEM 10% FBS was put into E-16 plates and they were incubated at RT for 15 min. Then, background impedance signal was measured.  $1.5 \times 10^4$  MCF-7 cells were resuspended into 100  $\mu$ l of complete DMEM 10% FBS and were placed into wells of E-16 plate. They were incubated for 30 min at RT and were placed into machine. Target cells were left to growth until cell index reached 1.  $3 \times 10^4$  effector NK-92 cells were resuspended into 100  $\mu$ l of complete RPMI 20% FBS with 1000 U/ml IL-2. E-16 plate was taken from incubator and 100  $\mu$ l medium was discarded from target cells and target cells were given. Plate was placed into machine and cell index measurement was taken every 15 minutes for 24 hours. RTCA software (version 1.2) was used for data analysis.

#### **3.2.2.11. Genomic DNA Isolation**

PureLink Genomic DNA Mini Kit was used according to manufacturer's protocol for genomic DNA isolation.

#### **3.2.2.12. RNA Isolation and qRT-PCR**

TRIzol reagent was used for RNA isolation and manufacturer's protocol was followed. As suggested,  $4-7 \times 10^6$  cells were used. Total RNA was loaded onto agarose gel to check that isolated RNA was intact. RevertAid First Strand cDNA Synthesis Kit was performed to synthesize cDNA by using 2 $\mu$ g RNA and by following manufacturer's protocol. QRT-PCR was done by LightCycler® 480 SYBR Green I Master kit and analysis was done according to  $2^{(-\Delta\Delta Ct)}$ .

### **3.2.2.13. Optimization for Concentration of Ganciclovir Drug and Feeder Cells Ratio**

Different concentration of ganciclovir (0.01-1 µg/ml) was given into  $2.5 \times 10^6$  NK-92 cells with TK/GFP which is called as a feeder cell. Cells were counted every two days and they were resuspended into fresh RPMI 20% as a 500000/ml. FACS analysis was performed every two days by using  $2-3 \times 10^5$  cells and GFP expression was analyzed into Flow Jo software.

Feeder cells and target cells (NK-92 cells with tdTomato) were cultured together in the different ratios, and different concentration of ganciclovir was given. Experiments were started by using totally  $2.5 \times 10^6$  into 5 ml RPMI. Cells were counted every two days and they were resuspended into fresh RPMI 20% in the presence of different ratios of ganciclovir. FACS analysis was performed every two days by using  $2-3 \times 10^5$  cells. The decrease in GFP expression and increase in tdTomato expression was analyzed by using Flow Jo software.

In the last version of that series of experiment, feeder and target cells were cultured in different higher ratios. Experiment was started by using  $1.75 \times 10^5$  cells into 500 µl medium in 24-well plate and using  $7 \times 10^5$  cells into 2 ml medium in 6-well plate. Cells were counted regularly and FACS was performed every two days. Ganciclovir selection was started when number of cells reached  $2.5 \times 10^6$ . First days, 0.01 µg/ml ganciclovir was given, and according to increase in tdTomato expression, ganciclovir concentration was increased up to 1 µg/ml.

### **3.2.3. Vector Constructions**

#### **3.2.3.1. General Vector Constructions Protocol**

Restriction Enzyme Digestion: Required amount of template DNA was mixed by required enzymes and their proper buffers, and ddH<sub>2</sub>O was added until 20 µl. Sample was placed into thermocycler and was incubated required temperature that depends on the type of enzyme and required time which is between 30 minutes and 2 hours.

De-phosphorylation of 5' phosphate groups: 5' phosphate groups of digested plasmid product have been removed to prevent self-ligation. Calf intestinal alkaline phosphatase (CIAP) and its buffer was added onto the digested product and they were incubated at 50 °C for 60 min for blunt ends and at 37° C for 30 min for sticky ends.

Agarose gel electrophoresis and DNA purification from the gel: Digested vectors or DNA templates and PCR products were loaded on the gel. Percentage of gel were decided

according to the length of bands or vector fragments. Low percentages (0.7-1% w/v) was used for longer product and higher percentages (1.5-2% w/v) was used for shorter products. Desired amount of agarose was weighed and put into 100 ml 0.5X TBE. It was heated by microwave until it was clear and homogenous. Then, it was allowed to cool, and 0.002% v/v ethidium bromide was added. It was poured into cassette and comb was placed properly. After solidification of gel, DNA samples with loading dye were loaded into gel. PCR products were run at 100V for 45 minutes and digested vectors were run at 100 V for 1 and half hour. Bands were visualized under UV light and were cut. Commercially available gel purification kit was used to purify DNA.

Ligation: T4 ligase enzyme and its proper buffer were mixed by DNA of vector and insert. It was incubated at 16°C for 16 hours or 25°C for 4 hours. Ratio for vector to inset was used 1 to 3. Serial diluted DNA of vector and insert was loaded onto control agarose gel and their concentrations were compared. Proper amount of vector and insert was decided according to control gel. Negative control which had only vector and enzyme was also performed. Then, 10 µl of ligation product was transformed into chemically competent *E. coli* DH5α or Top10 strain. Cells were spread onto LB-Agar plate with desired antibiotic by using glass beads. Plates were incubated at 37°C for 16 hours without shaking.

### **3.2.3.2. Donor DNA construction**

Herpes Simplex Virus-1 Thymidine Kinase (HSV-TK) gene was produced by using primers with BamHI and EcoRI from PL253 vector and it was cloned into BamHI and EcoRI digested LeGO-iG2-puro vector.

Production of TK gene: Phusion PCR was performed by forward primer with BamHI and reverse primer with EcoRI and Thymidine Kinase gene was taken. Phusion PCR mix was prepared according to below:

PL253 (1ng)	1 µl
5X Phusion Buffer	10 µl
10 mM dNTP	1 µl
10 µM Forward Primer with BamHI	2.5 µl
10 µM Reverse Primer with EcoRI	2.5 µl

Phusion DNA polymerase	0.5 $\mu$ l
ddH <sub>2</sub> O	32.5 $\mu$ l
	50 $\mu$ l

Annealing temperature for primers was decided by performing Gradient PCR. Settings for Phusion PCR is shown below:

Initial Denaturation	98°C	30 sec
30 Cycle	98°C	10 sec
	75°C	30 sec
	72°C	1 min
Final Extension	72°C	10 min
Final	4°C	$\infty$

After PCR was performed, PCR product was loaded onto 1% gel at 110V for 1 hour. Gel extraction was done. Gel Extracted PCR product was double digested by EcoRI-HF and BamHI-HF enzymes. Reaction mix was placed into Thermo Cycler at 37°C for 2 hours. Preparation of reaction mix is shown in the below:

Gel Extracted PCR product	10 $\mu$ l
Cut Smart	5 $\mu$ l
EcoRI-HF	1 $\mu$ l from 1:4 diluted
BamHI-HF	1 $\mu$ l from 1:4 diluted
ddH <sub>2</sub> O	33 $\mu$ l
	50 $\mu$ l

PCR clean-up was performed by a commercially available kit. LeGO-iG2-puro vector was double digested by EcoRI-HF and BamHI-HF enzymes. Reaction mix was placed into Thermo Cycler at 37°C for 2 hours. Preparation of reaction mix is shown in the below:

DNA(2 $\mu$ g)	2 $\mu$ l
----------------	-----------



Cut Smart	5 $\mu$ l
EcoRI-HF	1 $\mu$ l from 1:4 diluted
BamHI-HF	1 $\mu$ l from 1:4 diluted
ddH <sub>2</sub> O	41 $\mu$ l
	50 $\mu$ l

CIAP was performed after digestion and reaction mix is shown below:

Digested Vector Reaction Mix	50 $\mu$ l
Cut Smart Buffer	7 $\mu$ l
CIP Enzyme (10000U/ml NEB)	1 $\mu$ l
ddH <sub>2</sub> O	12 $\mu$ l
	70 $\mu$ l

Reaction mix was placed into Thermo Cycler at 37°C for 30 minutes. After CIAP, 1% agarose gel was poured, and it was run at 120V for 1 and half hour. Then, gel extraction was performed by a commercially available kit.

Digested PCR product and LeGO-iG2-puro vector were loaded onto gel by serial dilution volume. According to vector: insert molar ratio 1:3, volume of vector and insert was decided by using control gel. Then, three different ligation reaction mix was prepared, and it is shown in the below. They were incubated at RT for 4 hours.

	1. Condition	2. Condition	Only Vector
T4 Ligase Enzyme	1 $\mu$ l	1 $\mu$ l	1 $\mu$ l
Insert	1 $\mu$ l	2 $\mu$ l	-
Vector	2 $\mu$ l	4 $\mu$ l	4 $\mu$ l
10X T4 DNA Ligase Buffer	2 $\mu$ l	2 $\mu$ l	2 $\mu$ l
ddH <sub>2</sub> O	14 $\mu$ l	11 $\mu$ l	13
	20 $\mu$ l	20 $\mu$ l	20 $\mu$ l

10  $\mu$ l of Ligation products were transformed into chemically competent *E. coli* DH5 $\alpha$  bacteria and cells were spread onto LB-Agar plate with proper antibiotic. They were incubated at 37°C for 16 hours. Colonies were picked and were grown for plasmid DNA isolation. Then, Diagnostic digest was performed by using SmaI enzyme, and reaction is shown below:

Miniprep Product	5 $\mu$ l
SmaI	0.05 $\mu$ l
Cut Buffer	2 $\mu$ l
ddH <sub>2</sub> O	12.95 $\mu$ l
	20 $\mu$ l

Reaction mix was placed into Thermo Cycler and incubated 25°C for 2 hours. 1% agarose gel was poured, and samples were loaded. Positive colonies were sent to sequence company.

### 3.2.4. CRISPR/Cas9 Genome Editing by using pLentiCRISPRv2

pLentiCRISPRv2 plasmid was used to mutate NK-92 cell lines.

#### 3.2.4.1. sgRNA Design and off-target analysis

Exon which was common for all alternative splicing forms was chosen as a target. CRISPOR (<http://crispor.tefor.net/>) and CRISPR design tool (Zhang Lab, [www.crispr.mit.edu](http://www.crispr.mit.edu)) tools were used for designing proper sgRNA. Off-targets and scores were calculated by them and best sgRNA was chosen by considering that information.

#### 3.2.4.2. Phosphorylation and annealing of top and bottom oligonucleotide pairs

An order was given for selected sgRNA and they were synthesized as a top and bottom strand. Oligonucleotides were solved into newly autoclaved distilled water with a final concentration 100  $\mu$ M. Then, they were annealed with the following reaction and protocol:

sgRNA Top Oligonucleotide (100 $\mu$ M)	1 $\mu$ l
sgRNA Bottom Oligonucleotide (100 $\mu$ M)	1 $\mu$ l
10X T4 Ligase Buffer	1 $\mu$ l

T4 PNK Enzyme	1 $\mu$ l
ddH <sub>2</sub> O	6 $\mu$ l

Reaction mix was prepared and was placed into thermocycler. Settings are shown below:

37°C	30 minutes
95°C	5 minutes
Ramp down to 25°C	5°C/minute

#### 3.2.4.4. LentiCRISPRv2 plasmid digestion and dephosphorylation

Flank site of annealed oligonucleotide's is compatible by BsmBI digested plasmid. pLentiCRISPRv2 plasmid was digested with BsmBI enzyme at 55°C for 1 hour. Reaction is shown below:

pLentiCRISPRv2(5 $\mu$ g)	3.6 $\mu$ l
BsmBI(NEB)	1 $\mu$ l
NeBuffer 3	5 $\mu$ l
ddH <sub>2</sub> O	40.4 $\mu$ l
	50 $\mu$ l

Digested vector was loaded onto 1% gel and it was run at 100V for 1 and half hour. 2kb band was removed from the plasmid and 12 kb band was cut. Commercially available gen extraction kit was performed to get pure digested plasmid. Concentration and purity of digested plasmid were calculated by nanodrop. Ligation was done by using digested plasmid and annealed oligonucleotides. Reaction was prepared according to table:

BsmBI digested lentiCRISPRv2 plasmid	50 ng
Oligonucleotide duplex from step 3.2.4.2 (1:200 dilution)	1 $\mu$ l
10X T4 Ligase Buffer (NEB)	2 $\mu$ l
T4 Ligase (400,000 U/ml) (NEB)	1 $\mu$ l
ddH <sub>2</sub> O	to 20 $\mu$ l

Reaction mix incubated at RT for 1 hour.

### 3.2.4.5. Transformation of Cas9 plasmids

10 µl of ligation product was transformed into chemically made *E.coli* Top10 competent cells and they were spread onto LB-Agar plate with proper antibiotic. Plasmid DNA extraction was done, and plasmids were sent to sequencing. Primer which binding to Human U6 promoter was used to confirm sgRNA were cloned into a vector.

### 3.2.5. CRISPR/Cas9 Genome Editing by using pSpCas9(BB)-2A-GFP

pSpCas9(BB)-2A-Puro plasmid was used to try to mutate NK-92 cell lines by electroporation. Annealing of top and bottom oligonucleotides pairs are shown in the 3.2.4.2.

#### 3.2.5.1. pSpCas9(BB)-2A-GFP plasmid digestion and ligation

Flank site of annealed oligonucleotide's is compatible by BbsI digested plasmid. pSpCas9(BB)-2A-GFP plasmid was digested with BbsI enzyme and ligated with annealed oligonucleotides in the same reaction:

pSpCas9(BB)-2A-GFP (100 ng)	1 µl
Oligonucleotide duplex from step 3.2.4.2 (1:200 dilution)	2 µl
10X T4 Ligase Buffer (NEB)	2 µl
DTT (10 mM)	1 µl
ATP (10 mM)	1 µl
BbsI (10,000 U/ml) (NEB)	1 µl
T4 Ligase (400,000 U/ml) (NEB)	0.5 µl
ddH <sub>2</sub> O	Upto 20 µl

Incubated at:

37°C	5 minutes
21°C	5 minutes
Go to Step 1	5 times

Exonuclease treatment was done to ligation reaction to prevent unwanted recombination products by the following reaction:

Ligation reaction from step 3.2.5.1	20 $\mu$ l
10X Buffer 4 (NEB)	3 $\mu$ l
ATP (10 mM)	3 $\mu$ l
Exonuclease V (10,000 U/ml) (NEB)	1 $\mu$ l
ddH <sub>2</sub> O	To 30 $\mu$ l

Incubate at:

37°C	30 minutes
70°C for inactivation	30 minutes

### 3.2.5.2. Transformation of Cas9 plasmids

10  $\mu$ l of ligation product was transformed into chemically made *E.coli* Top10 competent cells and they were spread onto LB-Agar plate with proper antibiotic. Plasmid DNA extraction was done, and plasmids were sent to sequencing. Primer which binding to Human U6 promoter was used to confirm sgRNA were cloned into a vector.

### 3.2.6. Determination Genome Targeting Efficiency by T7 endonuclease I assay

Viruses were produced by using pLentiCRISPRv2 with sgRNA vector according to protocol written in section 3.2.2.4. Then, virus volume was decided by using protocol written in section 3.2.2.5. NK-92 cells were transduced according to protocol written in section 3.2.2.6. CRISPR/Cas9 mediated genome editing efficiency was check by using T7 endonuclease I assay. Firstly, genome DNA extraction was done in each pool. Then, targeted part of the genome was amplified by PCR reaction. In the second step, PCR products were denatured and re-annealed, and then they were digested with T7E1 enzyme. T7E1 enzyme can detect and cut non-perfectly match part of PCR product. Mutated pools were analyzed by using that method.

Amplification of targeted part for CCDC124 was performed by using Ccdc124\_CRISPR\_fwd and Ccdc124\_CRISPR\_rew primers. Their T<sub>m</sub> is 70°C.

Amplification of targeted part for C12ORF4 was performed by using C12orf4\_CRISPR\_fwd and C12orf4\_CRISPR\_rew primers. Their T<sub>m</sub> is 67.5°C.

Amplification of targeted part for Ctr9 was performed by using Ctr9\_CRISPR\_fwd and Ctr9\_CRISPR\_rew primers. Their  $T_m$  is 67.5°C.

Amplification of targeted part for CCDC124 was performed by using Dffb\_CRISPR\_fwd and Dffb\_CRISPR\_rew primers. Their  $T_m$  is 71.2°C.

Amplification of targeted part for CCDC124 was performed by using Usp30\_CRISPR\_fwd and Usp30\_CRISPR\_rew primers. Their  $T_m$  is 69.7°C.

Amplification of targeted part for CCDC124 was performed by using Arpc1b\_CRISPR\_fwd and Arpc1b\_CRISPR\_rew primers. Their  $T_m$  is 64.3°C.

Amplification of targeted part for CCDC124 was performed by using Tsg101\_CRISPR\_fwd and Tsg101\_CRISPR\_rew primers. Their  $T_m$  is 64.3°C.

Amplification of targeted gDNA part was performed by Q5 DNA Polymerase:

5X Q5 HF Buffer (NEB)	5 $\mu$ l
10 mM dNTPs	0.5 $\mu$ l
10 $\mu$ M forward primer	1.25 $\mu$ l
10 $\mu$ M reverse primer	1.25 $\mu$ l
Template DNA	20-50 ng
Q5 HF Polymerase (2,000 U/ml) (NEB)	0.25 $\mu$ l
ddH <sub>2</sub> O	To 25 $\mu$ l

Reaction mixes were prepared, and they were placed into Thermo Cycler:

Initial Denaturation	98°C	30 seconds
30 Cycles	98°C	10 seconds
	50-72°C	20 seconds
	72°C	20 seconds
Final Extension	72°C	2 minutes
Hold	4°C	$\infty$

T7E1 digestion reaction was prepared as follow:

PCR Reaction	10 $\mu$ l
10X Buffer 2 (NEB)	2 $\mu$ l
ddH <sub>2</sub> O	to 19.5 $\mu$ l

Mix was placed into thermo cycler:

Initial Denaturation	95°C	5 minutes
Annealing	Ramp down to 85°C	2°C/second
	Ramp down to 25°C	0.1°C/second
Hold 4	°C	$\infty$

Re-annealed products were digested by T7E1. Genomic DNA from WT cells was used as a negative control.

Annealed PCR Product	19.5 $\mu$ l
T7E1 (10,000U/ml) (NEB)	0.5 $\mu$ l

Reaction mix was incubated at 37°C for 30 min. Digested product was loaded onto 2% agarose gel at 100V for 45 min to analyze.

## 4. RESULTS

### 4.1. Optimization Trials of Electroporation for NK-92 cells by Neon Transfection System

NK-92 cells are difficult to transfect with plasmid DNA. We tried to optimize the Neon electroporation method. Programs suggested on the website were given on Table 4. 1.

Program	Pulse Voltage	Pulse Width	Pulse No	Cell Density (cells/ml)	Transfection Efficiency	Viability	Tip Type
P4	1300	10	3	1x10 <sup>6</sup>	29%	55%	10 µl
P5	1200	10	4	1x10 <sup>6</sup>	29%	55%	10 µl
P2	1250	10	3	1x10 <sup>6</sup>	17%	70%	100 µl

**Table 4. 1. Programs for Neon Transfection**

Previous attempts at optimization of Neon electroporation conditions of NK-92 cells from our laboratory are shown in Table 4. 2.

Program	Pulse Voltage	Pulse Width	Pulse No
P1	1225	10	3
P2	1250	10	3
P3	1275	10	3
P4	1300	10	3
P5	1200	10	4
P6	1250	10	4
P7	1300	10	4
P8	1350	10	4

**Table 4. 2. Programs for Neon Transfection Optimization**

#### 4.1.1. Neon Optimization Using Different Electroporation Conditions

For optimization of transfection conditions, we used pCDNA3 GFP, a transfection control plasmid which was previously generated in our laboratory. 2x10<sup>5</sup> cells (optimized number per well in 24-well plate) were resuspended in R buffer or HBS buffer with 1 µg pcDNA GFP plasmid, and cells were taken by 10 µl tip for electroporation. We tried to optimize



transfection conditions using HBS buffer because this was less costly and in some cell lines gives better efficiency compared to R buffer. Programs, which are shown in table 4.2, were used. After electroporation, cells were incubated in NK-92 medium in the presence of  $10^6$ U/ml IL-2. FACS analysis was done after 24 h. Transfection efficiencies were analyzed by recording GFP expression level. Cell viability percentage and transfection efficiencies were given in Table 4. 3.

	<b>R Buffer</b>		<b>HBS Buffer</b>	
	Cell Viability %	Transfection Efficiency%	Cell Viability %	Transfection Efficiency %
<b>P1</b>	23.6	31.2	18.7	28.2
<b>P2</b>	20.2	31.7	16.3	27.3
<b>P3</b>	17.1	34.0	12.6	23.6
<b>P4</b>	16.9	35.3	11.2	24.2
<b>P5</b>	19.9	30.2	16.3	20.8
<b>P6</b>	15.5	33.3	9.37	16.8
<b>P7</b>	11.6	38.3	6.84	16.2
<b>P8</b>	10.8	46.1	5.19	17.5

**Table 4. 3. Cell Viability and Transfection Efficiency of Neon Electroporation Using Different Electroporation Conditions**

We got higher transfection efficiency in our experiments than the manufacturer's recommended conditions; however, cell viabilities greatly reduced. We chose conditions P1, P4 and P5 because their cell viabilities were highest.

#### **4.1.2. Neon Optimization Using Conditioned Medium**

Conditions P1, P4 and P5 were performed by using 10  $\mu$ l tip and  $10^5$  cells per well of 24-well plate, which were suggested in the website. 1  $\mu$ l pcDNA GFP was transfected for  $10^5$  cells. To increase cell viability, we decided to repeat electroporation several times.  $10^4$  cells were electroporated at a time in total 10 times. Conditioned medium which is essential for NK-92 viability, was used to increase viability of NK-92 cells after electroporation. To prepare conditioned medium, cells were incubated at a concentration of  $5 \times 10^5$  cells/ml for 48 hours, and centrifuged. The culture supernatant was collected and filtered by 0.22-micron filters

into a 50 ml falcon. After electroporation, cells were resuspended into conditioned medium and they were incubated for 48 h. FACS analysis was performed and the resulting cell viability and transfection efficiencies were given in Table 4. 4.

	<b>R Buffer</b>		<b>HBS Buffer</b>	
	Cell Viability%	Transfection Efficiency %	Cell Viability %	Transfection Efficiency %
<b>P1</b>	16.8	5.8	10.8	4.89
<b>P4</b>	11	6.03	7.02	4.04
<b>P5</b>	10.4	5.07	11.7	4.63

**Table 4. 4. Cell Viability and Transfection Efficiency of Neon Electroporation Using Conditioned Medium**

Cell viabilities and transfection efficiencies were lower than the previous experiment. We concluded that using conditioned medium is not an advantage for the electroporation of NK-92 cells.

#### **4.1.3. Neon Optimization with Increasing Doses of Plasmid DNA**

We decided to continue with the high number of cells and to use only R buffer to overcome the decreased cell viability. We tried to optimize DNA concentration for the 100  $\mu$ l tip.  $1 \times 10^6$  NK-92 iT2 cells were electroporated twice by using 100  $\mu$ l tip. Titration was done for pcDNA GFP amount between 1 to 9  $\mu$ g using the P1 transfection condition. Cells were resuspended in normal NK-92 medium in the presence of  $10^6$  U/ml IL-2. After 48 hours, FACS was performed to check transfection efficiencies and cell viabilities (Table 4. 5)

<b>P1</b>	<b>R buffer</b>	
	Cell Viability %	Transfection Efficiency %
<b>Untransfected</b>	21.9	0.28
<b>1 <math>\mu</math>g</b>	8.80	0.92
<b>3 <math>\mu</math>g</b>	5.82	1.22
<b>5 <math>\mu</math>g</b>	3.88	2.60
<b>7 <math>\mu</math>g</b>	3.92	1.82
<b>9 <math>\mu</math>g</b>	2.50	1.67

**Table 4. 5. Cell Viability and Transfection Efficiency of Neon Electroporation with Increasing Doses of Plasmid DNA**

We conclude that increasing the amount of transfected plasmid DNA did not improve cell viability and transfection efficiency. Because these experiments were conducted using the Neon 100 µl tip, next we decided to change this variable and repeated the transfections with the Neon 10 µl tip.

**4.1.4. Neon Optimization using Alternative Electroporation Pipet Tips**

We decided to use the setting that worked well with 10 µl tip in a large scale. Previous experiments showed that optimum transfection efficiency and cell viability was achieved with 1 µg pcDNA GFP resuspended in R buffer for  $2 \times 10^5$  NK-92 WT cells by using Neon 10 µl tip using electroporation program P1. 45 µg pspCas9\_GFP\_ccdc124 plasmid was used to transfect  $9 \times 10^6$  cells. To this end we aliquoted  $2 \times 10^5$  NK-92 iT2 cells and electroporated using R buffer containing 1 µg plasmid and repeated the transfection with new aliquots 45 times by using a single 10 µl Neon transfection tip using the P1 electroporation conditions. All aliquots of transfected cells were resuspended into normal NK-92 medium after electroporation. We tried to use the optimum small-scale setting on large scale. After 48 h of transfection, FACS analysis was done and results are shown in Table 4. 6.

<b>P1</b>	<b>R buffer</b>	
	Cell Viability %	Transfection Efficiency %
<b>Untransfected</b>	23.5	0.44
<b>45 µg/ <math>9 \times 10^6</math> cells</b>	4.56	5.31

**Table 4. 6. Cell Viability and Transfection Efficiency of Neon Electroporation using Alternative Electroporation Pipet Tips**

These experiments show that repetitive use of the same scale tip with small amounts of plasmid also did not result in higher transfection efficiency. These experiments contained the same settings and transfection solution/plasmid DNA/cell concentration as previous experiments. Notably the type of cells and identity of the plasmid was different. pspCas9\_GFP\_ccdc124 is a larger plasmid than pcDNA GFP and this may have negatively affected the transfection efficiency. To eliminate the effects of these variables, we conducted

transfection experiments for NK-92 WT and NK-92 iT2 cells using the same settings and plasmids.

#### 4.1.5. Neon Optimization by Changing Plasmid and Target Cell Identity

10<sup>6</sup> NK-92 WT and NK-92 iT2 cells were transfected with 5 µg and 15 µg pcDNA GFP plasmid resuspended in R buffer. 2x10<sup>5</sup> NK-92 WT and NK-92 iT2 cells were electroporated by 5 repeated pulses using 10 µl tip under P1 electroporation conditions. Cells were resuspended with normal NK-92 medium with presence of IL-2 for 48 hours. Then, FACS analysis was done and results are shown in Table 4. 7.

P1	R buffer	
	Cell Viability %	Transfection Efficiency %
<b>Untransfected</b>	48.9	0.35
<b>5 µg/ 10<sup>6</sup> NK-92 WT cells</b>	14.9	35.5
<b>15 µg/ 10<sup>6</sup> NK-92 WT cells</b>	10.5	56.1
<b>Untransfected</b>	42.1	0.27
<b>5 µg/ 10<sup>6</sup> NK-92 iT2 cells</b>	10.6	30.8
<b>15 µg/ 10<sup>6</sup> NK-92 iT2 cells</b>	7.82	37.1

**Table 4. 7. Cell Viability and Transfection Efficiency of Neon Electroporation by Changing Plasmid and Target Cell Identity**

We observed that the cell viabilities were still quite low, but transfection efficiencies were increased. Also, we found that the that transfection efficiencies of un-transduced and transduced NK-92 cells were very similar. Indicating that the type of NK-92 cell that is used in these optimization studies is not critical. Rather, the identity of the plasmid may be the critical factor in determining transfection efficiency. Because we could not obtain high transfection efficiencies for this cell line, we decided to use third generation lentivirus to transduce this cell line, despite the potential problems of off target specificity due to continued expression. The lentiviral vector pLentiCRISPRv2 expresses both the Cas9 enzyme with single guide RNAs. Future experiments may try to eliminate continuous expression problems by using conditional expression constructs.

## 4.2. Generation of Feeder Cell Line and Single Cell Cloning Trials

Mutated pools which are created by the CRISPR/Cas9 genome editing method need to be single cell cloned to identify clonal cell population. Unfortunately, NK-92 cells cannot grow as a single cell. We decided to generate a feeder cell line by transduction of lentivirus encoding the Herpes Simplex Virus Thymidine Kinase type 1 gene (HSV-TK) into NK-92 cells. HSV-TK is a suicide gene. Cells with lentivirus encoding TK gene die under ganciclovir treatment. GFP-puromycin and TK gene is simultaneously expressed from this vector under the control of an SFFV promoter. We used the GFP gene as a marker for the presence of feeder cells in mixed cell populations. The puromycin gene was used to positively select cells that were stably infected with this lentiviral vector. We also used a line of NK-92 cells previously stably infected with a lentiviral vector encoding the tdTomato fluorescent protein gene. In our experiments we mixed GFP puromycin and TK expressing NK-92 cells with tdTomato expressing NK-92 cells. We used different selection conditions using ganciclovir to specifically eliminate the feeder cell population. To this end we first generated the lentiviral vector expressing GFP puromycin and TK.

### 4.2.1. Cloning of the TK gene into the LegoiG2puro vector

The TK gene was amplified by using primers with suitable restriction enzyme recognition sites (BamHI and EcoRI) from PL253 vector. LegoiG2puro vector was double digested by BamHI and EcoRI. PCR product was cloned into digested vector (Figure 4. 1) and sent to sequencing for confirmation.

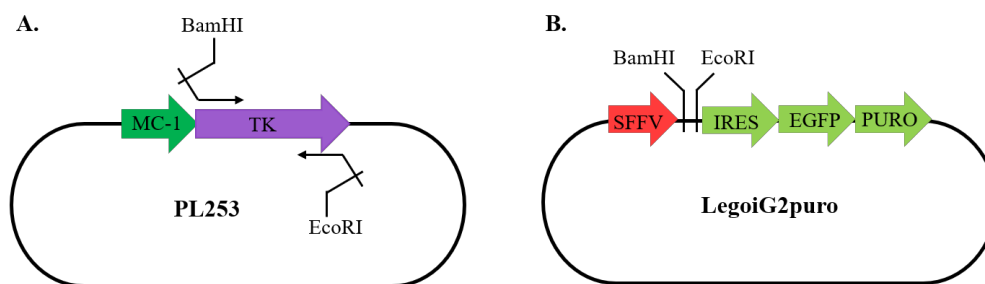


**Figure 4. 1. Cloning of the TK gene into the pLego-iG2Puro plasmid** (A) The pL253 plasmid from which the TK gene was amplified. (B) The pLego-iG2Puro plasmid into which the TK was cloned.

#### 4.2.2. Production and Transduction of Virus into NK-92 cell line

Vectors which were used for generating the lentivirus used for generating TK expressing feeder cell lines are shown in Figure 4. 22. LegoiG2puro\_TK and packaging plasmids were transfected into HEK293FT cells to produce lentivirus (Figure 4. 2).

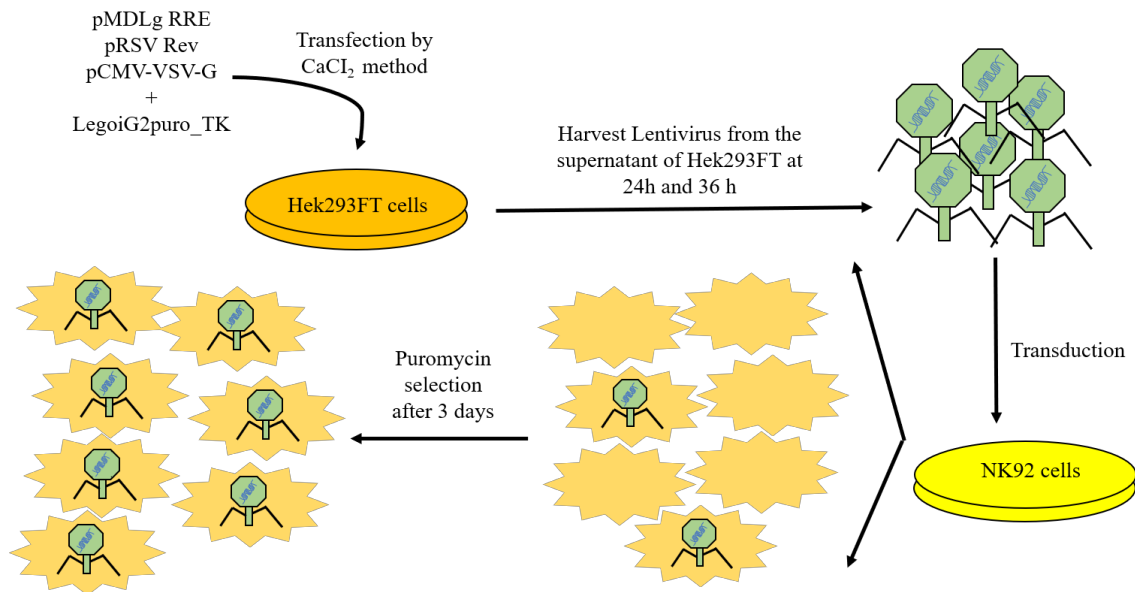


**Figure 4. 2. Experimental design of the production of the virus with TK gene and transduction into NK-92 cells.**

Cell supernatants with lentivirus was collected 24h and 36h after transfection. Virus titration was done and FACS was performed to calculate number of infectious particles per ml (calculated to be  $10^6$  infectious particles per ml at 24 h sample).  $2 \times 10^6$ -NK-92 cells in T25 plate were transduced at a defined multiplicity of infection (MOI=5) in the presence of the inhibitor BX795 (3  $\mu$ M final concentration was used),  $10^6$  U/ml IL-2 and 8  $\mu$ g/ml Proteamine Sulfate was added to the infection reaction for 6 hours to increase efficiency. After 6 hours, transduced NK-92 cells were washed and resuspended into NK-92 medium with  $10^6$  U/ml IL-2 at a concentration of  $4 \times 10^5$  cells/ml. FACS analysis was done after 3 days and the percentage of GFP expressing cells was approximately 7%. Puromycin selection (1  $\mu$ g/ml) was performed for 10 days to increase the number of cells transduced with lentivirus. After this selection, the percentage of GFP positively increased to 97% (Figure 4. 3).

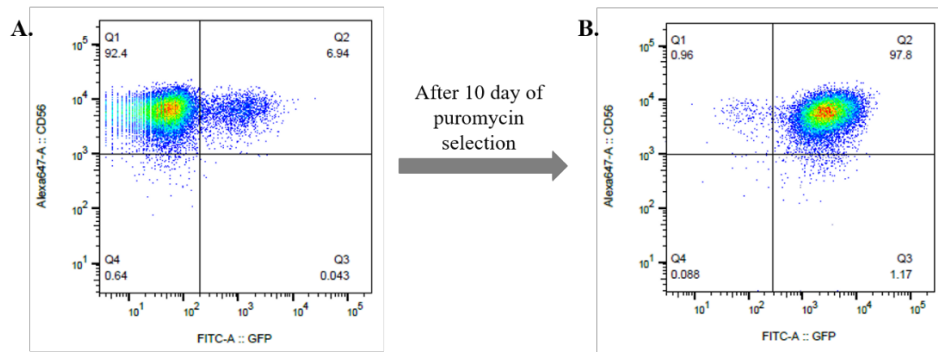


**Figure 4.3. FACS Analysis of Virus Transduction Efficiency:** Transduced NK-92 cells were stained with propidium iodide (PI) and anti-CD56 antibodies. Dead cells were selected by PI positivity and NK-92 cells were selected by CD56 positivity. **(A)** Percentage of GFP expressing cells 3 days after transduction. **(B)** Percentage of GFP expressing cells after 10 days of puromycin selection.

#### 4.2.3. Ganciclovir Titration

$10^6$  NK-92 cells transduced by lentivirus encoding GFP-puro-TK (which from this point onwards are named NK-92 TK/GFP) cells were set at a concentration of  $5 \times 10^5$  cells/ml in 2 ml. Cells were treated with different concentrations of ganciclovir which were 1  $\mu\text{g/ml}$ , 0.3  $\mu\text{g/ml}$ , 0.1  $\mu\text{g/ml}$ , 0.3  $\mu\text{g/ml}$  and 0.01  $\mu\text{g/ml}$  analyzed by flow cytometry and counted every 2 days and were plated again at a concentration of  $5 \times 10^5$  cells/ml. NK-92 WT and NK-92 TK/GFP cells were used as a control group. Cell numbers/ml is shown in Figure 4.4. Every concentration of ganciclovir resulted in cell death in this range. Interestingly the at the lowest concentration (0.01  $\mu\text{g/ml}$ ) ganciclovir killed cells until the fourth day after which a resistant population emerged. GFP expression levels are shown in Figure 4.5. We observed the appearance of a GFP negative population at the time of the maximum death of GFP positive cells treated with ganciclovir. At the time (day 4) of the appearance of this ganciclovir resistant GFP negative population, GFP positivity decreased from 98% to 2% and then increased up to 17.7% percent under 1  $\mu\text{g/ml}$  ganciclovir treatment.

We decided to positively select the GFP-puro-TK expressing cells by puromycin treatment and eliminate this GFP negative population.  $5 \times 10^5$  NK-92 TK/GFP cells/ml in 2 ml were treated by different concentrations of ganciclovir and 1  $\mu\text{g/ml}$  puromycin.  $5 \times 10^5$  NK-92 WT cells/ml in 2 ml were treated only 1  $\mu\text{g/ml}$  puromycin as a positive control group. Cells were

counted every two days and analyzed by FACS. Cell numbers per ml every two days is shown in Figure 4. 6. At the end of the tenth day, NK-92 TK/GFP cells that were treated with 0.01  $\mu\text{g/ml}$  ganciclovir and 1  $\mu\text{g/ml}$  puromycin died. However, we still observed a GFP negative population appearing on day 10 when analyzed by FACS which are shown in Figure 4. 7.

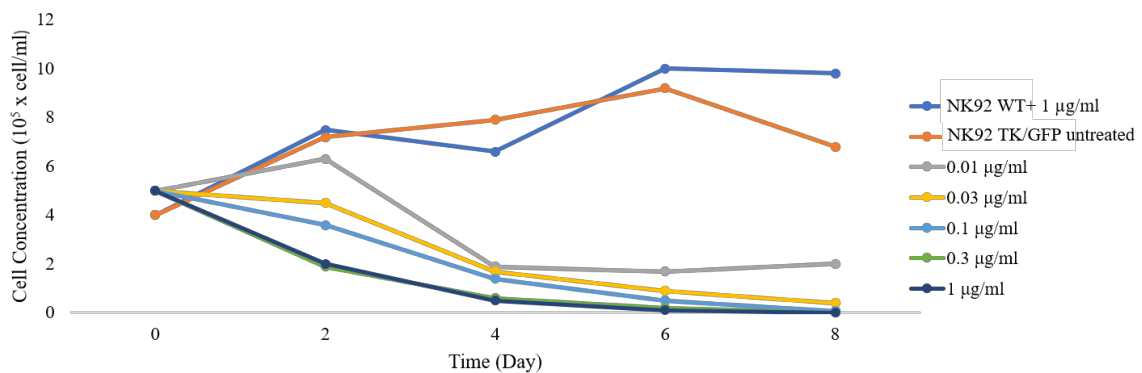


**Figure 4. 4. Cell concentration under different selection conditions with increasing concentrations of ganciclovir.** Different concentrations of ganciclovir (1  $\mu\text{g/ml}$ , 0.3  $\mu\text{g/ml}$ , 0.1  $\mu\text{g/ml}$ , 0.3  $\mu\text{g/ml}$  and 0.01  $\mu\text{g/ml}$ ) were given to NK92 WT and TK/GFP cells. Every 2 days, cells were counted and set again as a  $5 \times 10^5$  cells/ml.

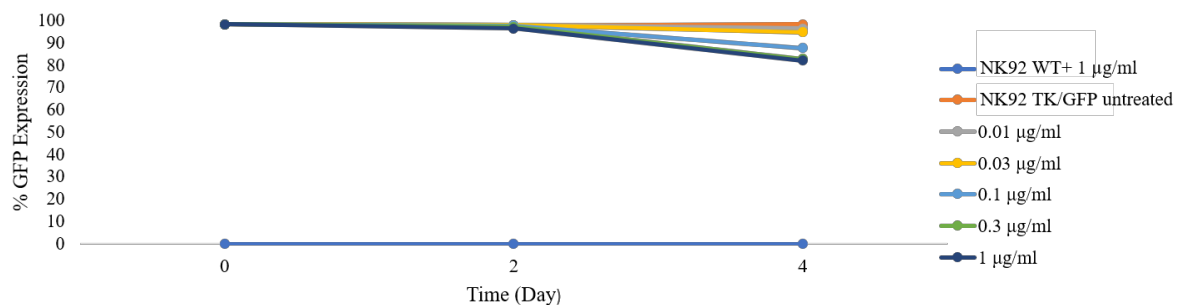


**Figure 4. 5. Percentage of GFP positive cells in the cell culture under ganciclovir treatment.**



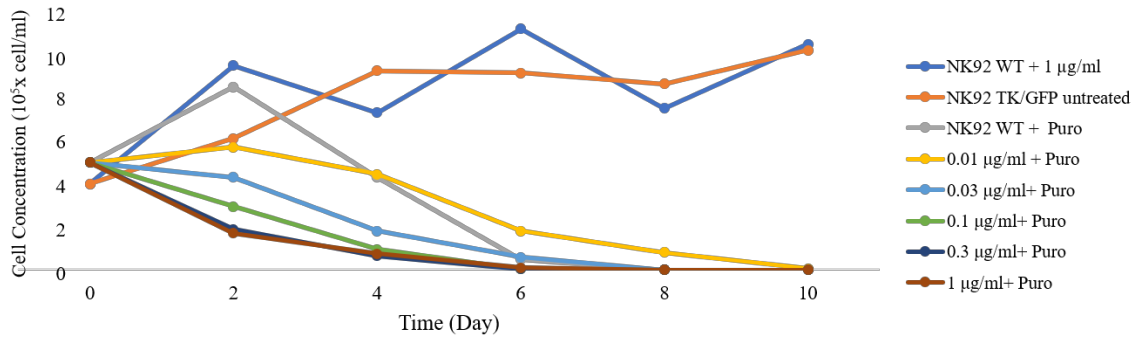


**Figure 4. 6. Cell concentration under the different selection conditions with increasing concentrations of ganciclovir and 1µg/ml puromycin.** Different concentrations of ganciclovir (1 µg/ml, 0.3 µg/ml, 0.1 µg/ml, 0.3 µg/ml and 0.01 µg/ml) were given to NK92 WT and TK/GFP cells. Only 1 µg/ml puromycin was given for NK-92 WT as a control. Every 2 days, cells were counted and set again as a  $5 \times 10^5$  cells/ml.

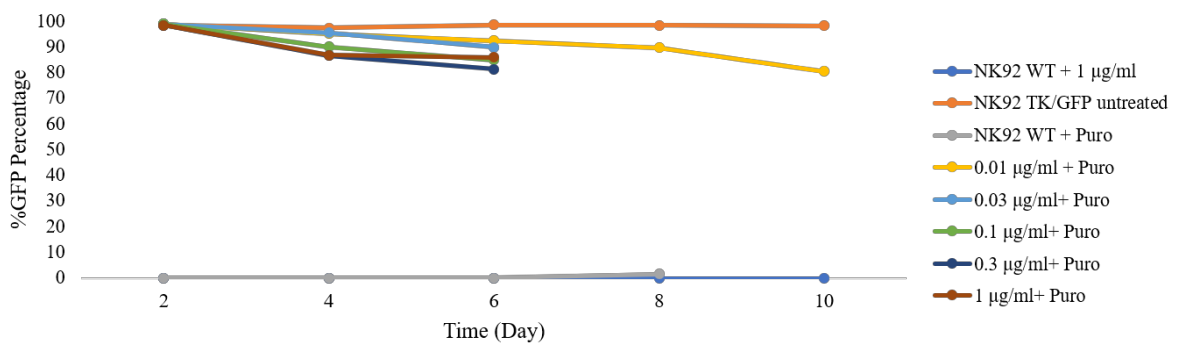


**Figure 4. 7. Percentage of GFP positive cells in the cell culture under ganciclovir treatment and 0.01 µg/ml puromycin treatment.**

We concluded from these experiments that under these selection conditions a GFP negative TK resistant population appears after prolonged culture. These may be cells that have lost TK expression by silencing of integrated lentiviral construct.

#### 4.2.4. Making a Single Cell Cloning From NK-92 Cells

NK-92 cells grow as clumps and are IL-2 dependent. Thus, it is difficult to grow these as a single cell.

First Trial: To be sure, we made single cell cloning by using the serial dilution method. A cell concentration corresponding to 0.3 cell per well was placed into each well of a 96-well

plate. The plates were incubated for at least one week by daily supplementation of  $10^6$ U/ml IL-2 but no wells with colonies could be observed under these conditions.

Second Trial: We supplemented the single cell colonies in 96 plates with conditioned medium in our second trial. Cells were plated at  $5 \times 10^5$  cells/ml and cell supernatant was collected after 48 hours, filtered thorough 0.22-micron filter and diluted with equal volume of NK-92 growth medium. Again, a cell concentration corresponding to 0.3 cell per well was placed into each well of 96-well plate, incubated with this conditioned medium with daily supplementation of  $10^6$ U/ml IL-2. At the time of plating each well was observed under the microscope and those containing single cells were marked. Out of 96 wells, 12 wells had single cells but on the second day of incubation only 6 wells contained live cells and after one week of incubation no well with a live cell could be observed.

Third Trial: Different dilutions were used to determine the fewest number of cells that could produce a viable colony of NK-92 cells. Experimental design is shown in Figure 4. 8. Cells were resuspended in 50% conditioned medium and  $10^6$ U/ml IL-2 was supplemented every day. 27.500 cells/ml and 2.750 cells/ml produced colonies after 2 or 3 days. However, 275 cells/ml produced very small colonies which were not viable.

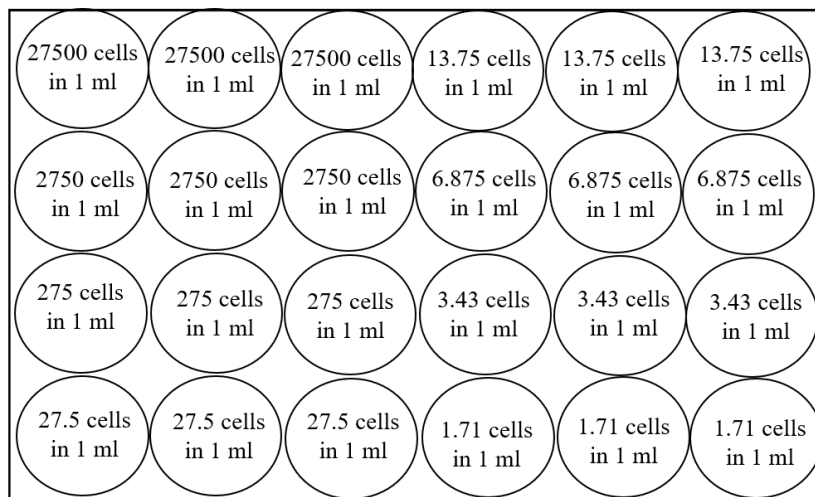


**Figure 4. 8. Different dilutions of NK-92 cells.** Cell numbers for each well are shown in the figure.

After these experiments, we decided to generate a feeder cell line by transduction of lentivirus encoding the TK gene into the NK-92 cell line.

#### 4.2.5. Single Cell Cloning by Using Feeder Cell Lines

The NK-92 TK/GFP cell was used as a feeder cell line and NK-92 iT2 cells were used to make single cell clone (Figure 4. 9). First, we made serial dilutions of the NK-92 iT2 cells into 96 well plates in 100  $\mu$ l normal NK medium. We waited for cells to settle down for 4 hours and identified those wells that had single cells by fluorescent microscopy. 3000 NK-92 TK/GFP feeder cells were resuspended in 100  $\mu$ l medium and added to the wells containing the single cells. Cells were incubated for 15 days by adding  $10^6$ U/ml IL-2 each day. The experimental design is shown in Figure 4. 10. Cell concentrations after 10 days of incubation were fixed to  $3 \times 10^5$  NK-92 cells per ml ( $6 \times 10^4$  cells in 200  $\mu$ l). We calculated that to reach  $6 \times 10^4$  cells in one well, in 10 days, we must start with 3750 cells/well. Our previous experiments indicated that 2750 cells/ml (550 cells in 200  $\mu$ l) can produce a colony. Thus 3000 cells/well for a starting culture was a good starting point to prevent cellular stress.

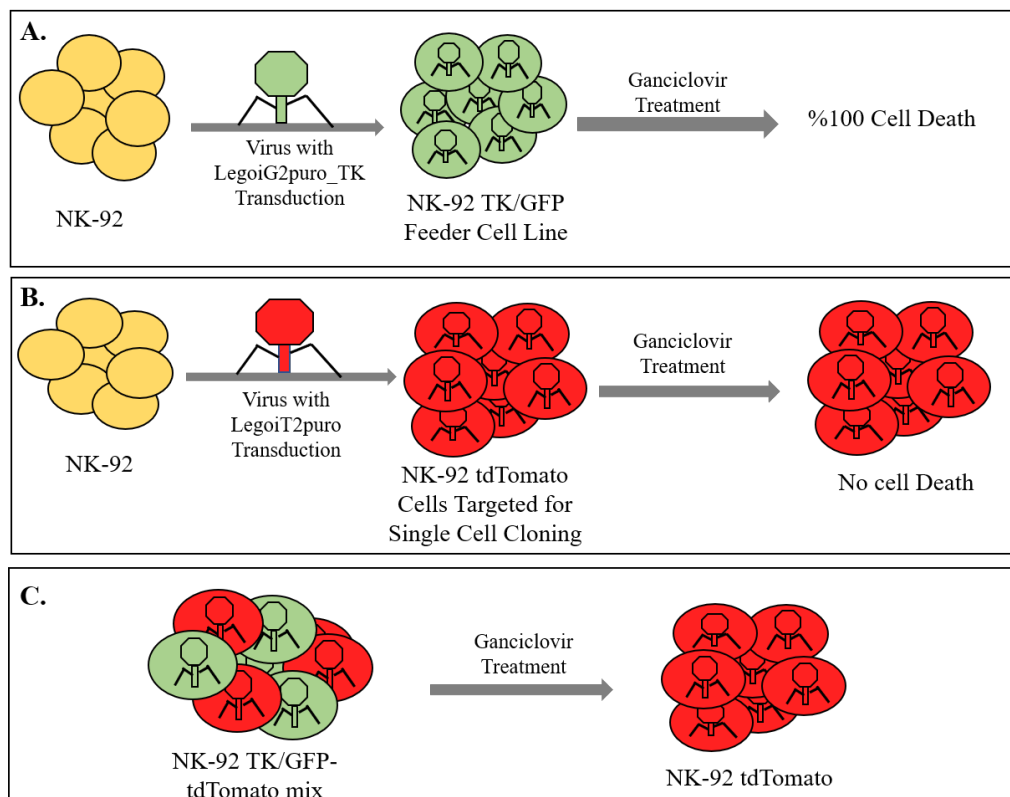


**Figure 4. 9. Schematic showing ganciclovir treatment of mixtures of the TK/GFP feeder cells and iT2 cells (A) Feeder cells die by ganciclovir treatment. (B) NK-92 iT2 cells are**

expected to be resistant to ganciclovir. (C) Ganciclovir treatment of a mix of GFP positive feeder cells and tdTomato positive cells.

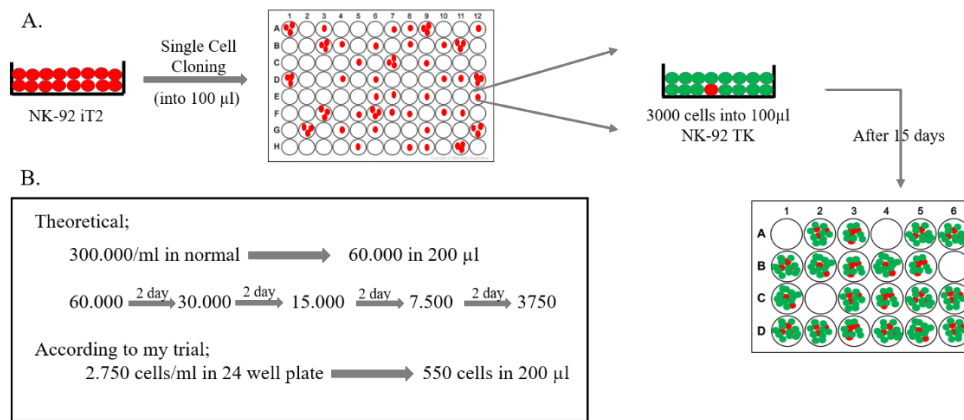


**Figure 4. 10. Experimental setups for single cell clone by co-incubation with feeder cells. (A)** Schematic demonstration of the experiment. **(B)** Calculations for deciding the number of feeder cells to be added to the culture.

After 15 days of incubation, feeder/single cell mixtures were counted and set to a concentration of  $3 \times 10^5$  cells/ml and transferred into 24-well plates and 6-well plates. Cells were examined under an inverted fluorescent microscope and a confocal microscope when they were in the 24 well plates. We observed that NK-92 iT2 cells and TK/GFP feeder cells produced a mixed colony (Figure 4. 11). Cells from three wells (D4, F8 and F1) grew and we analyzed them by flow cytometry to compare the relative composition of these colonies from tdTomato (single cells) and GFP (feeder cells) positive populations (Table 4. 8).

	<b>GFP%</b>	<b>tdTomato%</b>
<b>NK-92 WT</b>	0.78	0.65
<b>NK-92 iT2/TCR</b>	88	96.7
<b>D4</b>	94.1	0.32
<b>F8</b>	96.5	0.37
<b>F1</b>	95.9	4.13

**Table 4. 8. GFP and tdTomato Expressing Cell Ratio**

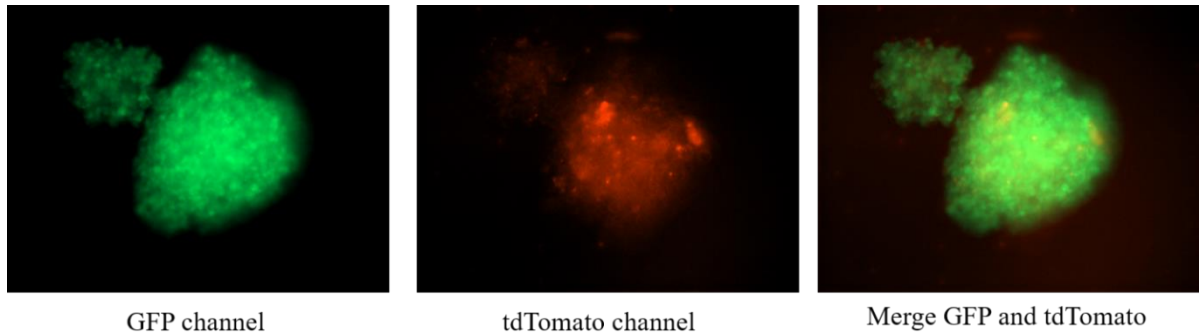


**Figure 4. 11. Fluorescent Imaging of a mixed origin colony.** 10 X magnification. Left is GFP channel, middle is tdTomato channel and right is a merged image.

Ganciclovir treatment of mixed origin colonies D4 and F8: Although we predicted NK-92 iT2 origin red fluorescent cells under microscopic analysis, we could not detect tdTomato expression after in flow cytometer analysis. This may be because of a malfunction of red channel in the flow cytometer. Regardless, we treated the D4 and F8 populations with ganciclovir to assess whether expression of tdTomato increased.  $10^6$  D4 and F8 cells were resuspended in 2 ml in the presence of 1  $\mu\text{g/ml}$  ganciclovir (Figure 4. 12). Cells were counted every two days and set to a concentration of  $5 \times 10^5$  cells per ml. After 16 days of selection, no viable cells could be observed in the F8 population. The D4 population continued to live and the percentage of tdTomato expressing cells were assessed by flow cytometry. However, we could observe any tdTomato expressing cells and most cells were GFP positive (approximately 94%), which was unexpected. We could not explain why TK/GFP positive cells did not die under the treatment of ganciclovir. It is possible that TK might undergo silencing during selection.

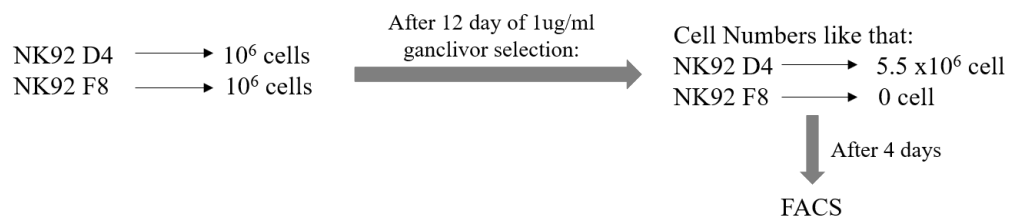


**Figure 4. 12. Experimental Design for D4 and F8 mixed colonies undergoing ganciclovir treatment.** Cell numbers in the beginning and end of the experiment were recorded.

To determine the mixed origin of the colonies, we examined the F1 population by confocal microscopy. A colony from this well was transferred into an imaging ring with a glass bottom appropriate for confocal microscopy. The imaging was performed by z-stack analysis using the 488 nm laser as an excitation source and a green and red channel to detect the different fluorophores (Figure 4. 13). Analysis of the z-stack image indicates that there are distinct GFP positive and tdTomato positive cells that make up this colony. We did not detect any double positive cells. One side of the colony was observed to be predominantly GFP positive while the other side was predominantly tdTomato positive.

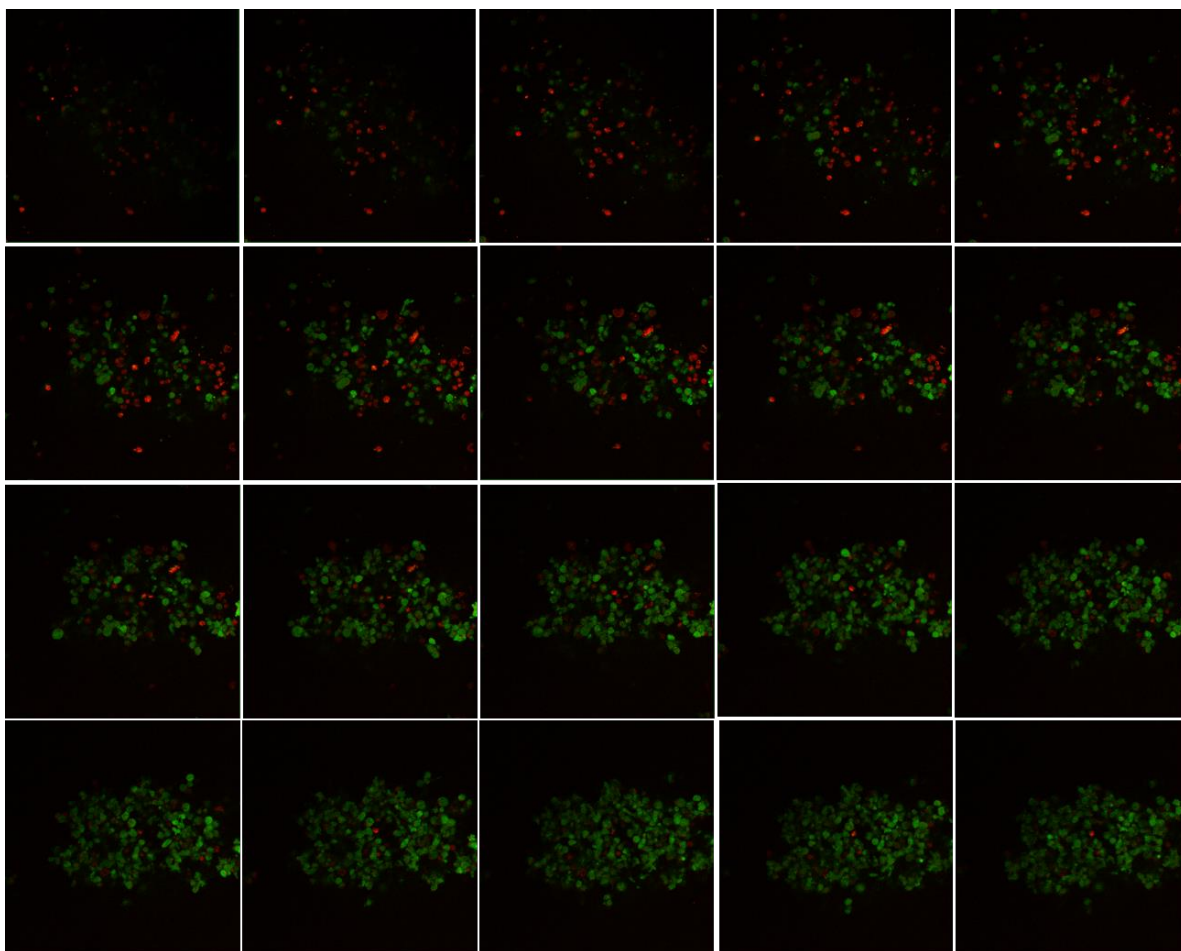


**Figure 4. 13. Confocal Z-stack Image of the F1 population**

Ganciclovir treatment of the F1 colony: 1  $\mu\text{g/ml}$  ganciclovir was given to  $10^6$  NK-92 WT and F1 cells. After 4 days, while the NK-92 WT cells thrived, all F1 cells were dead. This was likely due to the presence of a very few number of tdTomato positive cells (Table 4. 8). Thus, we increased the cell concentration to  $5 \times 10^5$ ,  $6.25 \times 10^5$  and  $7.5 \times 10^5$  per ml. Also, we decreased the concentration of ganciclovir to 0.2  $\mu\text{g/ml}$ . At the end of 4 days of selection, cell numbers were very low, indicating that ganciclovir could kill most cells and that the mixed population contained very few tdTomato positive cells. To increase the relative percentage of tdTomato positive cells in the mixture, we expanded this colony for 18 days and analyzed by flow cytometry (Table 4. 9 and Figure 4. 14)

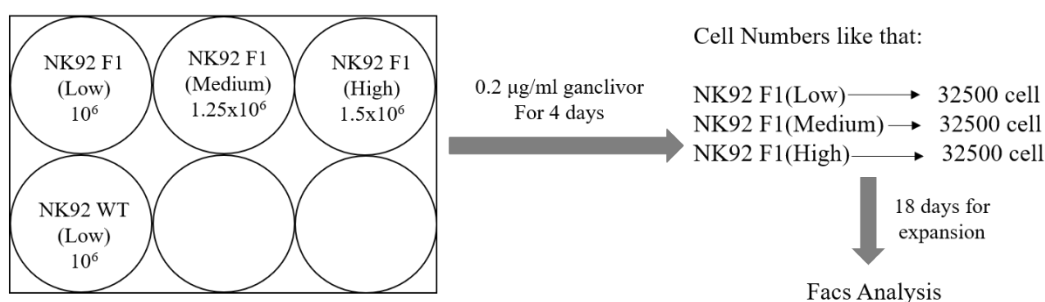


**Figure 4. 14. Experimental Design for F1 colony ganciclovir treatment:** F1(Low);  $5 \times 10^5$  cells per ml. F1(Medium);  $6.25 \times 10^5$  cells per ml. F1(High);  $7.5 \times 10^5$  cells per ml. NK-92 WT cells were set  $5 \times 10^5$  cells per ml. All cultures contained 2 ml.

	<b>GFP%</b>	<b>tdTomato %</b>
<b>NK-92 WT</b>	0.72	0.95
<b>NK-92 TK/GFP</b>	96.2	0.38
<b>NK-92 F1</b>	95.7	0.46
<b>F1(Low)</b>	1.43	0.93
<b>F1(Medium)</b>	2.03	0.52
<b>F1(High)</b>	2.57	0.52

**Table 4. 9. The percentage of GFP and tdTomato positive cells after ganciclovir treatment.**

In this experiment, we again could not detect tdTomato expression after ganciclovir treatment. We conclude that the numbers of tdTomato positive cells were quite low in the

beginning of drug treatment, which resulted in ineffective selection. To optimize the ratios of starting cell populations, we performed several additional experiments with different ratios of GFP positive TK expressing and tdTomato positive NK-92 cells.

#### 4.2.6. Coculturing feeder and target cells by using different ratios and different ganciclovir concentrations

We conducted a coculture experiment to grow a single tdTomato expressing cell in the presence of higher numbers of TK/GFP expressing cells. Experiments set up to contain different ratios (1:1, 1:2, 1:5, 1:10, 1:20, 1:50, 1:100, 1:200, 1:500, 1:1000, 1:10000, 1:100000) and different ganciclovir concentrations (0.01  $\mu\text{g/ml}$ , 0.1  $\mu\text{g/ml}$ , 1  $\mu\text{g/ml}$ , 2  $\mu\text{g/ml}$ ). Experimental designs are shown in Table 4. 10.

	<b>Ratio of tdTomato to TK/GFP</b>	<b>Ganciclovir Concentration</b>
<b>Experiment 1</b>	1:1-1:20	1 $\mu\text{g/ml}$
<b>Experiment 2</b>	1:50-1:1000	0.1 $\mu\text{g/ml}$
<b>Experiment 3</b>	1:50-1:1000	0.01 $\mu\text{g/ml}$
<b>Experiment 4</b>	1:100-1:100000	From 0.01 $\mu\text{g/ml}$ To 1 $\mu\text{g/ml}$

**Table 4. 10. Experimental Design for Coculture Experiments**

##### 4.2.6.1. Coculture Experiment 1

NK-92 TK/GFP and NK92-iT2 cells were cocultured starting at a concentration of  $5 \times 10^5$  cells/ml with different ratios (1:1, 1:2, 1:5, 1:10, 1:20) (shown in Table 4. 11) under  $1 \mu\text{g/ml}$  ganciclovir selection for 26 days. Cells were counted and FACS analysis was performed every two days. Ganciclovir concentration was altered at different times to retain a healthy culture of cells. Because of the stringent selection conditions, on day 4, the total cell number decreased to  $4 \times 10^5$  for the 1:10 and to  $2 \times 10^5$  for the 1:20 ratio cultures and we decreased the concentration of ganciclovir to 0.2  $\mu\text{g/ml}$ . The changes in the percentage of GFP and tdTomato expressing cells during the culture is shown in Figure 4. 15. tdTomato expressing cells increased to 83% (similar to the original tdTomato population) on day 10 for the 1:1 and the 1:2 ratios. All cells died at day 10 for the 1:20 ratio and at day 16 for the 1:5 ratio.



However, the 1:10 ratio starting culture survived and tdTomato expression reached approximately 94% on day 26.

NK92 tdTomato: NK92 TK/GFP	Cell Number of NK92 tdTomato	Cell Number of NK92 TK/GFP	Total Cell Number
<b>1:1</b>	$1.25 \times 10^6$	$1.25 \times 10^6$	$2.5 \times 10^6$
<b>1:2</b>	$8.33 \times 10^5$	$1.66 \times 10^6$	$2.5 \times 10^6$
<b>1:5</b>	$4.16 \times 10^5$	$2.08 \times 10^6$	$2.5 \times 10^6$
<b>1:10</b>	$2.27 \times 10^5$	$2.27 \times 10^6$	$2.5 \times 10^6$
<b>1:20</b>	$1.19 \times 10^5$	$2.38 \times 10^6$	$2.5 \times 10^6$

**Table 4. 11. Cell Numbers and Ratios for NK92 iT2 and TK/GFP populations in Coculture Experiment 1**

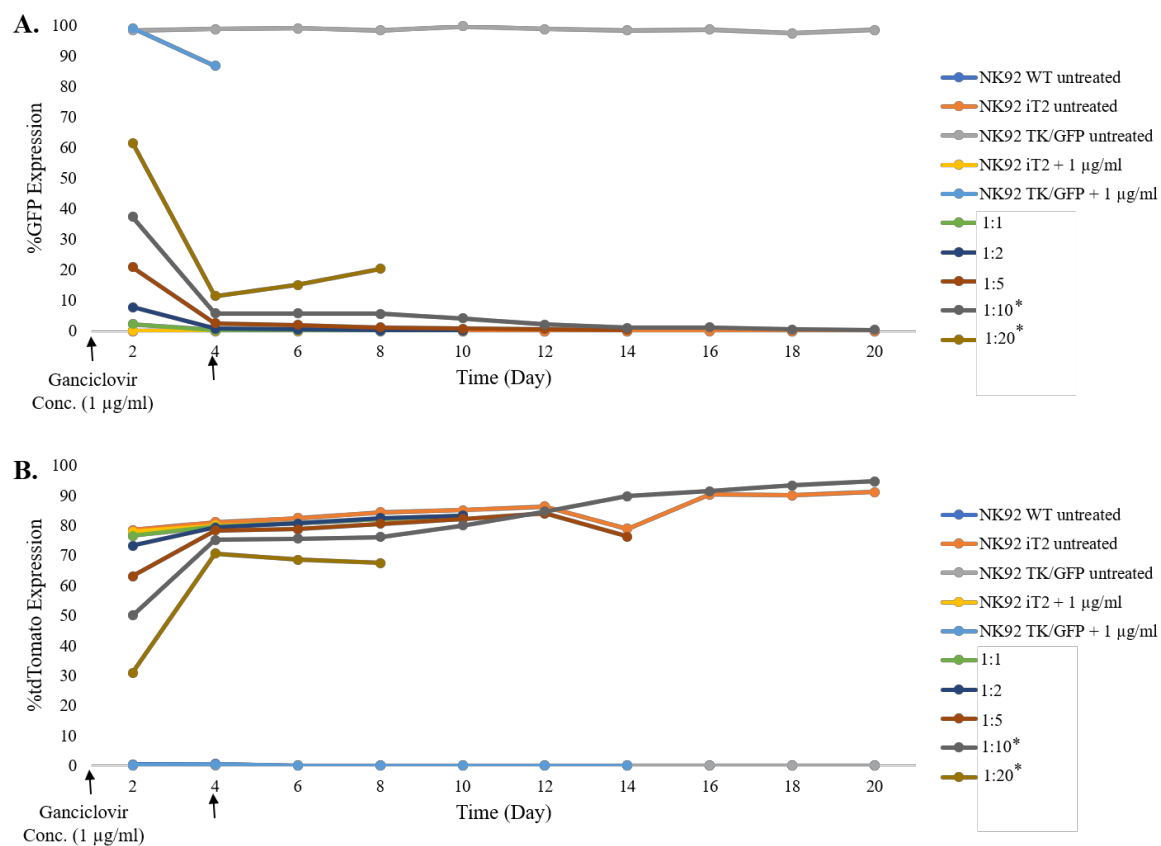


**Figure 4. 15. The percentage of GFP and tdTomato positive cells in Coculture Experiment 1** (A) Decrease in GFP expression is shown. (B) Increase in tdTomato expression is shown. All cells were incubated with 1 µg/ml ganciclovir except those indicated by (\*) which were switched to 0.2 µg/ml at the time points indicated by arrows.

#### 4.2.6.2. Coculture Experiment 2

NK-92 TK/GFP and NK92-iT2 cells were cocultured starting at a concentration of  $5 \times 10^5$  cells/ml in 5 ml with different ratios (1:50, 1:100, 1:200, 1:500, 1:1000) ( Table 4. 12) under 0.1µg/ml ganciclovir selection for 50 days. Cells were counted and FACS was done every two days. Ganciclovir concentration was altered at different times to retain a healthy culture of cells. Because of the stringent selection conditions, cultures with a starting ratio of 1:500 and 1:1000 died on day 12 and those with a 1:200 died on day 18. The starting cultures with a 1:50 and 1:100 ratios had roughly 145000 on day 32 where most of the cells were tdTomato positive (80%) and few were GFP positive (7%). To eliminate remaining GFP positive cells, we continued the experiment until day 50 increasing ganciclovir titration to 1 µg/ml ganciclovir between day 36 and 46 and to 2 µg/ml ganciclovir for the last 4 days. The percentage of GFP expression decreased to 2%. (Figure 4. 16)

<b>NK92 tdTomato: NK92 TK/GFP</b>	<b>Cell Number of NK92 tdTomato</b>	<b>Cell Number of NK92 TK/GFP</b>	<b>Total Cell Number</b>
<b>1:50</b>	$4.9 \times 10^4$	$2.45 \times 10^6$	$2.5 \times 10^6$
<b>1:100</b>	$2.47 \times 10^4$	$2.47 \times 10^6$	$2.5 \times 10^6$
<b>1:200</b>	$1.24 \times 10^4$	$2.48 \times 10^6$	$2.5 \times 10^6$
<b>1:500</b>	$4.99 \times 10^3$	$2.49 \times 10^6$	$2.5 \times 10^6$
<b>1:1000</b>	$2.49 \times 10^3$	$2.49 \times 10^6$	$2.5 \times 10^6$

**Table 4. 12. Cell Numbers and Ratios for NK92 iT2 and TK/GFP populations in Coculture Experiment 2**

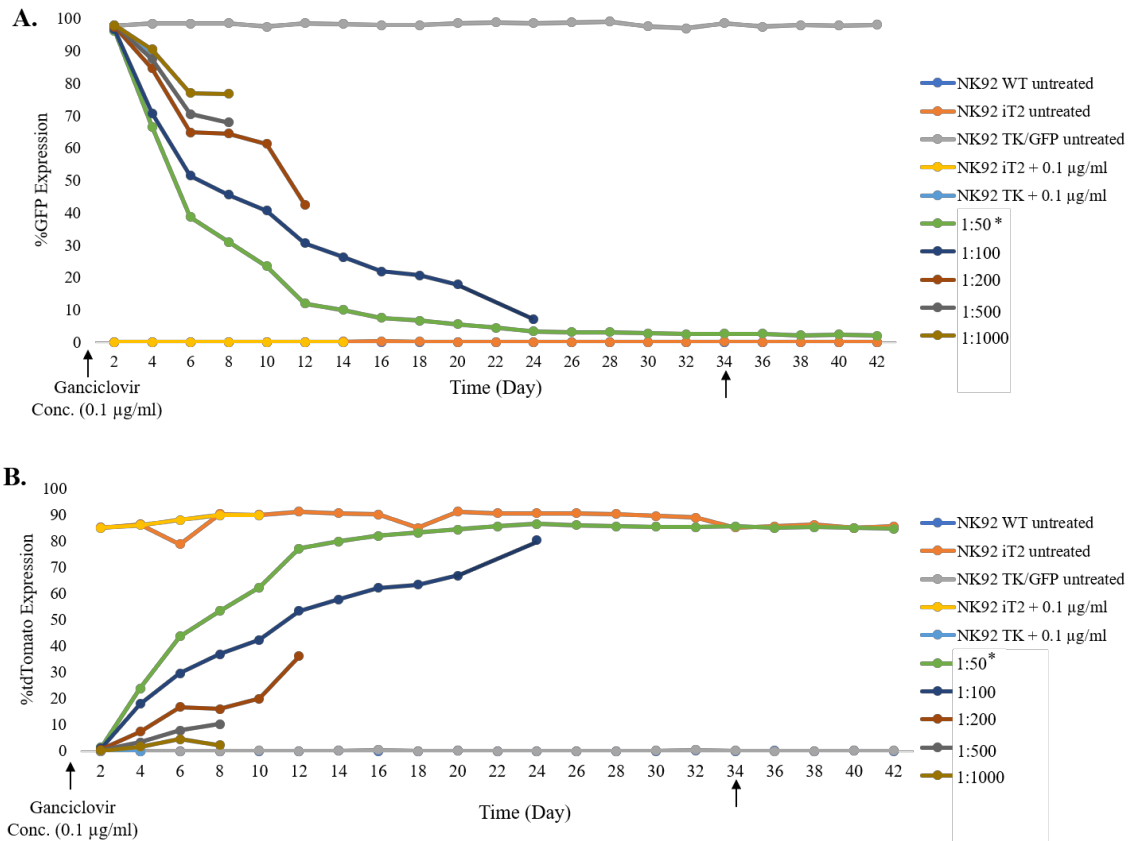


**Figure 4. 16. The percentage of GFP and tdTomato positive cells in Coculture Experiment 2 (A)Decrease in GFP expression is shown until day 42. (B) Increase in tdTomato expression is shown until day 40. All cells were incubated with 0.1 µg/ml ganciclovir except those indicated by (\*) which were switched to 1 µg/ml at the time points indicated by arrows.**

#### 4.2.6.3. Coculture Experiment 3

NK-92 TK/GFP and NK92-iT2 cells were cocultured starting at the concentration of  $5 \times 10^5$  cells/ml in 5 ml with different ratios (1:50, 1:100, 1:200, 1:500, 1:1000) (Table 4. 13) under 0.01µg/ml ganciclovir selection for 40 days. Cells were counted and FACS analysis was done every two days. Ganciclovir concentration was changed at different times to retain a healthy culture of cells. The starting culture with 1:50 ratio survived and reached 85% tdTomato positive cells on day 34, and ganciclovir concentration increased to with 0.1 µg/ml ganciclovir between day 16 and day 20 and to 1 µg/ml ganciclovir for last 12 days. The

starting culture with 1:100 and 1:200 ratios survived and percentage of tdTomato expressing cells reached to 83% and to 70% on day 40, respectively. Their ganciclovir concentration increased to 0.1 µg/ml between day 20 and day 22 and to 1 µg/ml ganciclovir for last 18 days. The 1:500 ratio starting culture survived and tdTomato expression reached 44% day 40, and ganciclovir concentration increased to 0.1 µg/ml between day 22 and 24 and to 1 µg/ml for last 16 days. The 1:1000 ratio starting culture also survived and tdTomato expression reached 22% day 40, and ganciclovir concentration increased to 0.1 µg/ml between day 24 and 26 and to 1 µg/ml for last 14 days (Figure 4. 17)

Cells treated by 0.01 µg/ml ganciclovir gain a resistant to ganciclovir. Death rate of them decrease to very low even with 1 µg/ml ganciclovir.

<b>NK92 tdTomato: NK92 TK/GFP</b>	<b>Cell Number of NK92 tdTomato</b>	<b>Cell Number of NK92 TK/GFP</b>	<b>Total Cell Number</b>
<b>1:50</b>	4.9x10 <sup>4</sup>	2.45x10 <sup>6</sup>	2.5x10 <sup>6</sup>
<b>1:100</b>	2.47x10 <sup>4</sup>	2.47x10 <sup>6</sup>	2.5x10 <sup>6</sup>
<b>1:200</b>	1.24x10 <sup>4</sup>	2.48x10 <sup>6</sup>	2.5x10 <sup>6</sup>
<b>1:500</b>	4.99x10 <sup>3</sup>	2.49x10 <sup>6</sup>	2.5x10 <sup>6</sup>
<b>1:1000</b>	2.49x10 <sup>3</sup>	2.49x10 <sup>6</sup>	2.5x10 <sup>6</sup>

**Table 4. 13. Cell Numbers and Ratios for NK92 iT2 and TK/GFP populations in Coculture Experiment 3**

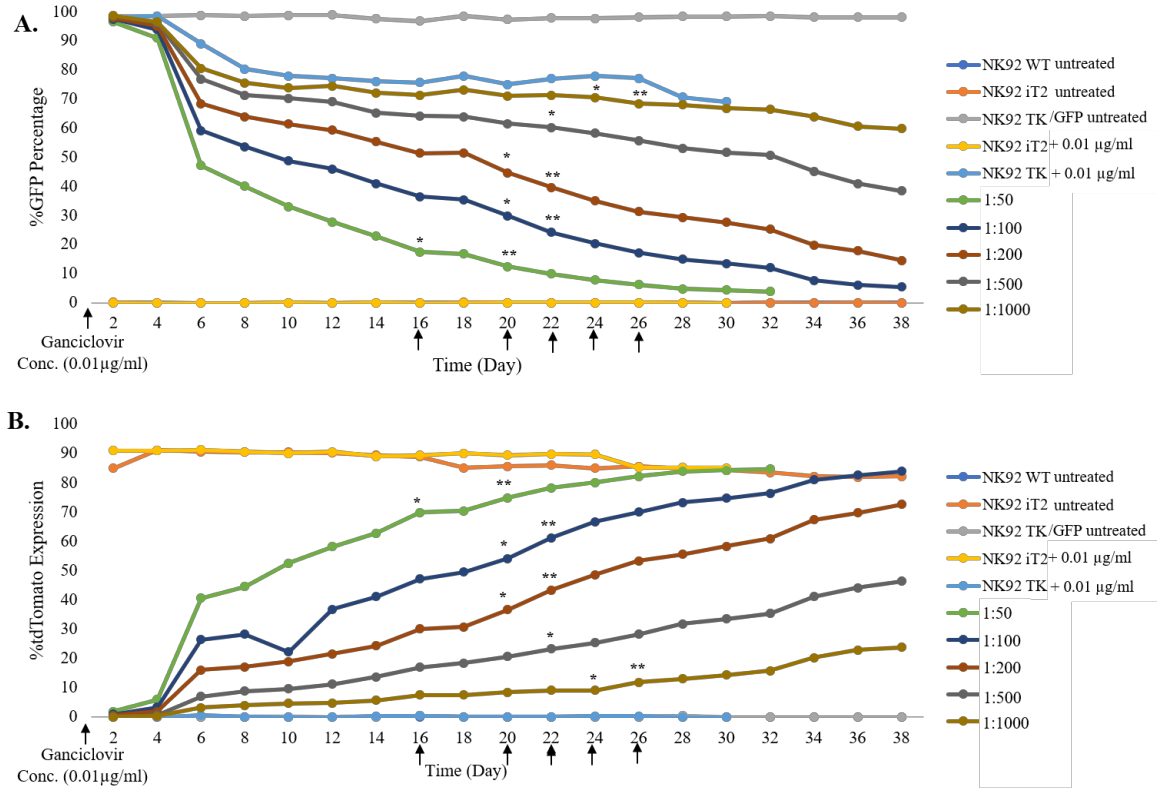


**Figure 4. 17. The percentage of GFP and tdTomato positive cells in Coculture Experiment 3. (A) Decrease in GFP expression is shown. (B) Increase in tdTomato expression is shown. All cells were incubated with 0.01 µg/ml ganciclovir except those indicated by (\*) which were switched to 0.1 µg/ml at the time points indicated by arrows, and by (\*\*) which were switched to 1 µg/ml at the time points indicated by arrows.**

#### 4.2.6.4. Coculture Experiment 4

NK-92 TK/GFP and NK92-iT2 cells were cocultured starting at a concentration of  $3.5 \times 10^5$  cells/ml in 500 µl with different ratios (1:100, 1:1000, 1:10000, 1:100000) (Table 4. 14). Ganciclovir was not given until they reached approximately  $2.5 \times 10^6$  cells. NK-92 TK/GFP and NK92-iT2 cocultures were set at a concentration of  $5 \times 10^5$  cells/ml in 5 ml and 0.01 µg/ml ganciclovir selection was started after 7 days. Cells were counted and FACS was performed every two days. Ganciclovir concentration was altered at the different times to retain a healthy culture of cells.

The ratio 1:100 starting culture survived and percentage of tdTomato expressing cells reach to 83.6% (similar to the original tdTomato expressing cells) on day 8. Ganciclovir concentration increased to 0.1µg/ml on day 6 and to 1 µg/ml on day 8.

The ratio 1:1000 and 1:10000 starting cultures survived and percentage of tdTomato expressing cells reach to 74% on day 20 and 30 % on day 30, respectively. Ganciclovir concentration of the 1:1000 starting culture increased to 0.1µg/ml between day 8 and 12 and to 1 µg/ml between day 12 and 26. Ganciclovir concentration of the 1:10000 starting culture increased directly to 1 µg/ml between day 12 and 26. The ratio 1:100000 starting culture survived but percentage of tdTomato expressing cells did not increased until the end of the experiment. Ganciclovir selection of the 1:100000 starting culture started with 0.1µg/ml on day 14 and increased to 1 µg/ml between day 12 and 26. The percentage of tdTomato expressing cells did not change significantly between day 20 and 28 under 1 µg/ml ganciclovir selection. To eliminate the remaining GFP positive cells and the remaining puromycin negative cells, we increased ganciclovir concentration to 2 µg/ml and added 1 µg/ml puromycin between day 28 and day 32. We did not detect significant increase the percentage of tdTomato expressing cells for last 4 days (Figure 4. 18).

The starting culture with 1:10000 ratio had only 17 NK-92 tdTomato expressing cells theoretically and this number of tdTomato expressing NK-92 cells could become a healthy tdTomato expression population by coculturing with TK/GFP expressing feeder cells.

<b>NK92 tdTomato: NK92 TK/GFP</b>	<b>Cell Number of NK92 tdTomato</b>	<b>Cell Number of NK92 TK/GFP</b>	<b>Total Cell Number</b>
<b>1:100</b>	1732	1.73x10 <sup>5</sup>	1.75x10 <sup>5</sup>
<b>1:1000</b>	174.8	1.74x10 <sup>5</sup>	1.75x10 <sup>5</sup>
<b>1:10000</b>	17.49	1.74x10 <sup>5</sup>	1.75x10 <sup>5</sup>
<b>1:100000</b>	1.74	1.74x10 <sup>5</sup>	1.75x10 <sup>5</sup>

**Table 4. 14. Cell Numbers and Ratios for NK92 iT2 and TK/GFP populations in Coculture Experiment 4.**

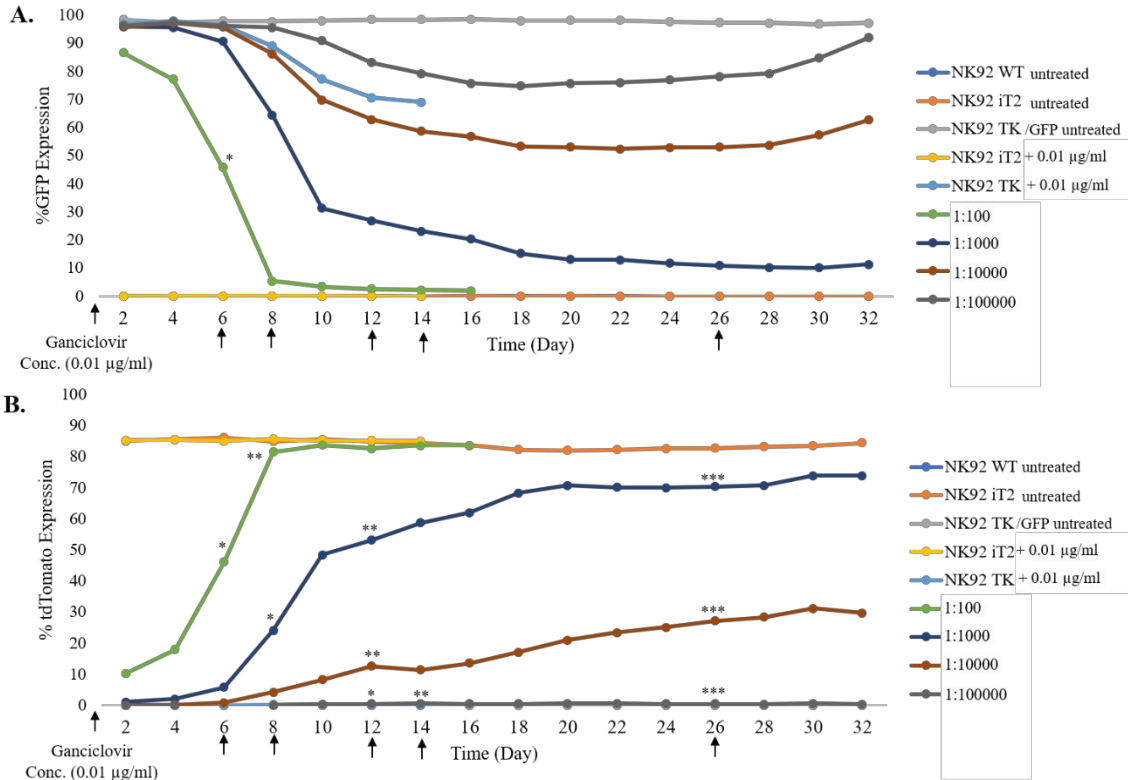


**Figure 4. 18. The percentage of GFP and tdTomato positive cells in Coculture Experiment 4. (A)** Decrease in GFP expression is shown. **(B)** Increase in tdTomato expression is shown. All cells were incubated with 0.01  $\mu$ g/ml ganciclovir except those indicated by (\*) which were switched to 0.1  $\mu$ g/ml at the time points indicated by arrows, and by (\*\*) which were switched to 1  $\mu$ g/ml at the time points indicated by arrows, and by (\*\*\*) which were switched to 2  $\mu$ g/ml ganciclovir and 1  $\mu$ g/ml puromycin at the time points indicated by arrows.

### 4.3. Production of Mutated Pools by CRISPR/Cas9 Genome Editing Method

Our aim is to find important immunological genes for cytotoxicity of the NK-92 cell line. Our starting point was a list of candidate genes identified by the 3i consortium that play a role in the cytotoxicity of CTLs. We first checked whether these genes were expressed by NK-92 cells by using the results of a previous RNA-seq experiment conducted in our laboratory. Transcripts per million were calculated and results were normalized to GAPDH expression (Figure 4. 19). We also targeted two other genes Ccdc124 and Tsg101 important for MTOC function and the formation of the cSMAC of the cytotoxic T cells respectively[108].

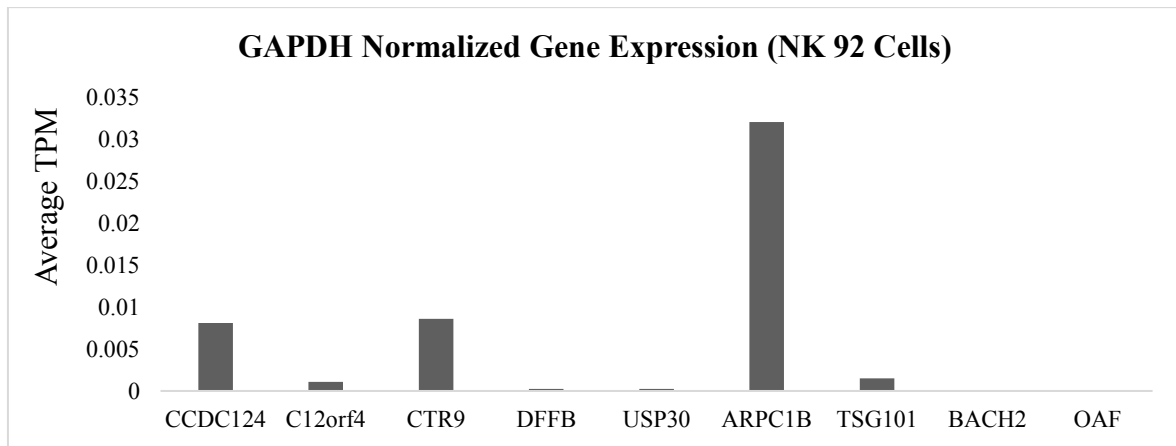


**Figure 4. 19. Expression pattern of candidate genes in NK-92 cells.** Average of TPM was calculated and they were normalized to GAPDH.

#### 4.3.1. Cloning of gRNA into pLentiCRISPR\_v2 plasmid

The CRISPR/Cas9 genome editing method was used to create mutated pools of NK-92 cells. gRNAs were designed to exons which are common for all alternative spliced transcripts of the genes. gRNAs sequences and the location of PAM sequences for each gene are shown in Figure 4. 20. Oligonucleotides encoding gRNA sequences were annealed and cloned into the BsmBI digested pLentiCRISPRv2 vector (Figure 4. 21). Ligated products were transformed into chemically competent Top10 strain of *E.coli* spread onto an agar plate with a proper antibiotic for 16 h incubation at 37°C. Colonies were selected and plasmid DNA isolation was performed. The presence of oligonucleotides cloned in the vector was checked by BsmBI digestion or EcoRI-HF and NdeI double digestion. The cutting site for BsmBI was destroyed upon ligation and the presence of an insert was determined by the absence of digestion by this enzyme. For plasmids with an insert, EcoRI-HF and NdeI double digestion yielded three bands of 10542, 2301 and 178 bp. Colonies that scored positive in the diagnostic digestions were verified by sequencing. We purified plasmids by Midiprep DNA purification from sequence verified colonies to be used for transfection.



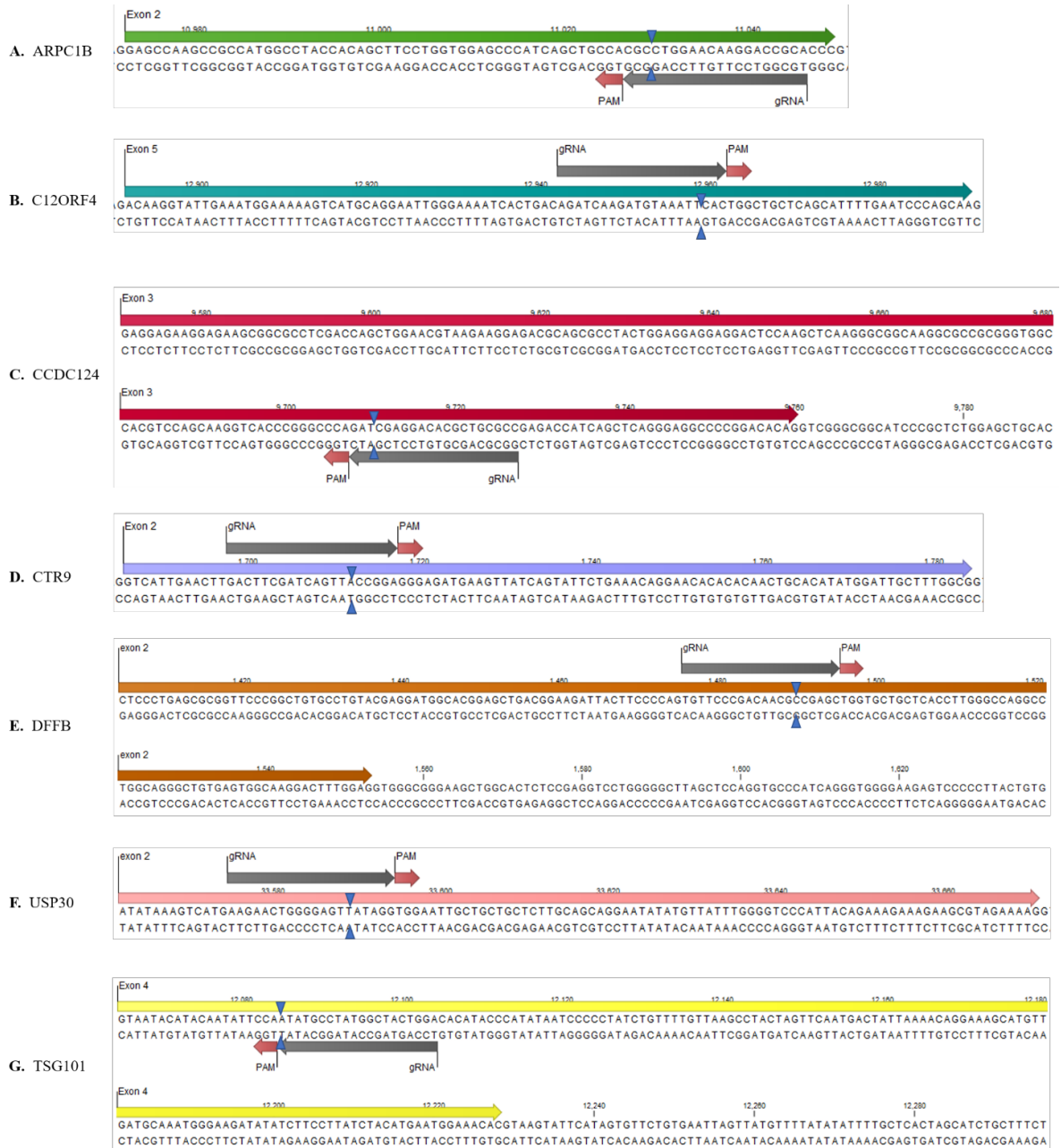


**Figure 4. 20. Guide RNA design for targeting candidate genes.** gRNAs are represented as grey and PAM sequences are represented as a pink. Blue arrow shows the location where Cas9 enzyme cut dsDNA. **(A)** Second exon of ARPC1B gene (green) was targeted. **(B)** Fifth exon of C12ORF4 gene (blue) was targeted. **(C)** Third exon of CCDC124 (red) was targeted. **(D)** Second exon of CTR9 gene (cyan) was targeted. **(E)** Second exon of DFFB (orange) was targeted. **(F)** Second exon of USP30 (light pink) was targeted. **(G)** Fourth exon of TSG101 (yellow) was targeted.

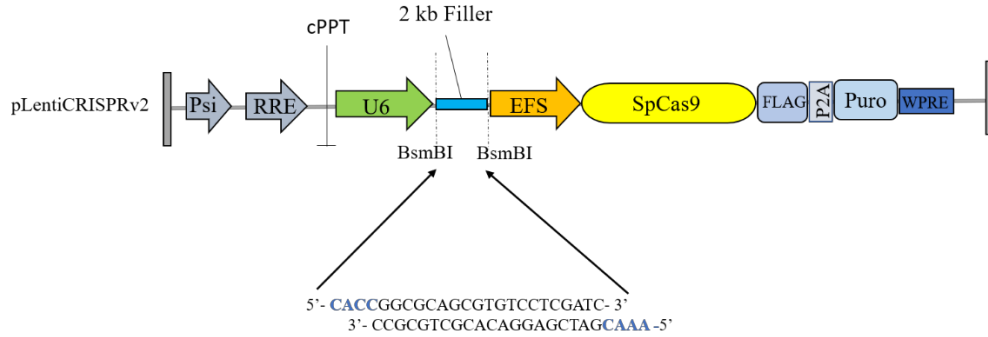
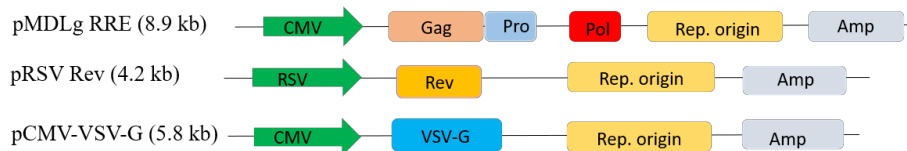


**Figure 4. 21. Map of the pLentiCRISPRv2 plasmid and a representative annealed oligonucleotide inserted into the BsmBI site.** Oligonucleotide was cloned into the pLentiCRISPRv2 plasmid by complementary flanking regions which are shown as a blue.

#### 4.3.2. Production and Transduction of Lentivirus into the NK-92 cell line

Vectors which were used for lentivirus production are shown in Figure 4. 22. pLentiCRISPRv2 with gRNAs and packaging plasmids were transferred into HEK293FT cells to produce lentiviruses (Figure 4. 23). Lentiviruses were collected 24h and 36h after transfection. For the pLentiCRISPRv2\_ccdc124 virus, 5 ml of supernatant was used to transduce  $10^6$  NK-92 cells and infected cells were selected with 1  $\mu$ g/ml puromycin for 10 days. For the viruses targeting the C12orf4/Ctr9/Dffb/Usp30/Arpc1b/Tsg101 genes, 10 ml supernatant was used to transduce  $2 \times 10^6$  NK-92 cells followed by the same puromycin selection.

Packaging Plasmids that express viral genes deleted from vector backbone:



Plasmid that expresses vector genome:

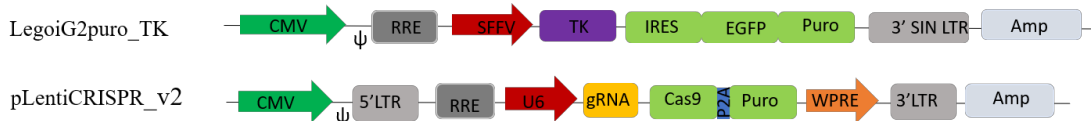


**Figure 4. 22. Vectors for third generation virus production.** Top part shows packaging plasmids. Bottom part shows vector we used to put gene of interest into virus.

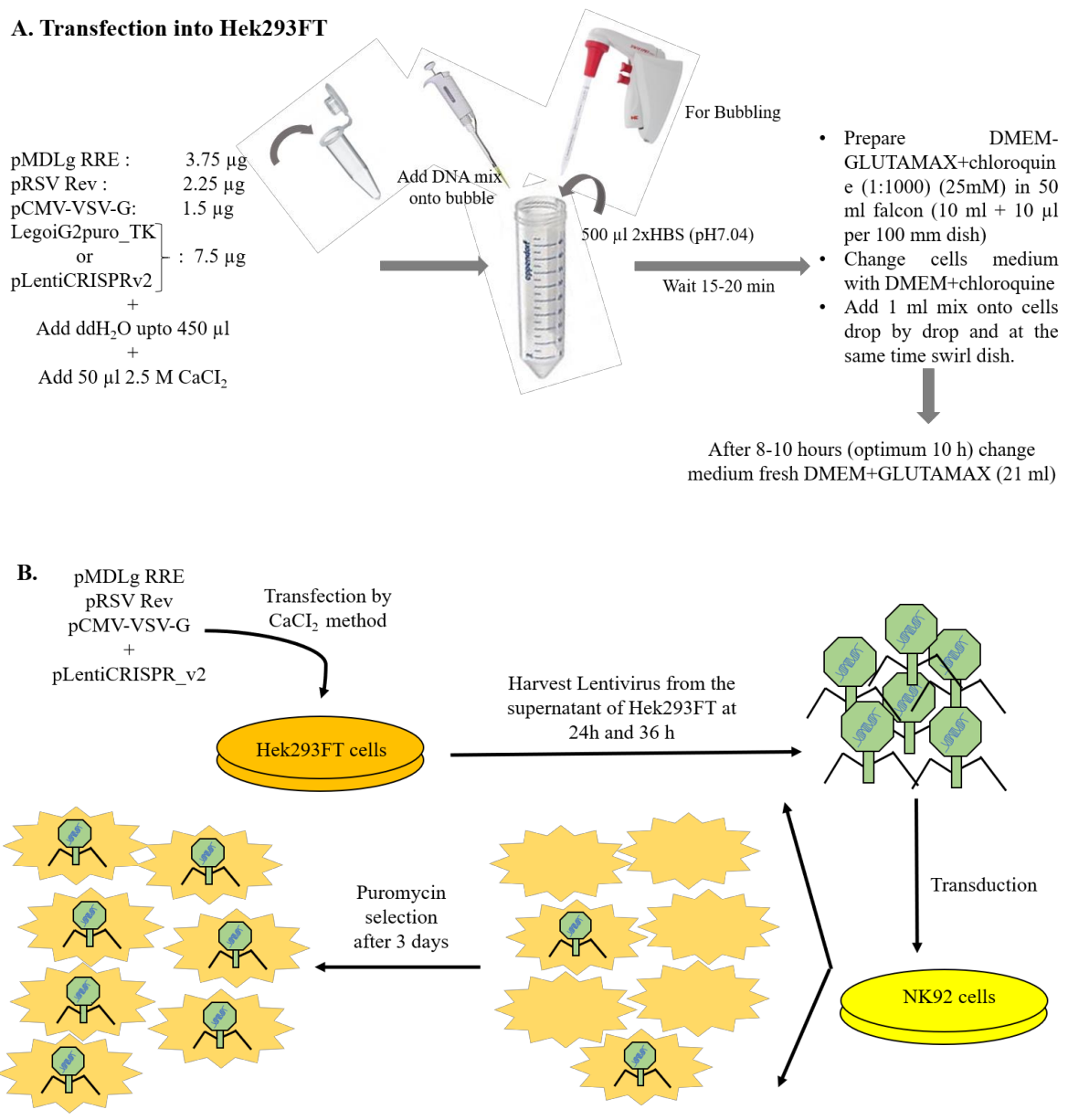


**Figure 4. 23. Experimental design of the production of lentivirus with expressing CRISPR/Cas9 targeting different genes in NK-92 cells (A) Protocol for transfection into the HEK293 packaging cells. (B) Protocol for the production and transduction with lentivirus.**

### 4.3.3. Analysis of Mutations by the T7 Assay and QRT-PCR

Genomic DNA isolation was performed from each pool of infected NK-92 cells and the T7 assay was performed. Genomic fragments from the targeted region were amplified with the identified primers. The length of the targeted region is shown for each genes in Table 4. 15.

	Length of DNA Fragment
<b>Arpc1b</b>	258 bp
<b>C12orf4</b>	309 bp
<b>Ccdc124</b>	385 bp
<b>Ctr9</b>	328 bp
<b>Dffb</b>	345 bp
<b>Usp30</b>	382 bp
<b>Tsg101</b>	298 bp

**Table 4. 15. Length of DNA fragment with targeted part**

PCR products were digested by the T7 endonuclease enzyme and digested products were analyzed on agarose gels (Figure 4. 24). NK-92 WT genomic DNA was used as a negative control.

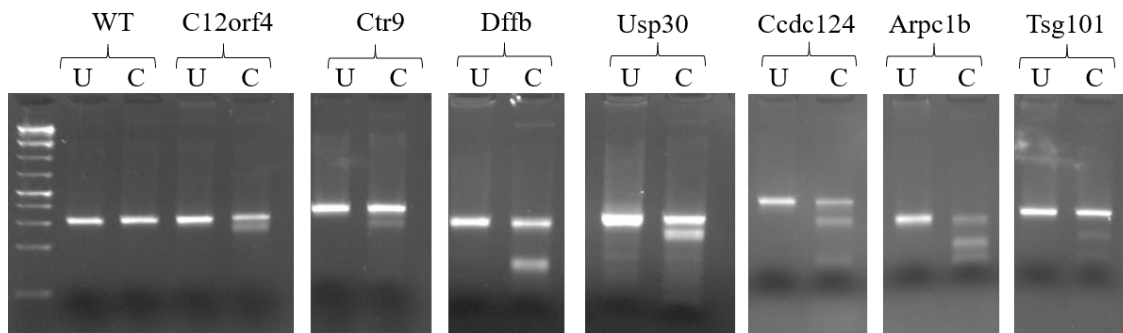


**Figure 4. 24. T7 Assay Results.** WT was a negative control group. U represent uncut non-T7 enzyme treated. C is cut meaning T7 enzyme treated.

The presence of mutations in each pool was confirmed by the T7 assay. Then, RNA isolation and qRT-PCR were performed to check mRNA expression level. RNA isolation was performed twice from cells that were thawed on different days by the Trizol method. They were loaded on the gel to check whether RNA is intact. Bands for 28S, 18S and 5S ribosomal RNA were used to confirm the intactness of mRNA (Figure 4. 25).

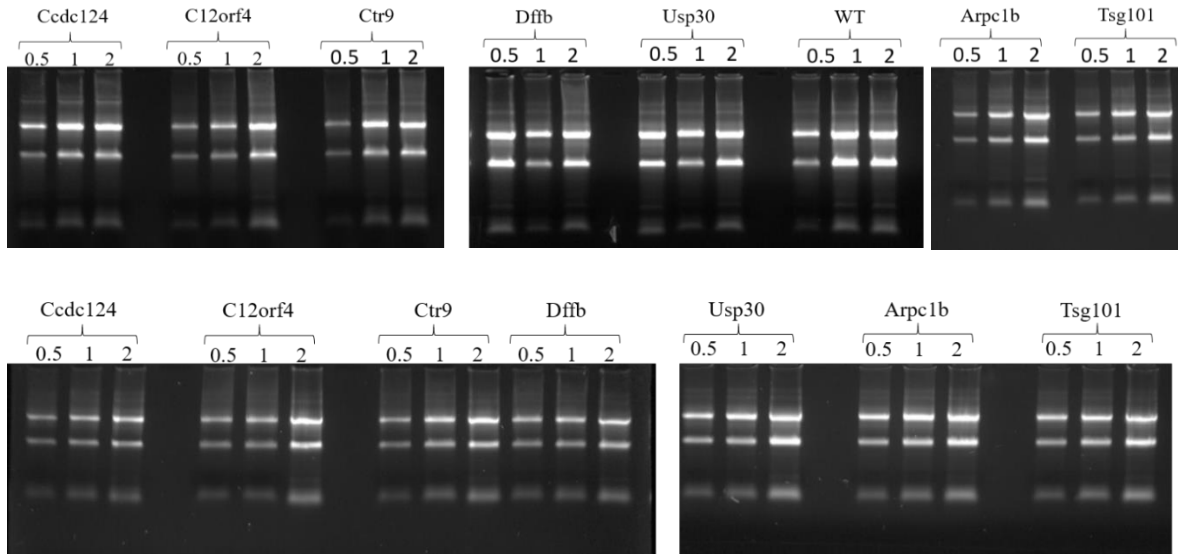


**Figure 4. 25. RNA Isolation Results.** (A) First RNA Isolation and (B) Second RNA Isolation: 0.5  $\mu$ l, 1  $\mu$ l and 2  $\mu$ l RNA were loaded.

cDNA synthesis was performed by using 2  $\mu$ g total RNA according to manufacturer's instructions using a reverse transcription kit. cDNAs were diluted 1 to 100 and QRT-PCR was performed with selected  $T_m = 57^\circ\text{C}$ . qRT-PCR repeated twice except for Ctr9 mutant pool. Relative fold changes of gene expressions was calculated, and normalized to GAPDH expression (Figure 4. 26). We found that in targeted NK-92 cells the mRNA expression levels decreased for each mutant pool.

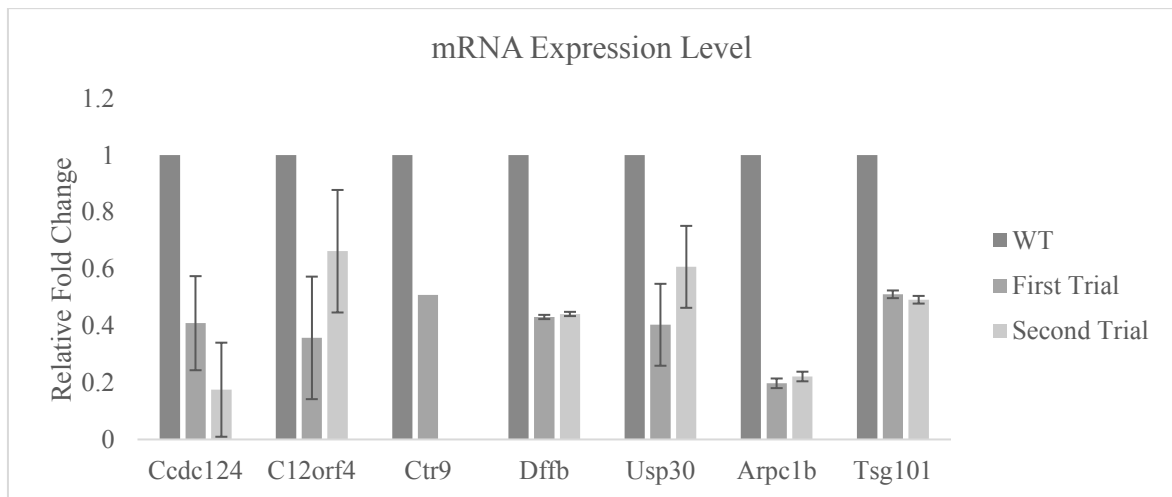


**Figure 4. 26. QRT-PCR quantification of gene expression in targeted NK-92 cells.** Relative fold change in gene expression for each candidate gene was calculated. RNA was

isolated from CRISPR targeted cells on two consecutive dates and independent qRT-PCR was performed.

#### **4.4. Cytotoxic Tests for Mutated Pools**

In the pools of cells that contained mutations (as determined by the T7 assay) and a decrease in targeted gene expression (as determined by QRT-PCR), we performed functional cytotoxicity tests such as a degranulation assay and an xCELLigence real time cell growth analysis assay to check role of these genes in the cytotoxicity of NK-92 cells.

##### **4.4.1. Degranulation Assay**

NK-92 cells release cytolytic granules when they recognize their target. Anti-CD107 $\alpha$ /LAMP-1 (Lysosome-associated membrane protein) antibody binds to a protein that translocate to the surface of NK cells that degranulate.  $2 \times 10^5$  target cells (MCF-7 and K562) were resuspended in NK-92 medium and plated in V-bottom 96 well plates.  $2 \times 10^5$  Effector cells (NK-92 WT and mutant cells) were resuspended in NK-92 medium in the presence of 1 $\mu$ l Anti-CD107 $\alpha$  antibody per well. For the negative control group, only effector cells were plated. For the positive control group, PMA (final concentration is 1.25  $\mu$ g)-Ionomycin (final concentration is 0.25  $\mu$ g) to effector cells. Cells were incubated for 1 hour and monensin (final concentration 2  $\mu$ M) were added into each well. Monensin prevents reinternalization of CD107 $\alpha$  via the endocytic pathway. Cells were incubated 4 more hours and FACS analysis was done to check the surface expression levels of CD107 $\alpha$ .

Each experiment was done in duplicate and repeated for twice. In the first experiment, K562 was used as a target cell. We used K562 cells which were transduced by lentivirus encoding the GFP-puro fusion protein. Normally, CD56 antibody is used to separate NK-92 cells from target cells. Instead of using CD56 antibody, we separated NK-92 cells from K562 by gating away GFP negative cells (Figure 4. 27). Surprisingly, the cytotoxicity of Tsg101 mutated NK-92 cell pools were higher than the cytotoxicity of WT cells. Except for Arpc1b and Tsg101, all other mutated pools showed less cytotoxicity to MCF-7 than WT.

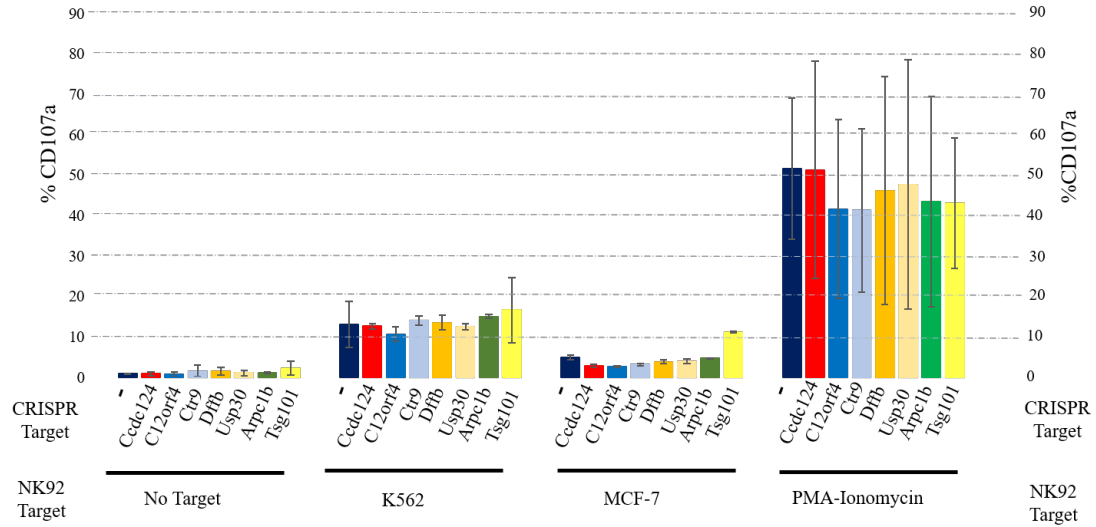


**Figure 4. 27. Expression of CD107a in the Degranulation Assay.** Degranulation of the NK-92 WT and mutant pools towards to K562 and MCF-7 are shown.

#### 4.4.2. xCELLigence Real Time Cell Analysis Assay

The xCELLigence RTCA experiment gives information about cell death and proliferation by using plates with gold electrodes. Attachment of adherent cells on the E-plate impede electrical current, and signal change is recorded as a cell index (CI). Effector cells were added to the wells before the cell index of target cells reach to 1. To determine the proliferation properties of the target cells in 24 hours we plated and incubated different numbers of MCF-7 cells (Figure 4. 28). A starting population of  $1.5 \times 10^4$  MCF-7 cells were selected for further experiments.

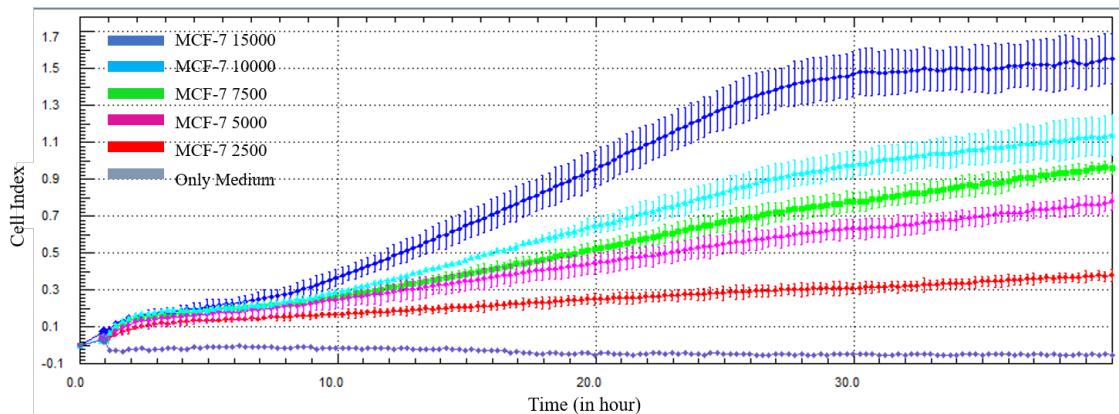
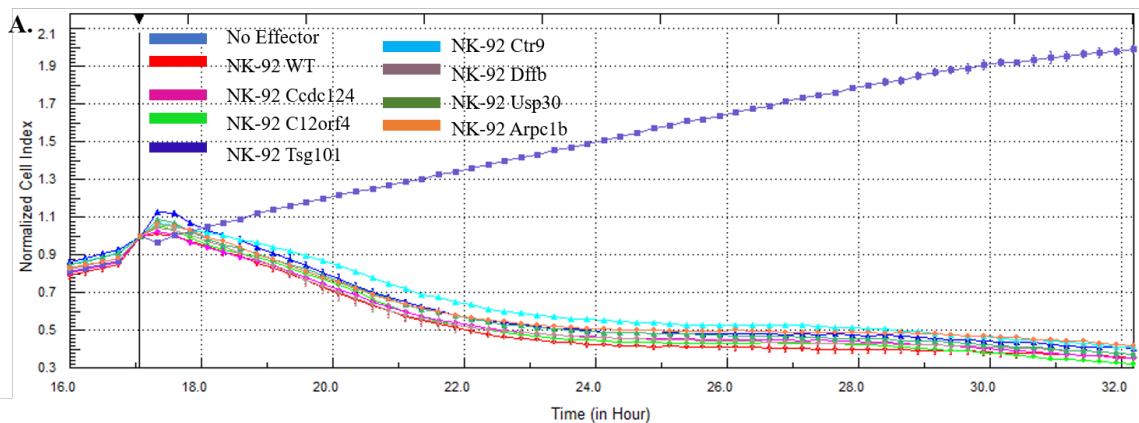


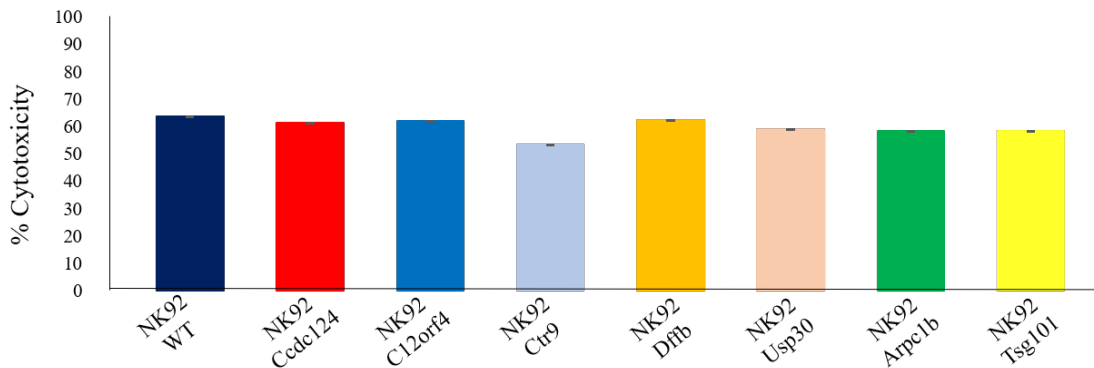
**Figure 4. 28. Proliferation of MCF-7 cells in the xCELLigence RTCA machine.** Different number of MCF-7 cells were seeded on the plate. Cell proliferation was checked around 24 h and  $1.5 \times 10^4$  MCF-7 cells were chosen.

We chose a 2:1 Effector:Target Ratio, thus  $1.5 \times 10^4$  MCF-7 cells were seeded and after 17 hours,  $3 \times 10^4$  Effector NK-92 WT or Mutant cell pools were plated on top of the target cells. Killing of target cells was assessed until 32 hours (Figure 4. 29). Cytotoxicity becomes evident when target cells start detaching from the plate and the CI starts to decrease. We noted that among all the mutants, only the cytotoxicity of the Ctr9 targeted NK-92 pools were significantly different from the cytotoxicity of NK-92 WT cells. This effect was only evident at short timepoints (eg. 5 hr) and not after prolonged incubation (eg. 18 hr). We hypothesized that Ctr9 protein may have a role in the attachment of NK-92 cells to target cells and the formation of the immune synapse. It does not look like Ctr9 mutant cells have significant defects in degranulation of the NK-92 cells.





### B. Cytotoxicity at 5 hour



### C. Cytotoxicity at 18 hour

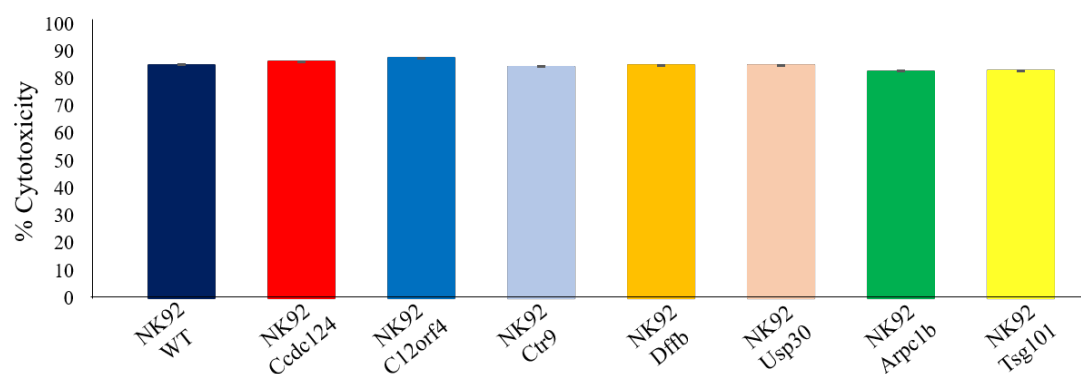


**Figure 4. 29. xCELLigence RTCA results for NK-92 WT and Mutant & MCF-7 target cells. (A)** Time & Normalized Cell Index graph is shown. **(B)** Cytotoxicity Percentage of the NK-92 WT and Mutant Pools towards to MCF-7 is shown at hour 5 after addition of effector cells. **(C)** Cytotoxicity Percentage of the NK-92 WT and Mutant Pools towards MCF-7 targets is shown at hour 18 after addition of effector.

## 5. DISCUSSION

NK cells are the crucial protectors of the body against cancer cells and infected cells. Using engineered NK-92 cells in the treatment of disease is a hot and developing topic. Tools which are used to engineer NK-92 cells should be optimized. Also, the cytotoxic mechanisms of the NK-92 cells should be investigated to make them a stronger candidate for immunotherapies. Previous work demonstrated that administered NK-92 cells in malignant melanoma decreased tumor burden and increased viability of mice 1.5-2.5 fold in a xenograft model [36].

In order to identify efficient methods for gene transfer into NK cell, we tried to optimize of Neon Electroporation methods and generation of single cell clones. NK-92 cells are resistant to gene delivery and previous studies demonstrated that plasmid delivery into these cells by transfection is almost impossible. Most transfected cells were not viable and compared to other lymphoid cell lines, transfection efficiencies were very low. Transduction by using third generation lentivirus method is the best way to deliver plasmids into NK-92 cells. However, this method is not very safe for delivering genome editing enzymes. Although in this study we transferred the Cas9 and gRNA encoding genes by lentiviral transduction into the genome of NK-92 cells, this results in a stable expression of this genome editing enzyme. This approach has the potential to increase the off-target effects of the CRISPR/Cas9 enzyme. To solve this problem, we aimed to optimize the Neon Electroporation technique on this cell line. We could only obtain a transfection efficiency of 30-46% and cell viability around 10-25%. We further tried to optimize conditions by changing cell number, electroporation number, DNA concentration, tip type and by using condition medium. We could not find suitable conditions for Neon transfection that are better than the suggested methods especially when large plasmids containing the Cas9 and guide RNA encoding genes were used. Therefore, we concluded that lentiviral gene transfer methods are the optimal when using this cell line.

CRISPR/Cas9 methods create double strand breaks which are repaired by NHEJ or HDR. In our study, we relied on NHEJ because we did not supply donor DNA for HR. In CRISPR/Cas9 genome editing, each cell in the pool of mutated cells contains a different mutation due to the random nature of double stranded break repair by NHEJ. For that reason, single cell cloning must be performed to obtain isogenic mutated cells. Even so, the

possibility exists that a single cell cloned line may have two different mutant alleles. Making a single cell clone from the NK-92 cells is a problem because these cells grow in colonies and cannot thrive as single cells. We generated a feeder NK-92 cell line by transduction of lentivirus encoding HSV-TK gene into the parental NK-92 cell line. Cells expressing HSV-TK can be negatively selected by ganciclovir treatment. Because the lentiviral vector expressing the HSV-TK gene also expressed GFP, we used expression of GFP as a surrogate to HSV-TK gene expression. FACS analysis showed that feeder cell pools were 98% GFP positive and 2% GFP negative. Even one cell that does not express TK gene is a problem for our experiment because ganciclovir treatment must negatively select all feeder cells. We thought that we could kill the GFP negative NK-92 cells by puromycin selection but were not successful in removing this GFP negative population. The NK-92-iT2 cell line was selected for limiting dilution assays. The increase in the percentage of tdTomato expressing NK-92-iT2 cells in a mixed population containing GFP expressing feeder NK-92 TK cells was interpreted as successful negatively of the feeder population by ganciclovir. After various optimization culture, we could grow a healthy culture starting with only 17 NK-92 iT2 cells by using a 1:10000 ratio of ganciclovir sensitive feeder cells selected under increasing doses of ganciclovir. In this selection experiment, at the end of day 26, tdTomato expressing cell reached 27% of the total. It is important to note that starting the selection with low doses (0.01  $\mu\text{g/ml}$ ) of ganciclovir generated ganciclovir resistant TK/GFP cells. We think it is a success to grow a healthy population of NK-92 cells originating from as few as 17 cells. Further purification likely will require single cell cloning by sorting by flow cytometry. We also attempted to clone tdTomato expressing NK-92 cells by starting an iT2:TK/GFP ratio of 1:100000. This ratio corresponds to approximately 1.7 cells in each originating well. While we could not isolate any cells from these originating wells, repetitions with higher numbers of single wells containing single cells may yield successful clones.

Our main aim in the third part of this study was to check whether genes which were defined by the 3i project have a role in the cytotoxicity of NK-92 cells. gRNAs were designed and cloned into the pLentiCRISPRv2 vector which was delivered into NK-92 cells by using third generation lentivirus. Validation of mutations in genomic DNA and decreases in mRNA expression level was performed by the T7 assay and QRT-PCR analysis. We identified that in all targeted cells, the mRNA for the corresponding gene expression levels were decreased

significantly. Then, cytotoxic analysis was done by the degranulation assay and xCELLigence RTCA experiments. As these CRISPR/Cas9 genome edited cells were not single cell cloned, it is possible that in the pool of mutated cells, there may be many different mutant alleles generated by NHEJ. It is our experience that the expression of pLentiCRISPR plasmid is so successful that the majority of the cells in the pool of targeted cells have mutant targeted loci. Because NHEJ is random, it is likely that 2/3 of these mutant cells harbor out of frame mutations that result in premature stop codons. It is well known that mRNAs encoding premature stop codons are degraded by nonsense mediated decay (NMD). We surmise that the reason for the dramatically decreased mRNA levels for the targeted genes is due to NMD. When we repeated the QRT-PCR at a later passage number from mutated cell pools, we obtained variable results. While gene specific mRNA expression level continued to decrease for Ccdc124 mutated cells, mRNA expression was increased for C12orf4 and Usp30 mutated cells, and was not altered for Dffb, Arpc1b and Tsg101 mutated cells. Because the Cas9 and gRNA encoding genes were stably inserted and expressed from the genome of the NK-92 cells, it is possible that selection events may favor cells that lack or express these targeted genes. The cytotoxicity of mutant pools of cells determined by the xCELLigence RTCA experiment indicated that Ctr9 mutated NK-92 cells showed lower cytotoxicity toward MCF-7 targets up to 9 hours. After this timepoint, the cytotoxicity of these Ctr9 mutated NK-92 caught up to their WT counterparts. It is possible that both WT and Ctr9 mutated cells can degranulate, so we did not see any significant differences in the degranulation assay. However, while Ctr9 mutated cells could degranulate, they could not direct their granules towards their specific targets. Under prolonged incubation of the target and the NK cells culture, it is possible that non-specifically released granules result in cytotoxicity of targets. Previous work has demonstrated that repression of Ctr9 expression increases the differentiation of naive T cells into Th17 cells and abolishes IL-6 responsive gene expression. IL-6 responsive genes were repressed by interacting with JAK/STAT3 pathway. IL-6 stimulation activates STAT3 and STAT3 binds to promoter of target gene where it associates with Ctr9-containing complex. This complex induces expression of target genes [88,89]. Those activated target genes might have a role in the movement or specific degranulation of NK-92 cells to target cells or in the production of cytolytic granules or their

release toward target cells. The role of Ctr9 gene in the cytotoxicity of NK-92 cells need further investigation.

We were surprised that there were no differences in the cytotoxicity of Arpc1b, C12orf4, Ccdc124 and Tsg101 mutated pools. Arpc1b is a member of the Arp2/3 complex. Arpc2/3 actin filament branching has a role in the formation of the immunological synapse of T cells [81,82]. Decreased F actin was observed in the IS in Arpc1b deficient T cells [83]. Arpc1b has an isoform which is Arpc1a. Isoform Arpc1a is expressed in tissue cells and Arpc1b is expressed in the hematopoietic cell lines. Arpc1b deficient Primary fibroblast cells did not show any impairment in migration behavior. It is possible that the expression of Arpc1a can rescue fibroblast cells from deficiency of Arpc1b [109]. RNA-seq results indicate that the NK-92 cell line also express Arpc1a. Thus, mutation in the Arpc1b gene may be rescued by its homolog and not affect actin branching. C12orf4 has a role in the activation and degranulation of mast cells[85], Ccdc124 is centrosomal protein[85] which is localized to the MTOC, and Tsg101 has a role in the translocation of the TCR into the IS and incorporation of TCR into microvesicles [74].

To see more accurate results for each mutated pool, fewer number of cells, 17 cells for example, should be grown to increase a chance to get more critical mutations in the pool. Less number of mutations can be analyzed by sequencing and we can the ratio of these mutations that cause early stop codon. Besides that, western blotting should be performed to check protein levels of mutated pools. After these confirmations, we can comment better why some genes did not have any effect while others had. Other cytotoxicity tests should be performed to better define minor but critical differences in the cytotoxicity mechanisms of these mutated cells.

## 6. REFERENCES

- [1] Hato T, Dagher PC. How the innate immune system senses trouble and causes trouble. *Clin J Am Soc Nephrol*. 2015;10(8):1459-1469. doi:10.2215/CJN.04680514.
- [2] Hamon MA, Quintin J. Innate immune memory in mammals. *Semin Immunol*. 2016;28(4):351-358. doi:10.1016/j.smim.2016.05.003.
- [3] Kato J, Svensson CI. Role of extracellular damage-associated molecular pattern molecules (DAMPs) as mediators of persistent pain. *Progress in Molecular Biology and Translational Science*. 2015. doi:10.1016/bs.pmbts.2014.11.014.
- [4] Iwasaki A, Medzhitov R. Control of adaptive immunity by the innate immune system. *Nat Immunol*. 2015;16(4):343-353. doi:10.1038/ni.3123.
- [5] Cooper MD, Herrin BR. How did our complex immune system evolve? *Nat Rev Immunol*. 2010;10(1):2-3. doi:10.1038/nri2686.
- [6] Janeway CA, Medzhitov R. Innate immune recognition. *Annu Rev Immunol*. 2002;20(1):197-216. doi:10.1146/annurev.immunol.20.083001.084359.
- [7] Leone P, Shin EC, Perosa F, Vacca A, Dammacco F, Racanelli V. MHC class I antigen processing and presenting machinery: Organization, function, and defects in tumor cells. *J Natl Cancer Inst*. 2013;105(16):1172-1187. doi:10.1093/jnci/djt184.
- [8] Roche PA, Furuta K. The ins and outs of MHC class II-mediated antigen processing and presentation. *Nat Rev Immunol*. 2015;15(4):203-216. doi:10.1038/nri3818.
- [9] Malissen B, Bongrand P. Early T cell activation : Integrating biochemical , structural , and biophysical cues. *Annu Rev Immunol*. 2015. doi:10.1146/annurev-immunol-032414-112158.
- [10] Davis MM. A new trigger for T cells. *Cell*. 2002;110(3):285-287. doi:10.1016/S0092-8674(02)00865-6.
- [11] Smith-garvin JE, Koretzky GA, Jordan MS. T cell activation. *Annu Rev Immunol*. 2009:591-619. doi:10.1146/annurev.immunol.021908.132706.
- [12] Chakraborty AK, Weiss A. Insights into the initiation of TCR signaling. *Nat Immunol*. 2014;15(9):798-807. doi:10.1038/ni.2940.
- [13] Yablonski D, Kuhne MR, Kadlecsek T, Weiss A. Uncoupling of nonreceptor tyrosine kinases from PLC- $\gamma$ 1 in an SLP-76- deficient T cell. *Science*. 1998;281(5375):413-416. doi:10.1126/science.281.5375.413.
- [14] Quann EJ, Liu X, Altan-Bonnet G, Huse M. A cascade of protein kinase C isozymes promotes cytoskeletal polarization in T cells. *Nat Immunol*. 2011;12(7):647-654. doi:10.1038/ni.2033.
- [15] Dieckmann NMG, Frazer GL, Asano Y, Stinchcombe JC, Griffiths GM. The cytotoxic T lymphocyte immune synapse at a glance. *J Cell Sci*. 2016;129:2881-2886. doi:doi: 10.1242/jcs.186205.

- [16] Dustin, Michael L., Long EO. Cytotoxic immunological synapses. *Immunol Rev.* 2011;235(1):24-34. doi:10.1111/j.0105-2896.2010.00904.x.
- [17] Lettau M, Qian J, Linkermann A, et al. The adaptor protein Nck interacts with Fas ligand: Guiding the death factor to the cytotoxic immunological synapse. *PNAS.* 2006;103:5911–5916. doi:doi10.1073pnas.0508562103.
- [18] Pegram HJ, Andrews DM, Smyth MJ, Darcy PK, Kershaw MH. Activating and inhibitory receptors of natural killer cells. *Immunology&Cell Biology.* 2010; 216-224. doi:10.1038/icb.2010.78.
- [19] Zotto G Del, Marcenaro E, Vacca P, et al. Markers and Function of Human NK Cells in Normal and Pathological Conditions. *Clinical Cytometry.* 2017;114:100-114. doi:10.1002/cyto.b.21508.
- [20] Geiger TL, Sun JC. Development and maturation of natural killer cells. *Curr Opin Immunol.* 2016;39:82-89. doi:10.1016/j.coi.2016.01.007.
- [21] Thomas LM, Peterson ME, Long EO, Thomas LM, Peterson ME, Long EO. Cutting edge: NK cell licensing modulates adhesion to target cells. *J Immunol.* 2013;191:3981-3985. doi: 10.4049/jimmunol.1301159.
- [22] Saunders PM, Vivian JP, Connor GMO, et al. A bird ' s eye view of NK cell receptor interactions with their MHC class I ligands. *Immunol Rev.* 2015;267:148-166.
- [23] Watzl C, Long EO. Signal transduction during activation and inhibition of natural killer cells. *Curr Protoc Immunol.* 2010. doi:10.1002/0471142735.im1109bs90.
- [24] Mart B, Suñe G, Perez-amill L, Castella M. Natural Killer cells : Angels and devils for immunotherapy. *Int. J. Mol. Sci.* 2017. doi:10.3390/ijms18091868.
- [25] Borg C, Jalil A, Laderach D, et al. NK cell activation by dendritic cells ( DCs ) requires the formation of a synapse leading to IL-12 polarization in DCs. *Blood.* 2004;104(10):3267-3276. doi:10.1182/blood-2004-01-0380.
- [26] Lanier LL. Up on the tightrope: natural killer cell activation and inhibition. *Nat Immunol.* 2009;9(5):495-502. doi:10.1038/ni1581.
- [27] Pegram HJ, Andrews DM, Smyth MJ, Darcy PK, Kershaw MH. Activating and inhibitory receptors of natural killer cells. *Immunol Cell Biol.* 2011;89(2):216-224. doi:10.1038/icb.2010.78.
- [28] Rosen DB, Araki M, Hamerman JA, Chen T, Yamamura T, Lanier LL. A Structural basis for the association of DAP12 with mouse, but not human, NKG2D. *J Immunol.* 2004;173(4):2470-2478. doi:10.4049/jimmunol.173.4.2470.
- [29] Chen R, Latour S, Shi X, Veillette A. Association between SAP and FynT: Inducible SH3 domain-mediated interaction controlled by engagement of the SLAM receptor. *Mol Cell Biol.* 2006;26(15):5559-5568. doi:10.1128/MCB.00357-06.
- [30] March ME, Ljunggren H, Long EO. Costimulation of resting human natural killer cells. *Immunol Rev.* 2006;214:73-91. doi: 10.1111/j.1600-065X.2006.00457.x

- [31] Seifried E. Cellular immunotherapy of malignancies using the clonal Natural Killer cell line NK-92. *J Hematother Stem Cell Res.* 2001;10(4):535-544. doi: 10.1089/15258160152509145.
- [32] Childs H, Reilly JO. Antileukemia activity of a natural killer cell line against human leukemias. *Clin cancer Res.* 1998;4(11):2859-2868. pmid: 9829753
- [33] Suck G, Odendahl M, Nowakowska P, et al. NK - 92 : an ‘ off - the - shelf therapeutic ’ for adoptive natural killer cell - based cancer immunotherapy. *Cancer Immunol Immunother.* 2016;65(4):485-492. doi:10.1007/s00262-015-1761-x.
- [34] Kalina U, Kauschat D, Koyama N, et al. IL-18 activates STAT3 in the Natural Killer cell line 92, augments cytotoxic activity, and mediates IFN- $\gamma$  production by the stress kinase p38 and by the extracellular regulated kinases p44<sup>erk-1</sup> and p42<sup>erk-2</sup>. *J Immunol.* 2000;165(3):1307-1313. doi:10.4049/jimmunol.165.3.1307.
- [35] Maki, G., Klingemann, H.G., Martinson, J.A, and Tam KT. Factors regulating the cytotoxic activity of the human natural killer cell line, NK-92. *J Hematother Stem Cell Res.* 2001;10:369-383. doi: 10.1089/152581601750288975.
- [36] Tam YK, Miyagawa B, Ho VC, Klingemann H-G. Immunotherapy of malignant melanoma in a SCID mouse model using the highly cytotoxic natural killer cell line NK-92. *J Hematother.* 1999;8(3):281-290. doi:10.1002/jps.2600840122.
- [37] Maki G, Tam YK, Berkahn L, Klingemann HG. Ex vivo purging with NK-92 prior to autografting for chronic myelogenous leukemia. *Bone Marrow Transplant.* 2003;31(12):1119-1125. doi:10.1038/sj.bmt.1704117.
- [38] Burshtyn DN, Scharenberg AM, Wagtmann N, et al. Recruitment of tyrosine phosphatase HCP by the killer cell inhibitory receptor. *Immunity.* 1996;4(1):77-85. doi:10.1016/S1074-7613(00)80300-3.
- [39] Carbone E, Ruggiero G, Terrazzano G, et al. A new mechanism of NK cell cytotoxicity activation: the CD40-CD40 ligand interaction. *J Exp Med.* 1997;185(12):2053-2060. doi:10.1084/jem.185.12.2053.
- [40] Kashii Y, Giorda R, Herberman R, Whiteside T, Vujanovic N. Constitutive expression and role of the TNF family ligands in apoptotic killing of tumor cells by human NK cells. *J Immunol.* 1999;163(10):5358-66. pmid: 10553060.
- [41] Sutlu T, Gilljam M, Stellan B, Applequist SE, Alici E. Inhibition of intracellular antiviral defense mechanisms augments lentiviral transduction of human natural killer cells: Implications for gene therapy. *Hum Gene Ther.* 2012;23:1090-1100. doi:10.1089/hum.2012.080.
- [42] Ladd B, O’Konek JJ, Ostruszka LJ, Shewach DS. Unrepairable DNA double-strand breaks initiate cytotoxicity with HSV-TK/ganciclovir. *Cancer Gene Ther.* 2011;18(10):751-759. doi:10.1038/cgt.2011.51.
- [43] Burkhardt JK, Carrizosa E, Shaffer MH. The actin cytoskeleton in T cell activation. *Annu Rev Immunol.* 2008. doi:10.1146/annurev.immunol.26.021607.090347.



- [44] Varma R, Campi G, Yokosuka T, Saito T, Dustin ML. T cell receptor-proximal signals are sustained in peripheral microclusters and terminated in the central supramolecular activation cluster. *Immunity*. 2006;117-127. doi:10.1016/j.immuni.2006.04.010
- [45] Ritter AT, Angus KL, Griffiths GM. The role of the cytoskeleton at the immunological synapse. *Immunol Rev*. 2013;256(1):107-17. doi: 10.1111/imr.12117.
- [46] Higgs HN, Pollard TD. Regulation of actin filament network formation through Arp2/3 complex : Activation by a diverse array of proteins. *Annu Rev Biochem*. 2001;70:649–76. doi: 10.1146/annurev.biochem.70.1.649.
- [47] Cullinan P, Sperling AI, Burkhardt JK. The distal pole complex : a novel membrane domain distal to the immunological synapse. *Immunological Rev*.2002;189:111-122. doi:https://doi.org/10.1034/j.1600-065X.2002.18910.x.
- [48] Dustin ML, Choudhuri K. Signaling and polarized communication across the T cell immunological synapse. *Annual Review of Cell and Developmental Biology*. 2016; 32:303-325. doi:10.1146/annurev-cellbio-100814-125330.
- [49] Beemiller P, Krummel MF. Mediation of T-cell activation by actin meshworks. *Cold Spring Harb Perspect Biol*. 2010;2(9). doi: 10.1101/cshperspect.a002444.
- [50] Asano Y, Griffiths GM. Origins of the cytolytic synapse. *Nature Reviews Immunology*. 2016;16:421–432. doi:10.1038/nri.2016.54.
- [51] Irvine DJ. Function-specific variations in the immunological synapses formed by cytotoxic T cells. *PNAS*. 2003;100(24):13739-13740. https://doi.org/10.1073/pnas.2536626100
- [52] Geiger B, Rosen D, Berke G. Spatial relationships of microtubule-organizing centers and the contact area of cytotoxic T lymphocytes and target cells. *J Cell Biol*. 1982;(5):10-12. doi: 10.1083/jcb.95.1.137.
- [53] Verret CR, Firmenich AA, Ahne DM. Resistance of cytotoxic t lymphocytes to the lytic effects of their toxic granules. *J Exp Med*. 1987;166. doi: 10.1084/jem.166.5.1536.
- [54] Stinchcombe JC, Griffiths GM. Secretory mechanisms in cell-mediated cytotoxicity. *Annual Review of Cell and Developmental Biology*. 2007:495-517. doi:10.1146/annurev.cellbio.23.090506.123521.
- [55] Urlaub D, Höfer K, Müller M-L, Watzl C. LFA-1 activation in NK cells and their subsets: Influence of receptors, maturation, and cytokine stimulation. *J Immunol*. 2017;198(5):1944-1951. doi:10.4049/jimmunol.1601004.
- [56] Lopez-verge S, Milush JM, Pandey S, et al. CD57 defines a functionally distinct population of mature NK cells in the human CD56<sup>dim</sup> CD16<sup>+</sup> NK-cell subset. *Blood*. 2010;116(19):3865-3875. doi:10.1182/blood-2010-04-282301.
- [57] Hogg N, Leitinger B. Shape and shift changes related to the function of leukocyte integrins LFA-1 and Mac-1. *J Leukoc Biol*. 2001;69:893-898. doi:10.1189/jlb.69.6.893.

- [58] Dransfield I, Cabanas C, Craig A, Hogg N. Divalent cation regulation of the function of the leukocyte integrin LFA1. *J Cell Biol.* 1992;116(1). doi: 10.1083/jcb.116.1.219.
- [59] Bryceson YT, Chiang SCC, Darmanin S, et al. Molecular mechanisms of natural killer cell activation. *J Innate Immun.* 2011;3(3):216-226. doi:10.1159/000325265.
- [60] Mccann FE, Vanherberghen B, Carlin LM, et al. The size of the synaptic cleft and distinct distributions of filamentous actin, ezrin, CD43, and CD45 at activating and inhibitory human NK cell immune synapses. *J Immunol.* 2003;170(6):2862-2870. doi:10.4049/jimmunol.170.6.2862.
- [61] Orange JS, Ramesh N, Donnell ER, et al. Wiskott – Aldrich syndrome protein is required for NK cell cytotoxicity and colocalizes with actin to NK cell-activating immunologic synapses. *PNAS.* 2002;99(17):1-6. doi:https://doi.org/10.1073/pnas.162376099.
- [62] Krzewski K, Strominger JL. The killer's kiss : the many functions of NK cell immunological synapses. *Curr Opin Cell Biol.* 2008;20(5):597-605. doi:10.1016/j.ceb.2008.05.006.
- [63] Sanborn KB, Orange JS. Navigating barriers: The challenge of directed secretion at the natural killer cell lytic immunological synapse. *J Clin Immunol.* 2010;30(3):358-363. doi:10.1007/s10875-010-9372-y.
- [64] Fauriat C, Long EO, Ljunggren HG, and Bryceson YT. Regulation of human NK-cell cytokine and chemokine production by target cell recognition. *Blood.* 2010;115(11):2167–2176. doi:10.1182/blood-2009-08-238469.
- [65] Szabo SJ, Sullivan BM, Peng SL, Glimcher LH. Molecular mechanisms regulating Th1 immune responses. *Annu Rev Immunol.* 2003;21(1):713-758. doi:10.1146/annurev.immunol.21.120601.140942.
- [66] Erskine RA, Deacon MP, Strominger JL, Reyburn HT. The role of zinc in the binding of killer cell Ig-like receptors to class I MHC proteins. *PNAS.* 2001;98(4):1734-1739. doi:https://doi.org/10.1073/pnas.98.4.1734.
- [67] Matalon O, Fried S, Ben-shmuel A, et al. Dephosphorylation of the adaptor LAT and phospholipase C- $\gamma$  by SHP-1 inhibits natural killer cell cytotoxicity. *Immunology.* 2016;9(429):1-16. doi:10.1126/scisignal.aad6182.
- [68] Davis DM, Chiu I, Fassett M, Cohen GB, Mandelboim O, Strominger JL. The human natural killer cell immune synapse. *Proc Natl Acad Sci USA.* 1999;96(26):15062-7. pmid: 10611338
- [69] Lema F, Santo JP Di, Bouso P, Deguine J. Article intravital imaging reveals distinct dynamics for Natural Killer and CD8<sup>+</sup> T Cells during tumor regression. *Immunity.* 2010;33(4):632-644. doi:10.1016/j.immuni.2010.09.016.
- [70] De Saint Basile G, Ménasché G, Fischer A. Molecular mechanisms of biogenesis and exocytosis of cytotoxic granules. *Nat Rev Immunol.* 2010;10(8):568-579. doi:10.1038/nri2803.

- [71] Sanborn KB, Rak GD, Maru SY, et al. Myosin IIA associates with NK cell lytic granules to enable their interaction with F-actin and function at the immunological synapse. *J Immunol.* 2009;182(11):6969-6984. doi:10.4049/jimmunol.0804337.
- [72] MacE EM, Dongre P, Hsu HT, et al. Cell biological steps and checkpoints in accessing NK cell cytotoxicity. *Immunol Cell Biol.* 2014;92(3):245-255. doi:10.1038/icb.2013.96.
- [73] Telkoparan P, Erkek S, Yaman E, Alotaibi H, Bayik D, Tazebay UH. Coiled-coil domain containing protein 124 is a novel centrosome and midbody protein that interacts with the ras-guanine nucleotide exchange factor 1b and is involved in cytokinesis. *PLoS One.* 2013;8(7). doi:10.1371/journal.pone.0069289.
- [74] Choudhuri K, Llodrá J, Roth EW, et al. Polarized release of T-cell-receptor-enriched microvesicles at the immunological synapse. *Nature.* 2014;507(7490):118-123. doi:10.1038/nature12951.
- [75] Ran FA, Hsu PD, Wright J, Agarwala V, Scott DA, Zhang F. Genome engineering using the CRISPR-Cas9 system. *Nat Protoc.* 2013;8(11):2281-2308. doi:10.1038/nprot.2013.143.
- [76] Brouns SJJ, Jore MM, Lundgren M, Westra ER, Slijkhuis RJH, Snijders APL, Dickman MJ, Makarova KS, Koonin EV, van der Oost J. Small CRISPR RNAs guide antiviral defense in prokaryotes. *Science.* 2008;321(5891):960-964. doi:10.1126/science.1159689.
- [77] Cong L, Ran FA, Cox D, Lin S, Barretto R, Habib N, Hsu PD, Wu X, Jiang W, Marraffini LA, Zhang F. Multiplex genome engineering using CRISPR/Cas systems. *Science.* 2013;339(6121):819-823. doi:10.1126/science.1231143.
- [78] Zhang JH, Adikaram P, Pandey M, Genis A & Simonds WF. Optimization of genome editing through CRISPR Cas9 engineering. *Bioengineered.* 2016;7(3):166-74. doi:10.1080/21655979.2016.1189039.
- [79] Zhang F, Wen Y & Guo X. CRISPR/Cas9 for genome editing: progress, implications and challenges. *Human Molecular Genetics.* 2014. doi:10.1093/hmg/ddu125
- [80] Kahr WHA, Pluthero FG, Elkadri A, et al. Loss of the Arp2/3 complex component ARPC1B causes platelet abnormalities and predisposes to inflammatory disease. *Nat Commun.* 2017;8:1-14. doi:10.1038/ncomms14816.
- [81] Abella JVG, Galloni C, Pernier J, et al. Isoform diversity in the Arp2/3 complex determines actin filament dynamics. *Nat Cell Biol.* 2016;18(1):76-86. doi:10.1038/ncb3286.
- [82] Chinen J, Cowan MJ. Advances and highlights in primary immunodeficiencies in 2017. *J Allergy Clin Immunol.* 2018;142(4):1041-1051. doi:10.1016/j.jaci.2018.08.016.
- [83] Brigida I, Zoccolillo M, Cicalese MP, et al. T cell defects in patients with *ARPC1B* germline mutations account for their combined immunodeficiency. *Blood.* 2018. doi:10.1182/blood-2018-07-863431.

- [84] Somech R, Lev A, Lee YN, et al. Disruption of thrombocyte and T lymphocyte development by a mutation in *ARPC1B*. *J Immunol.* 2017. doi:10.4049/jimmunol.1700460.
- [85] Mazuc E, Guglielmi L, Bec N, et al. In-cell intrabody selection from a diverse human library identifies C12orf4 protein as a new player in rodent mast cell degranulation. *PLoS One.* 2014;9(8). doi:10.1371/journal.pone.0104998.
- [86] Wu P, Farrell WE, Haworth KE, et al. Maternal genome-wide DNA methylation profiling in gestational diabetes shows distinctive disease-associated changes relative to matched healthy pregnancies. *Epigenetics.* 2018;13(2):122-128. doi:10.1080/15592294.2016.1166321.
- [87] Li S, Wang L, Berman M, Kong YY, Dorf ME. Mapping a dynamic innate immunity protein interaction network regulating type I interferon production. *Immunity.* 2011;35(3):426-440. doi:10.1016/j.immuni.2011.06.014.
- [88] Yoo H-S, Choi Y, Ahn N, et al. Transcriptional regulator CTR9 inhibits Th17 differentiation via repression of IL-17 expression. *J Immunol.* 2014;192(4):1440-1448. doi:10.4049/jimmunol.1201952.
- [89] Youn MY, Yoo HS, Kim MJ, et al. hCTR9, a component of Paf1 complex, participates in the transcription of interleukin 6-responsive genes through regulation of STAT3-DNA interactions. *J Biol Chem.* 2007;282(48):34727-34734. doi:10.1074/jbc.M705411200.
- [90] Hanks S, Perdeaux ER, Seal S, et al. Germline mutations in the PAF1 complex gene CTR9 predispose to Wilms tumour. *Nat Commun.* 2014;5:1-7. doi:10.1038/ncomms5398.
- [91] Rodrigues J, Lydall D. Cis and trans interactions between genes encoding PAF1 complex and ESCRT machinery components in yeast. *Curr Genet.* 2018;64(5):1105-1116. doi:10.1007/s00294-018-0828-6.
- [92] Judson H, Van RN, Strain L, et al. Structure and mutation analysis of the gene encoding DNA fragmentation factor 40 (caspase-activated nuclease), a candidate neuroblastoma tumour suppressor gene. *Hum Genet.* 2000;106(4):406-413. doi:10.1007/s004390000257.
- [93] Yerlikaya A, Okur E, Baykal AT, Acilan C, Boyaci I, Ulukaya E. A proteomic analysis of p53-independent induction of apoptosis by bortezomib in 4T1 breast cancer cell line. *J Proteomics.* 2014;113:315-325. doi:10.1016/j.jprot.2014.09.010.
- [94] Malecki M, Dahlke J, Haig M, Wohlwend L & Malecki R. Eradication of human ovarian cancer cells by transgenic expression of recombinant DNASE1, DNASE1L3, DNASE2, and DFFB controlled by EGFR promoter: Novel strategy for targeted therapy of cancer. 2014;4. doi:10.4172/2157-7412.1000152.
- [95] Bingol B, Sheng M. Mechanisms of mitophagy: PINK1, Parkin, USP30 and beyond. *Free Radic Biol Med.* 2016;100:210-222. doi:10.1016/j.freeradbiomed.2016.04.015.

- [96] Bingol B, Tea JS, Phu L, et al. The mitochondrial deubiquitinase USP30 opposes parkin-mediated mitophagy. *Nature*. 2014;510(7505):370-375. doi:10.1038/nature13418.
- [97] Liang J-R, Martinez A, Lane JD, Mayor U, Clague MJ, Urbe S. USP30 deubiquitylates mitochondrial Parkin substrates and restricts apoptotic cell death. *EMBO Rep*. 2015;16(5):618-627. doi:10.15252/embr.201439820.
- [98] Gersch M, Gladkova C, Schubert AF, Michel MA, Maslen S, Komander D. Mechanism and regulation of the Lys6-selective deubiquitinase USP30. *Nat Struct Mol Biol*. 2017;24(11):920-930. doi:10.1038/nsmb.3475.
- [99] Wauer T, Swatek KN, Wagstaff JL, et al. Ubiquitin Ser65 phosphorylation affects ubiquitin structure, chain assembly and hydrolysis. *EMBO J*. 2015;34(3):307-325. doi:10.15252/emj.201489847.
- [100] Auth T, Schlüter S, Urschel S, et al. The TSG101 protein binds to connexins and is involved in connexin degradation. *Exp Cell Res*. 2009;315(6):1053-1062. doi:10.1016/j.yexcr.2008.12.025.
- [101] Yanagida-Ishizaki Y, Takei T, Ishizaki R, et al. Recruitment of Tom1L1/Srcasm to endosomes and the midbody by Tsg101. *Cell Struct Funct*. 2008;33(1347-3700 (Electronic)):91-100. doi:10.1247/csf.07037.
- [102] Cheng -H, Cohen SN. Human MDM2 isoforms translated differentially on constitutive versus p53-regulated transcripts have distinct functions in the p53/MDM2 and TSG101/MDM2 feedback control loops. *Mol Cell Biol*. 2007;27(1):111-119. doi:10.1128/MCB.00235-06.
- [103] Li L, Liao J, Ruland J, Mak TW, Cohen SN. A TSG101/MDM2 regulatory loop modulates MDM2 degradation and MDM2/p53 feedback control. *Proc Natl Acad Sci*. 2001;98(4):1619-1624. doi:10.1073/pnas.98.4.1619.
- [104] Liu Z, Tian Z, Cao K, et al. TSG101 promotes the proliferation, migration and invasion of hepatocellular carcinoma cells by regulating the PEG10. *J Cell Mol Med*. 2018;1-13. doi:10.1111/jcmm.13878.
- [105] Hewitt EW, Duncan L, Mufti D, Baker J, Stevenson PG, Lehner PJ. Ubiquitylation of MHC class I by the K3 viral protein signals internalization and TSG101-dependent degradation. *EMBO J*. 2002;21(10):2418-2429. doi:10.1093/emboj/21.10.2418.
- [106] Chiou CT, Hu CCA, Chen PH, Liao CL, Lin YL, Wang JJ. Association of Japanese encephalitis virus NS3 protein with microtubules and tumour susceptibility gene 101 (TSG101) protein. *J Gen Virol*. 2003;84(10):2795-2805. doi:10.1099/vir.0.19201-0.
- [107] McDonald B & Martin-Serrano J. Regulation of Tsg101 expression by the steadiness box: A role of Tsg101-associated ligase. *Mol Biol Cell*. 2008;19(2):754-63. doi:10.1091/mbc.e07-09-0957
- [108] Vardhana S, Choudhuri K, Varma R, Dustin ML. Essential role of ubiquitin and TSG101 protein in formation and function of the central supramolecular activation cluster. *Immunity*. 2010;32(4):531-540. doi:10.1016/j.immuni.2010.04.005.

- [109] Kuijpers TW, Toor ATJ, van der Bijl I, et al. Combined immunodeficiency with severe inflammation and allergy caused by ARPC1B deficiency. *J Allergy Clin Immunol.* 2017;140(1):273-277. doi:10.1016/j.jaci.2016.09.061.
- [110] Green MR & Sambrook J. *Molecular Cloning: A Laboratory Manual (Fourth Edition)* 2012 ISBN:978-1936113-42-2

## 7. APPENDICES

### 7.1. APPENDIX A- Chemicals

<b>Chemicals and Media Components</b>	<b>Supplier Company</b>
Acetic acid (glacial)	Merck Millipore, USA
Agarose	Sigma, Germany
Ampicillin Sodium Salt	Cellgro, USA
Boric Acid	Molekula France
BX795	Sigma, Germany
Chloroquine	Sigma, Germany
Distilled Water	Merck Millipore, USA
DMEM	GIBCO, USA
DMSO	Sigma, Germany
DNA Gel Loading Dye, 6X	NEB, USA
DPBS	Sigma, Germany
DTT	Fermentas, USA
EDTA	Sigma, Germany
Ethanol	Sigma, Germany
Ethidium Bromide	Sigma, Germany
Fetal Bovine Serum	Thermo Fischer Scientific, USA
Ganciclovir	Sigma, Germany
Glycerol	Sigma, Germany
HEPES Solution, 1 M	Sigma, Germany
Hydrochloric Acid	Sigma, Germany
Interleukin2	Proleukin, Novartis
Ionomycin	Sigma, Germany
Isopropanol	Sigma Germany
L-glutamine	Thermo Fischer Scientific, USA
LB Agar	Sigma, Germany
LB Broth	Invitrogen, USA
MEM Non-Essential Amino Acid Solution	Thermo Fischer Scientific, USA
MEM Vitamin Solution	Thermo Fischer Scientific, USA

Methanol	Sigma, Germany
Monensin	Biolegend, USA
PBS	Thermo Fischer Scientific, USA
Penicillin/Streptomycin	Thermo Fischer Scientific, USA
pH4.0 Buffer Solution	Merck Millipore, USA
pH7.0 Buffer Solution	Merck Millipore, USA
PIPES	Sigma, Germany
Poly-D-Lysine	BD, USA
Proteamine Sulfate	Sigma, Germany
Potassium Acetate	Merck Millipore, USA
Potassium Chloride	Sigma, Germany
RNase A	Roche, Germany
RPMI 1640	Thermo Fischer Scientific, USA
SDS	Sigma, Germany
Sodium Acetate	Sigma, Germany
Sodium Azide ?	Amresco, USA
Sodium Chloride	Amresco, USA
Sodium Hydroxide	Sigma, Germany
Tris Base	Sigma, Germany
Tris Hydrochloride	Amresco, USA
Trypan Blue Solution	Thermo Fischer Scientific



## 7.2 APPENDIX B – Equipment

<b>Equipment</b>	<b>Supplier Company</b>
Autoclave	HiClave HV-110, Hirayama, Japan
Balance	Isolab, Germany
Centrifuge	5418R, Eppendorf, Germany 5702, Eppendorf, Germany 5415R Eppendorf, Germany Allegra X-15R, Beckman Coulter, USA
CO2 Incubator	Binder, Germany
Deepfreeze	-80, Forma 88000 Series, Thermo Fischer Scientific, USA -20, Bosch, Germany
Electrophoresis Apparatus	VWR, USA
Electroporator	Neon Transfection System, Thermo Fischer Scientific, USA
Filters (0.22 µm and 0.45 µm)	Merck Millipore, USA
Flow Cytometer	BD FACSCanto, USA BD LSR Fortessa USA
Freezing Container	Mr. Frosty, Thermo Fischer Scientific, USA
Gel Documentation	Gel Doc EZ, Biorad, USA
Heater	Thermomixer Comfort, Eppendorf, Germany
Hemocytometer	Neubauer Improved, Isolab, Germany Hausser Scientific, Blue Bell Pa., USA
Ice Machine	AF20, Scotsman Inc., USA
Incubator	BE300, Memmert, Germany Mettmert, Modell 300, Germany Mettmert, Modell 600, Germany
Incubator Shaker	Innova 44, New Brunswick Scientific, USA
Laminar Flow	HeraSafe HS15, Heraeus, Germany HeraSafe HS12, Heraeus, Germany Heraeus, HeraSafe KS, Germany

LightCycler® 480	Roche, Switzerland
Liquid Nitrogen Tank	Taylor-Wharton, 300RS, USA
Magnetic Stirrer	SB162, Stuart, UK
Microliter Pipettes	Thermo Fischer Scientific, USA Gilson, Pipetman, France Isolab, Germany
Microscope	Primovert, Zeiss, Germany CK40, Olympus, Japan
Microwave Oven	Bosch, Germany
pH Meter	SevenCompact, Mettler Toledo, USA
Refrigerator	Bosch, Germany Arcelik, Turkey Panasonic, Japan
Spectrophotometer	NanoDrop 2000, Thermo Fischer Scientific, USA Ultrospec 2100 pro, Amersham Biosciences, UK
Thermal Cycler	C1000 Touch, Biorad, USA PTC-200, MJ Research Inc., Canada
xCELLigence RTCA	ACEA, USA
Vortex	VWR, USA
Water Bath	Innova 3100, New Brunswick Scientific, USA

### 7.3. APPENDIX C- Molecular Biology Kits

<b>Commercial Kit</b>	<b>Company</b>
GenElute Agarose Spin Columns	Sigma-Aldrich, USA
InsTAclone PCR Cloning Kit	Thermo Fischer Scientific, USA
Neon Transfection Kit	Invitrogen, USA
NuceloSpin Gel and PCR Clean-up	Macherey-Nagel, USA
PureLink HiPure Plasmid Midiprep Kit	Invitrogen, USA
PureLink Quick Gel Extraction Kit	Invitrogen, USA
RevertAid First Strand cDNA Synthesis Kit	FERMENTAS (K1622)
SuperScript Double-Stranded cDNA Synthesis Kit	11917-020, INVITROGEN
LightCycler® 480 SYBR Green I Master	Fermentas

### 7.4. APPENDIX D- Antibodies

<b>Antibody</b>	<b>Company</b>	<b>Catalog Number</b>
APC Mouse Anti-Human CD107a	BD Biosciences, USA	560664
PE/Cy7 Anti-Human CD107a	Biologend	328618
7AAD	BD Biosciences, USA	51-68981E

## 7.5. APPENDIX E – DNA Molecular Weight Marker

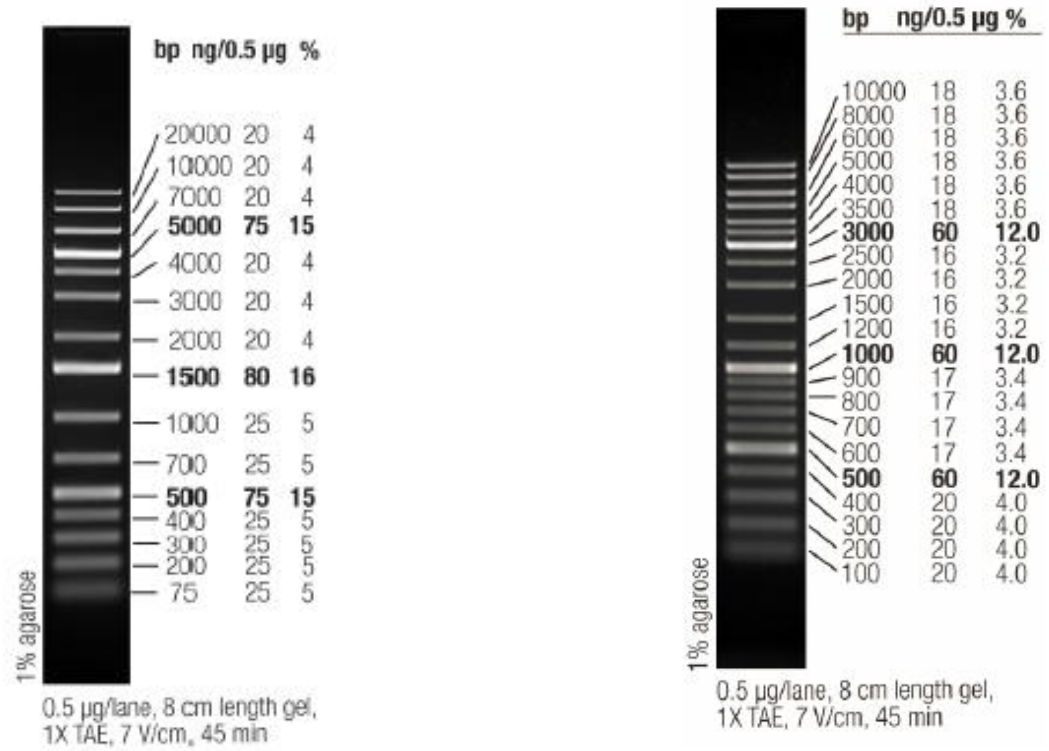


**Figure 7. 1. Thermo Scientific GeneRuler DNA Ladders 1 kb Plus DNA Ladder (SM1331) and (SM0331)**

## 7.6. APPENDIX F- Plasmid Maps

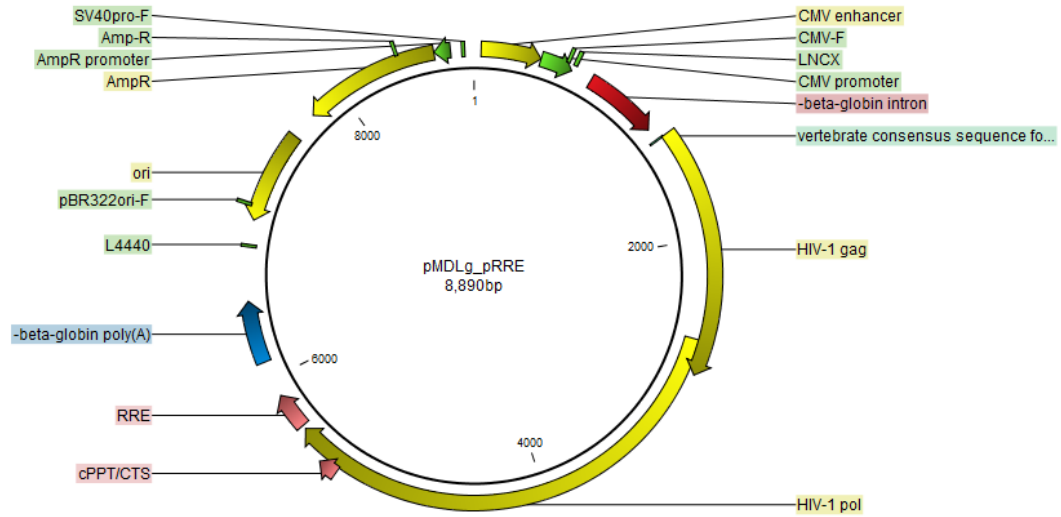


Figure 7. 2. The plasmid map of pMDLg\_pRRE

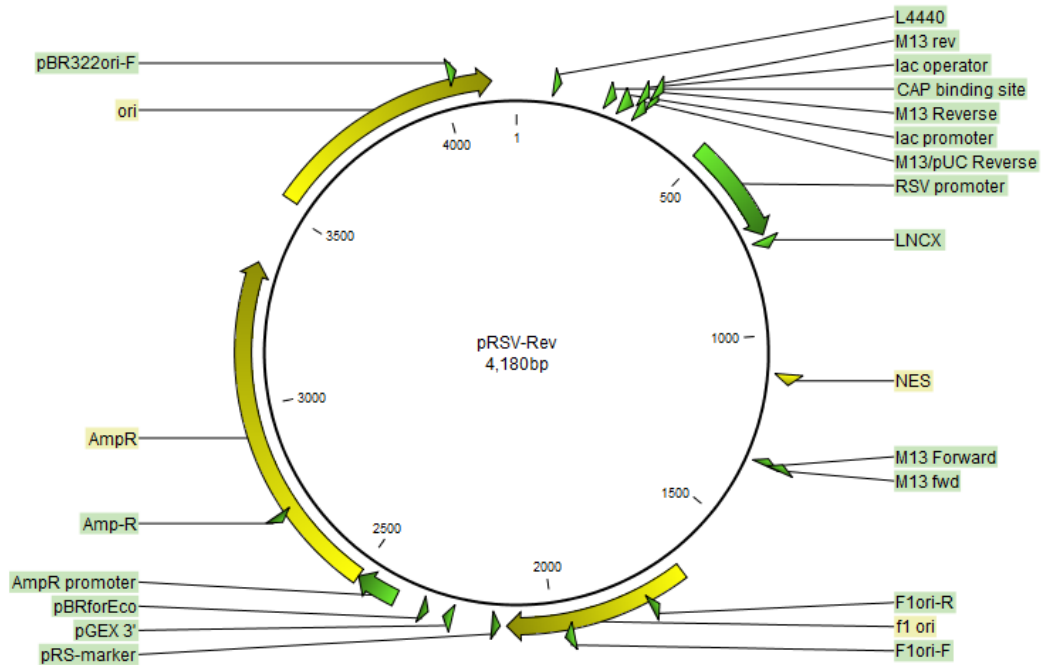


Figure 7. 3. The plasmid map of pRSV-Rev

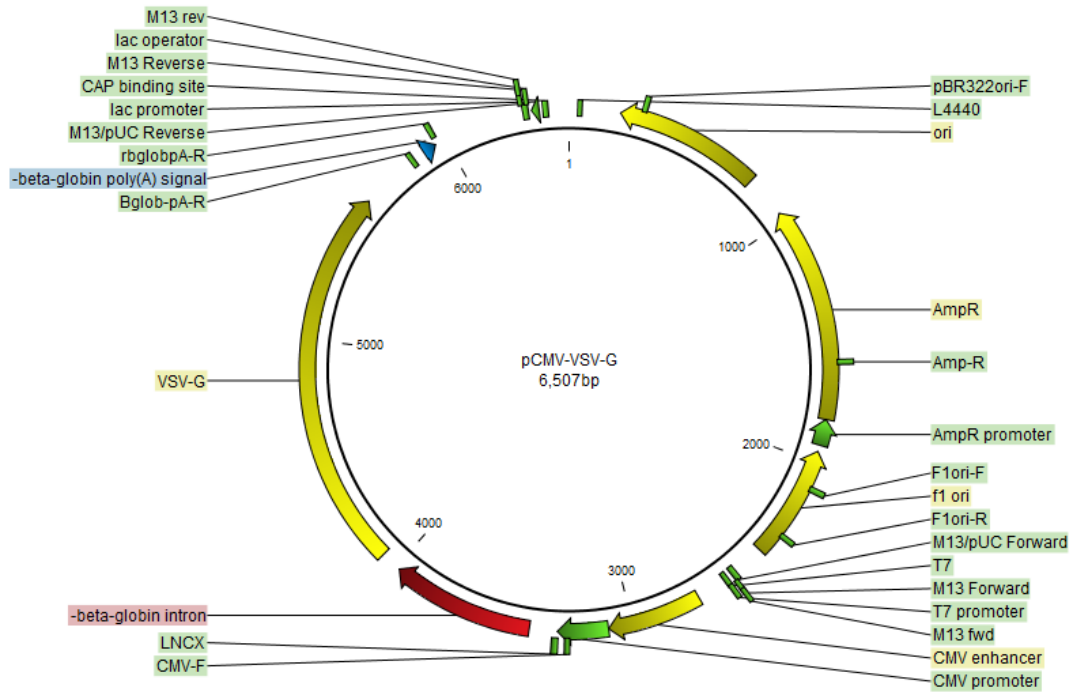


Figure 7. 4. The plasmid map of pCMV-VSV-G

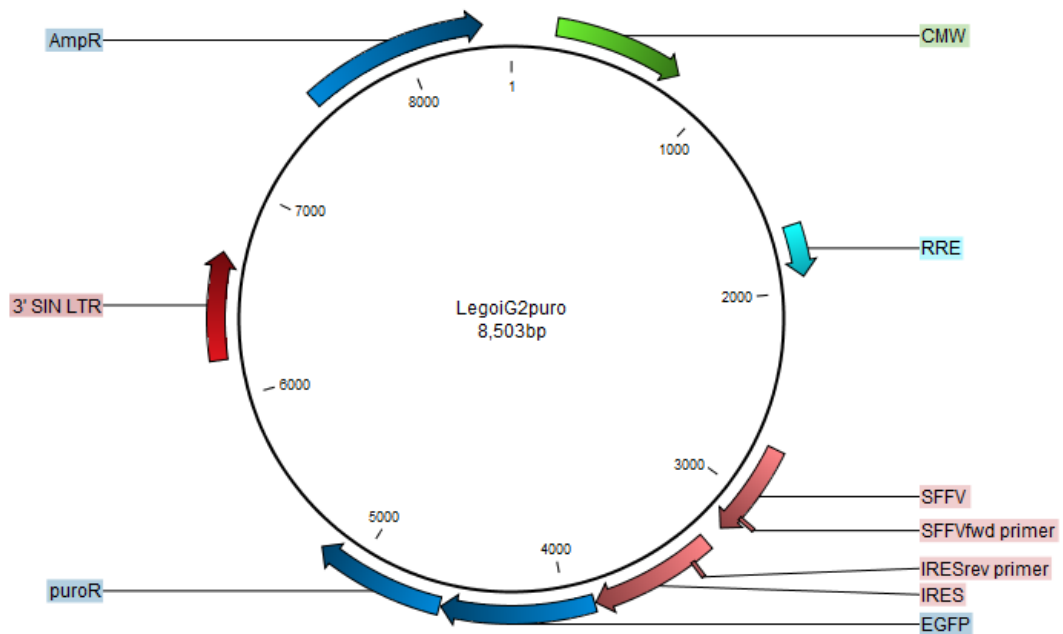


Figure 7. 5. The plasmid map of LegoiG2puro

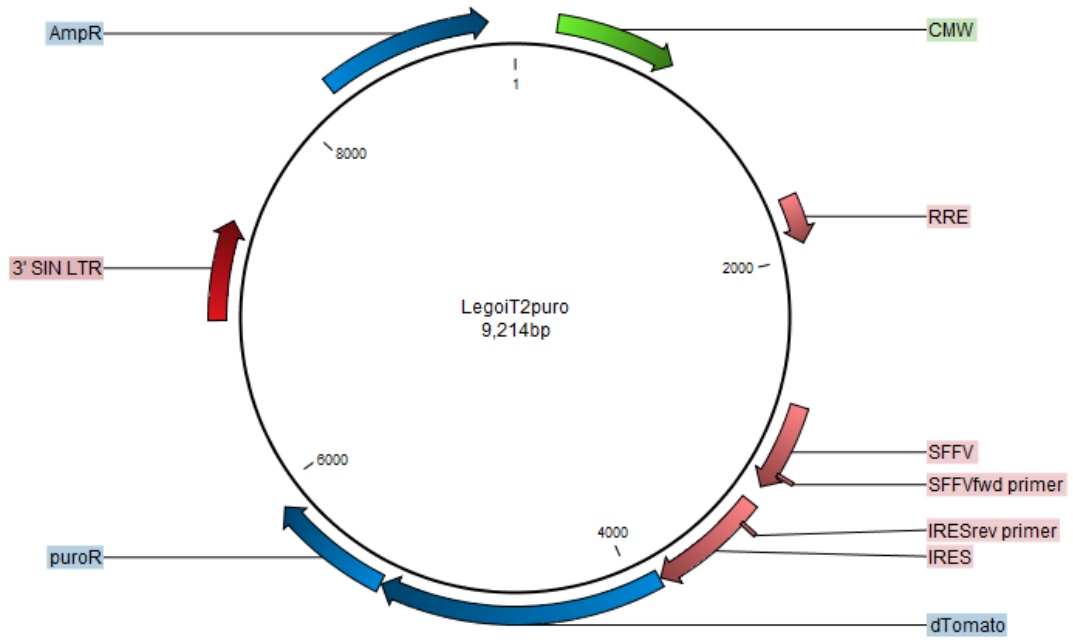


Figure 7. 6. The plasmid map of LegoIT2puro

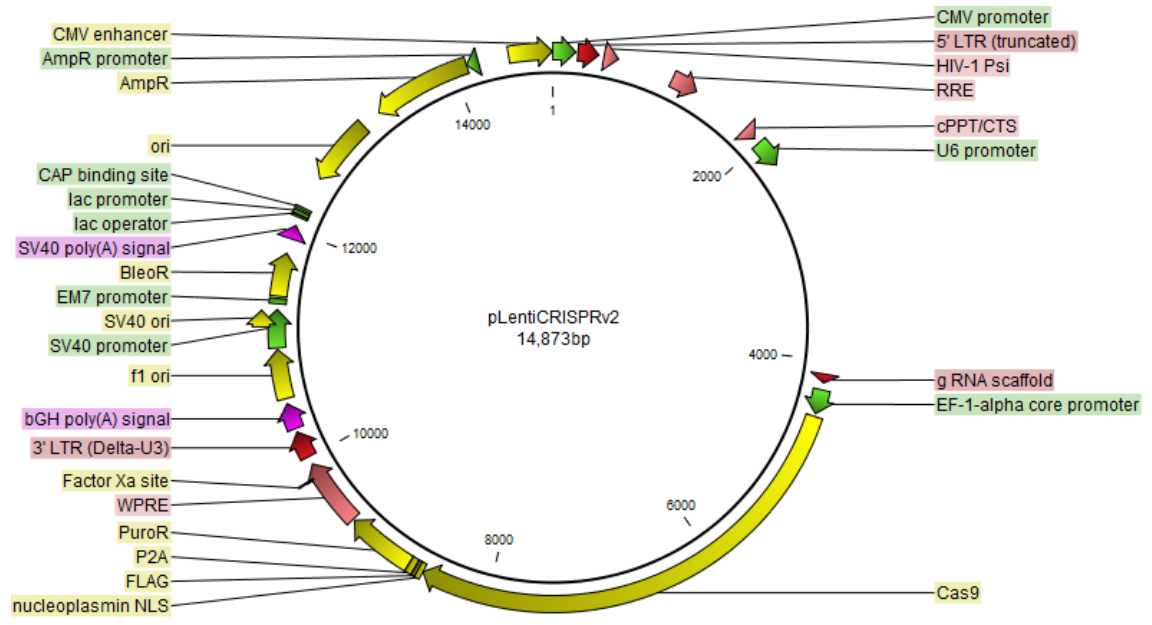
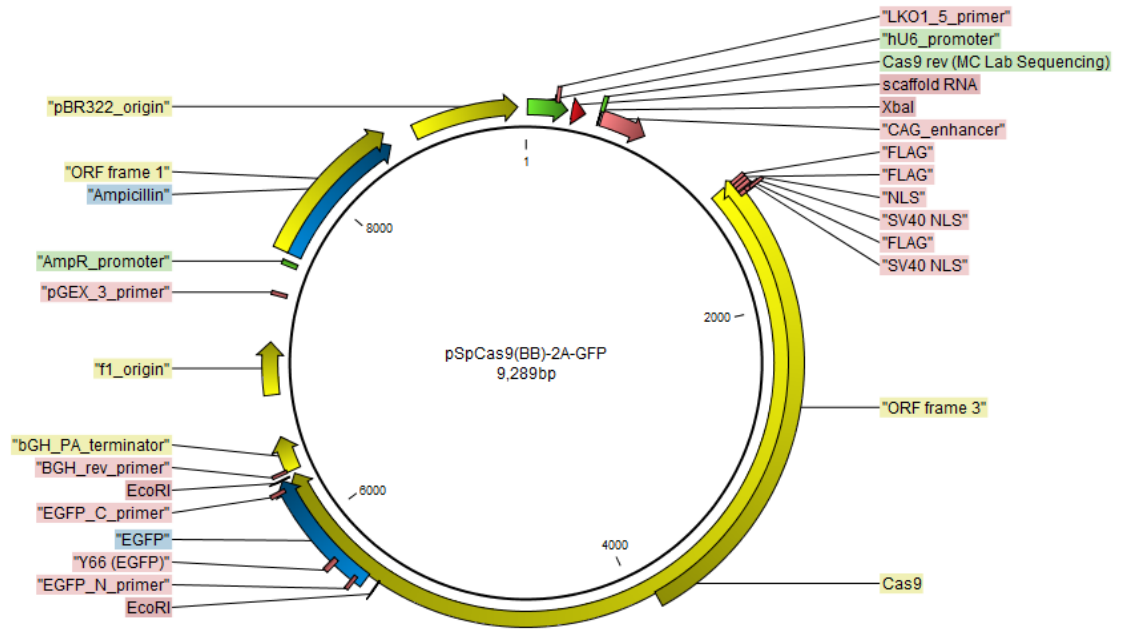
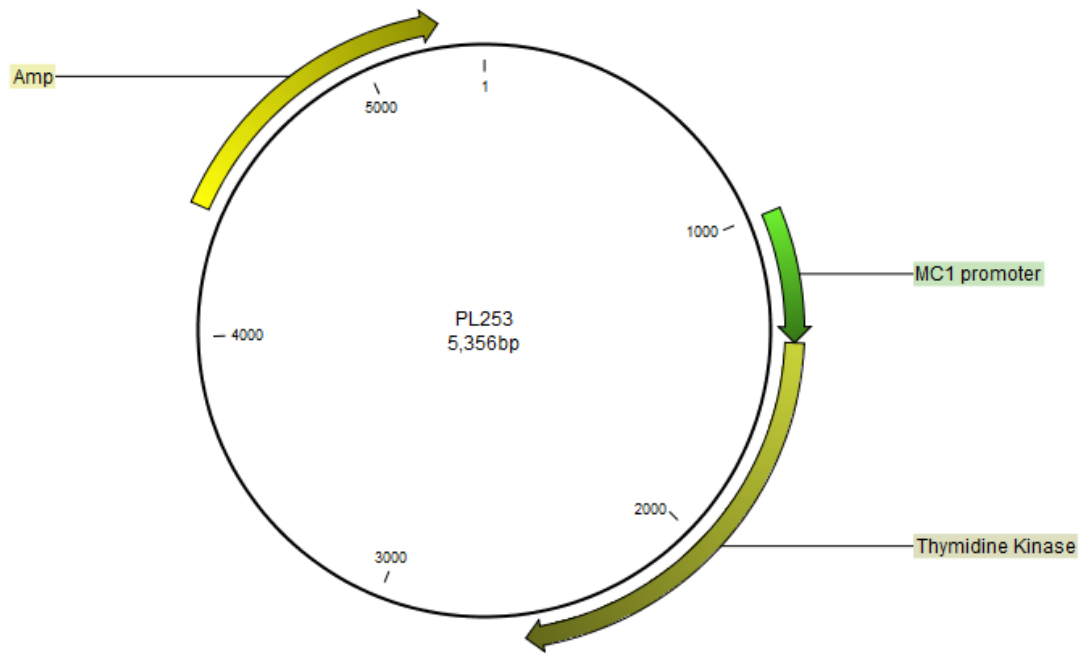


Figure 7. 7. The plasmid map of pLentiCRISPRv2



**Figure 7. 8. The plasmid map of pSpCas9(BB)-2A-GFP**



**Figure 7. 9. The plasmid map of PL253**



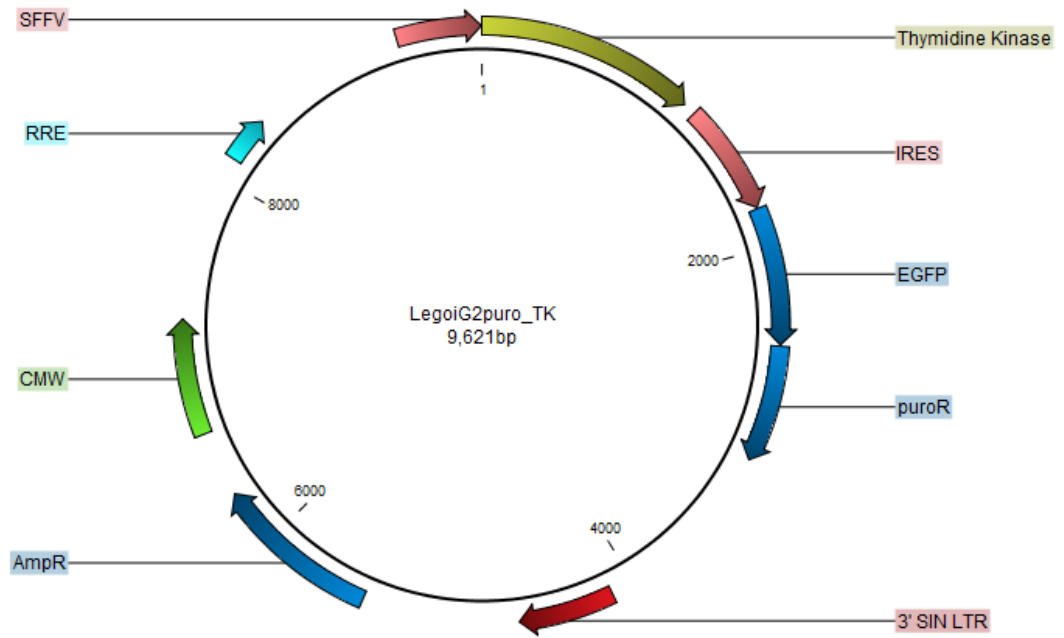


**Figure 7. 10. The plasmid map of LegoiG2puro\_TK**